Quantifying Within-field Variability in Soil Moisture and Nutrients and Scheduling Site-Specific Irrigation Using Numerical Modeling

by

Hemendra Kumar

A dissertation submitted to the Graduate Faculty of
Auburn University
in partial fulfillment of the
requirements for the Degree of
Doctor of Philosophy

Auburn, Alabama
August 6, 2022

Keywords: Soil Moisture, Nutrient Management, Spatial and Temporal Variability, HYDRUS Modeling, Irrigation Thresholds, Field Capacity

Approved by

Puneet Srivastava, Chair, Professor, Department of Biosystems Engineering
Jasmeet Lamba, Co-Chair, Associate Professor, Department of Biosystems Engineering
Brenda V Ortiz, Professor, Crop, Soil, and Environmental Sciences
Frances O'Donnell, Assistant Professor, Civil and Environment Engineering
Nedret Billor, Professor, Mathematics and Statistics
Thomas R. Way, Agricultural Engineer, National Soil Dynamics Laboratory, USDA-ARS

Abstract

The increasing global population is expected to increase pressure on water and food demands, which means intensification and improvements in irrigated agriculture are required to satisfy future needs. More than 70% of freshwater is destined for irrigation water withdrawal from streams, lakes, and groundwater. Managing irrigation based on crop demand using soil moisture variability can help improve agricultural water management. The distribution of precipitation over the growing season plays a very important role in scheduling irrigation. To improve agricultural systems, site-specific management of irrigation and nutrients are critical components of precision agriculture. To better understand irrigation and nutrient management in cropland fields, this research was conducted in the Tennessee Valley Region of Alabama.

Understanding the spatial and temporal variability in soil moisture (or soil water [L^3L^{-3}]) (Dissertation Objective 1) in different croplands can help improve the need for site-specific irrigation. We will be using soil moisture, soil moisture content, soil water, or soil water content synonymously, and all these terminologies represent volumetric soil water or moisture content in vol/vol. Estimating the mean soil water status within a field is crucial for effective irrigation water management. Various problems may arise with determining field mean soil moisture. These problems include soil physical properties, field attributes, and meteorological factors. Spatial and temporal variability in soil moisture showed maximum variability in deep and topsoil layers of the corn and cotton fields, respectively. Average soil moisture content had different patterns of variability depending on the soil depth in both corn and cotton fields. The topography of the cornfield and soil properties of the cotton field were found to be important in finding a representative location for average soil moisture content. We determined that to capture maximum

spatial and temporal variability within a field, the number of soil moisture sensors to be installed can be reduced relative to the sensors installed at the beginning of crop growing season and a temporally stable location can be identified to represent average soil moisture content within a field to schedule uniform irrigation.

Within-field variability in soil nutrients (phosphorus-P and nitrogen-N) has an effect on nutrient uptake by plants (Dissertation Objective 2). A cornfield divided into three irrigation management zones showed that uniform application of nutrients across the field resulted in inadequate nutrients in one zone and adequate nutrients in others, which had an impact on plant growth. The high P and N concentration zone had higher plant growth and higher corn grain yield during the 2019 growing season. However, lower P and N zone had reduced plant growth and lower corn grain yield. Plants in the high yield zone had greater nutrient uptake than plants in the low yield zone. Incorporating nutrient variability for site-specific management in management zone delineation can improve nutrient use efficiency and reduce nutrient loss during the growing season. The field hydrologic properties are important factors to be considered for irrigation and nutrient management in a field.

The site-specific irrigation and nutrient management are highly dependent on site-specific properties. Soil water dynamics are controlled by soil hydraulic properties (SHPs), which can vary greatly from one zone to another. Nutrient movement within the soil profile also depends on water movement within the soil profile. For better irrigation management, knowledge about SHPs is the most critical information in determining irrigation amount (Dissertation Objective 3). Optimizing SHPs using the HYDRUS modeling of zone-specific soil matric potentials (h) can determine accurate irrigation thresholds. The SHPs had differences between the irrigation management zones (zone 1 and zone 2). Determined irrigation thresholds and amounts using optimized SHPs were reduced as compared to laboratory-drawn (raw or observed) SHPs. Also, optimized irrigation

thresholds were not uniform between two zones of a cornfield. The optimizing SHPs address the discrepancies associated with laboratory and field observations since they account for measurements recorded for soil matric potential or soil water pressure heads to optimize the SHPs. However, raw SHPs cannot consider field measurements in determining accurate irrigation thresholds. Using the HYDRUS-1D model for irrigation scheduling can increase the actual root water uptake to meet the potential water demands for a crop during the growing season. Different irrigation thresholds and amounts were used to trigger the irrigation within the zones. Accurate and efficient irrigation adoption due to precipitation distribution over the growing season is important to meet crop water demands on time. Results show that farmers may delay irrigation for a few days after reaching at the irrigation threshold of h, and irrigation can be scheduled at different times in different zones. Installing soil moisture sensors at 15 cm and 30 cm depths can improve the actual to potential root water uptake ratios, which defines the water stress in the crop.

The accuracy in irrigation thresholds and depths is highly dependent on accurate field capacity (FC). The determination of FC, irrigation thresholds, and irrigation depths is characterized using site-specific SHPs (Dissertation Objective 4). Determination of FC within the field conditions is onerous and time-consuming. Therefore, FC was optimized using a negligible drainage-flux criterion at 0.01 cm/day for each zone within the field. Optimized FC was different from the FC obtained from raw SHPs and benchmark FC (33 kPa) for fine-textured soils. The differences in the determination of FC and irrigation thresholds using optimized SHPs considered soil water dynamics discrepancies associated with h measurements within the zones. The relationship between accumulated crop evapotranspiration and required irrigation amount showed a strong correlation for optimized SHPs and FC. The FC based on raw SHPs and benchmarks can be a

flawed irrigation strategy to determine irrigation threshold and depths during the growing season. Therefore, optimizing FC and the irrigation thresholds can improve irrigation water management.

Overall, this dissertation helps improve precision management of irrigation and nutrients during the growing seasons. This study can help provide a better understanding of the site-specific problems and can provide solutions for farmers to plan future growing seasons.

Acknowledgments

I want to THANK GOD for his supreme guidance and wisdom throughout my life and for putting me in the hands of bright mentors to give me direction in this Ph.D. adventure, which I could have only imagined. I would only begin by expressing my sincere gratitude to my esteemed advisor Dr. Puneet Srivastava, who first believed in me and made this incredible adventure achievable. He has provided me with constant and wise guidance. The faith he placed in me has been an inspiration to continuously improve myself as a researcher as well as an independent scholar, including academic and non-academic activities. His invaluable expertise helped me design the research questions and methodology independently. I am equally grateful to Dr. Jasmeet Lamba for being my co-advisor for believing in me and for providing me with continued guidance, support, and time as I worked towards completing my Ph.D. He has provided me the opportunities of teaching in the classes, interacting with students, and advising them with their homework or class projects. Dr. Lamba has been a bright mentor, always supporting and answering my questions related or non-related to research. Moreover, his way of being has inspired me and spurred me on during these years. I am extremely thankful to Dr. Brenda Ortiz for providing me with support, time, and ample opportunities to work with farmers and irrigation to build my research interests as I progressed in my Ph.D. She has always helped me at the time when needed in my academic and non-academic growth. I would say that my Ph.D. adventure would not have been so satisfying without meeting Dr. Ortiz. I am very grateful to Dr. Frances O'Donnell, who has provided me with my first experience of teaching at Auburn. She let me lead the lectures and articles in a graduate-level class. She has been a great mentor since a master's in Civil Engineering. She inspired me to earn master's in Civil Engineering with my Ph.D. in Biosystems Engineering. She was always

available when I needed her to discuss my research. I am equally thankful to Dr. Nedret Billor for serving on my committee. She has been a wonderful teacher in my statistics courses. She always motivated and supported me to earn a Ph.D. minor in Statistics. I am especially very grateful to Dr. Thomas Way (Tom) for serving on my committee and providing suggestions and insightful feedback on my research. I am very thankful to him for providing me the opportunity to work in the USDA lab with Mr. Gary Foster, who not only trained me in nutrient analyses, but also taught me the chemistry behind those analyses. With Dr. Way's help and mentorship, this Ph.D. journey has been a pleasant track. Working in NSDL USDA-ARS under his guidance has been an excellent learning experience for me. Thank you, everyone, for being my mentors. I sincerely believe in these words.

I am very thankful for the time and support provided by Dr. Efstathios Diamantopoulos (University of Copenhagen, Denmark) in helping me with HYDRUS modeling. I would also like to express my gratitude to Dr. Bruno Lena and Dr. Roberto Molinari for their valuable help and feedback in this research. I am thankful to my colleagues Bijoychandra, Ritesh Karki, Laljeet Sangha, and Suman Budhathoki in the research group for their continuous support and friendship during all these years. I would also like to thank my friends Guilherme Morata, Poulmi Roy, Luca Bondesan, Jenna Platt, Tayler Schillerberg, Danielle Tadych, Luan, and Rich Morbidelli for being there when I needed them. A special thanks to Gary Foster, as I and he worked days and nights for seven days a week on soil samples in the USDA lab.

I dedicate this Ph.D. to my grandfather (Zhandu Singh), my parents (Prem Pal Singh and Kalawati Devi), and my brothers (Devesh, Neeraj, and Kailash) for their unconditional and unceasing love and support. Lastly, I would like to express my heartfelt appreciation to my wife, Rashmi Sahu, whom I married during my Ph.D. journey.

Table of Contents

List of Tables

List of Figures

Chapter 1

Introduction

1.1 Background and problem statement

Increasing food and freshwater demands are the main challenges faced by agriculture due to projected population increment from 8.27 billion in 2030 to 9.322 billion in 2050 (FAO, 2012). More than 40% of the earth's population is already experiencing water security problems (Kummu et al., 2016). Thus, any improvements in the current irrigation practices can help conserve limited water resources and promote sustainable agriculture (Himanshu et al., 2021). The advancements in precision agriculture such as improvements in irrigation scheduling and nutrient management can play an important role in reducing water and nutrient losses from agricultural landscapes and help increase the crop yield. Therefore, it is important to understand soil water and nutrient variability at the field scale and develop appropriate management strategies that would contribute to food security and reduce stress on natural water resources.

The vadose zone or unsaturated or partially saturated soil media consists of the soil profile below the earth surface and above the groundwater table (Radcliffe and Simunek, 2018), which is comprised of three phases, i.e., solid, liquid, and gas. The soil water and nutrient dynamics within the soil profiles are very complicated to understand and they depend on soil type, texture, structure, and other soil properties. Therefore, it is important to have knowledge of the soil water retention curve (SWRC), which defines the soil matric potential (h) and soil water content (θ) relation is very critical in soil water dynamics. The hydraulic conductivity (K) of a soil profile defines the K-h-θ relationship, which helps understand the soil water movement within the soil profile. The accurate and effective relationship is important in irrigation scheduling and soil water status in the soil profile.

Irrigation is an essential and influencing component of the hydrological cycle and food production (Filippucci et al., 2020). Better understanding of spatial and temporal soil moisture variability within a field is of utmost importance for irrigation scheduling and for understanding transport of water, nutrients, and contaminants (Kumar et el., 2021b). Due to a lack of knowledge about soil moisture variation within a field, farmers can over-and under-irrigate the field. Over-irrigation can result in nitrate leaching, crop disease, and loss of water as runoff, which can erode soil and the nutrients contained therein, from the field (Irmak and Rathje, 2008). Under-irrigation can result in a lack of water available for plants to meet the crop water demands. In both situations, crop productivity is negatively affected. Therefore, knowing spatial and temporal variability in soil water can help identify the need for irrigation and adoption of best irrigation management practices. Like soil water variability, soil nutrients including phosphorus (P) and nitrogen (N), also vary within the fields, and this affects the crop productivity during the growing season (Kumar et al., 2021a). The excess application of water and nutrients in agricultural fields leads to contamination of surface waters by runoff, or groundwater by leaching (Hanrahan et al., 2019). Precision agriculture aims to improve the crop productivity and optimize the agricultural system by adopting best irrigation and nutrient management practices to achieve the increasing food and water demands. A uniform application of water and nutrients leads to excessive amounts in some areas and inadequate amounts in others due to within-field variability (Chen et al., 2020). Therefore, it is very important to understand within-field variation at different soil depths and different times during a growing season. This can help with enhancing site-specific recommendations in farming practices and environmental protection, improving yield management, delineating management zones, and contributing to the refinement of existing decision support tools.

Soil moisture variability causes variability in irrigation water demands in the field. The future forecast of precipitation data showed the 14% increment in the annual average of precipitation by 2059, which would alter the time, erosivity characteristics, and distribution of the precipitation events (Takhellambam et al., 2021, 2022). Depending on climate conditions, irrigation water demands vary greatly from arid to humid climate regions (O'Shaughnessy et al., 2018; Rolle et al., 2021). In humid climate regions, irrigation is needed due to non-uniform rainfall distribution (Sangha et al., 2020), distribution of precipitation over the growing season (Filho et al., 2020), and soil moisture variation within a crop field during a growing season (Kumar et al., 2020, 2021b). Uniform irrigation does not account for within-field variability in soil moisture; therefore, site-specific irrigation can be a solution to address soil moisture variability within a field. To adopt site-specific irrigation, such as variable-rate irrigation (VRI), a field can be delineated in different management zones (Filho et al., 2020). Applying zone-specific irrigation can help increase in water use efficiency, reduce crop water stress, and increase crop productivity. Sensor-based irrigation has received much attention in the past decade since it provides real-time soil moisture status by monitoring h or θ during the growing season (Irmak, 2012). In sensor-based irrigations, knowledge about soil hydraulic properties (SHPs) is critical for scheduling irrigation, root water uptake, and determining the irrigation threshold, which is defines as a point of h to start irrigation (Lena et al., 2022). A single rate of irrigation throughout a field can result in over-irrigation in some areas and under-irrigation in others. Therefore, determining a correct irrigation amount is critical in irrigation scheduling. Since the determination of irrigation amount is decided with field capacity (FC) as an upper limit on the soil moisture content, it is difficult to measure FC within the field conditions. Therefore, estimation of accurate FC is important to determine effective irrigation thresholds and amounts.

1.2 Dissertation Objectives

The overarching goal of this dissertation is to help improve the precision agricultural system by developing a better understanding of the site-specific need and refinements in irrigation and nutrient management. This dissertation includes these specific objectives:

Chapter	Objectives
2	Characterize the Field-Scale Spatial and Temporal Soil Water Variability in Irrigated Croplands (*published in Transactions of ASABE*)
3	Understand Within-Field Variability in Soil Nutrients for Site-Specific Agricultural Management in an Irrigated Cornfield (*published in Journal of ASABE*)
4	Scheduling Site-Specific Irrigation Using One-Layer Zone-Specific Soil Hydraulic Properties and Inverse Modeling
5	Optimizing Zone-Specific Field Capacity and Irrigation Thresholds Using A Numerical Modeling Approach

1.3 Dissertation Organization

Chapter 1 discussed the background and problem statement of the dissertation. It covered important issues in site-specific precision agricultural management for irrigation and nutrient management.

Chapter 6 presents spatial and temporal variability in soil moisture in the uniformly irrigated corn (*Zea mays* L.) and cotton (*Gossypium hirsutum* L.) fields during a growing season. This chapter also discusses different hydrological and meteorological factors affecting the spatial and temporal variability in soil moisture. Finally, this chapter optimizes the number of samples required to determine average soil

moisture content to represent the field. In this chapter, we will use “soil water” instead of soil water content or soil moisture content as recommended by the Transactions of ASABE.

Chapter 6 comprises the within-field variability of soil nutrients during a growing season in an irrigated cornfield. This chapter discusses variability in soil phosphorus and nitrogen within the field and the impact on crop growth. The spatial and temporal variability in soil nutrients causes spatial variability in crop yield.

Chapter 4 includes the site-specific irrigation management utilizing the soil hydraulic properties (SHPs) with numerical modeling. This chapter discusses the importance of optimizing site-specific SHPs to schedule the irrigation and avoid discrepancies between raw or observed SHPs (lab) and soil water dynamic measured within the field.

Chapter 5 includes the determination of site-specific field capacity using the optimized SHPs with numerical modeling for site-specific irrigation management. This chapter discusses the importance of accurate FC determination in determining the correct irrigation thresholds and amounts needed for scheduling site-specific irrigation.

Chapter 6 provides the overall summary and major findings of this dissertation. This chapter also discusses the in-field implications of the research and future recommendations to improve site-specific irrigation management.

1.4 References

Chen, S., Wang, S., Shukla, M.K., Wu, D., Guo, X., Li, D., Du, T., 2020. Delineation of management zones and optimization of irrigation scheduling to improve irrigation water productivity and revenue in a farmland of Northwest China. Precis. Agric. 21, 655–677. https://doi.org/10.1007/s11119-019-09688-0

FAO, 2012. AQUASTAT Online Database. Available at:. Food and Agriculture Organization of the United Nations (FAO). http://www.fao.org/ag/agl/aglw/

Filippucci, P., Tarpanelli, A., Massari, C., Serafini, A., Strati, V., Alberi, M., Raptis, K.G.C., Mantovani, F., Brocca, L., 2020. Soil moisture as a potential variable for tracking and quantifying irrigation: A case study with proximal gamma-ray spectroscopy data. Adv. Water Resour. 136, 103502. https://doi.org/10.1016/j.advwatres.2019.103502

Filho, J.F.L.C. Da, Ortiz, B. V, Damianidis, D., Balkcom, K.S., Dougherty, M., Knappenberger, T., Franco, J., Cunha, D., Filho, L., 2020. Irrigation Scheduling to Promote Corn Productivity in Central Alabama. J. Agric. Sci. 12. https://doi.org/10.5539/jas.v12n9p34Gao, L., Peng, X., Biswas, A., 2020. Temporal instability of soil moisture at a hillslope scale under subtropical hydroclimatic conditions. CATENA 187, 104362. https://doi.org/10.1016/j.catena.2019.104362

Hanrahan, B.R., King, K.W., Williams, M.R., Duncan, E.W., Pease, L.A., LaBarge, G.A., 2019. Nutrient balances influence hydrologic losses of nitrogen and phosphorus across agricultural fields in northwestern Ohio. Nutr. Cycl. Agroecosystems 113, 231–245. https://doi.org/10.1007/s10705-019-09981-4

Himanshu, S.K., Fan, Y., Ale, S., Bordovsky, J., 2021. Simulated efficient growth-stage-based deficit irrigation strategies for maximizing cotton yield, crop water productivity and net returns. Agric. Water Manag. 250, 106840. https://doi.org/10.1016/j.agwat.2021.106840

Irmak, S., Burgert, M.J., Yang, H.S., Cassman, K.G., Walters, D.T., Rathje, W.R., Payero, J.O., Grassini, P., Kuzila, M.S., Brunkhorst, K.J., Eisenhauer, D.E., Kranz, W.L., VanDeWalle, B., Rees, J M, Zoubek, G.L., Shapiro, C A, Teichmeier, G J, Rees, Jennifer M, Shapiro, Charles A, Teichmeier, Gregory J, 2012. Large-Scale On-Farm Implementation of Soil Moisture-Based Irrigation Management Strategies for Increasing Maize Water Productivity. Trans. ASABE 55, 881–894. https://doi.org/10.13031/2013.41521

Irmak, S., Rathje, W.R., 2008. Plant Growth and Yield as Affected by Wet Soil Conditions Due to Flooding or Over-Irrigation. Publ. Univ. Nebraska-Lincoln Extension, Lincoln.

Kumar, H., Srivastava, P., Lamba, J., Ortiz, B. V., Way, T.R., Sangha, L., Takhellambam, B.S., Morata, G., 2021a. Phosphorus variability in the irrigated cropland during a growing season. Am. Soc. Agric. Biol. Eng. Annu. Int. Meet. ASABE 2021 4, 1-. https://doi.org/10.13031/AIM.202100886

Kumar, H., Srivastava, P., Ortiz, B. V., Morata, G., Takhellambam, B.S., Lamba, J., Bondesan, L., 2021b. Field-Scale Spatial and Temporal Soil Water Variability in Irrigated Croplands. Trans.

ASABE 64, 1277–1294. https://doi.org/10.13031/TRANS.14335

Kumar, H., Srivastava, P., Ortiz, B.V., Bijoychandra, T.S., Morata, G., Bondesan, L. and Lamba, J., 2020. Spatiotemporal Soil Moisture Variability in Corn and Cotton Fields with Uniform Irrigation During the Growing Season. In: AGU Fall Meeting Abstracts (Vol. 2020, pp. H209-05).

Kummu, M., Guillaume, J.H.A., de Moel, H., Eisner, S., Flörke, M., Porkka, M., Siebert, S., Veldkamp, T.I.E., Ward, P.J., 2016. The world's road to water scarcity: shortage and stress in the 20th century and pathways towards sustainability. Sci. Rep. 6, 38495. https://doi.org/10.1038/srep38495

Lena, B.P., Bondesan, L., Pinheiro, E.A.R., Ortiz, B., Morata, G., Kumar, H., 2022. Determination of irrigation scheduling thresholds based on HYDRUS-1D simulations of field capacity for multilayered agronomic soils in Alabama, USA. Agric. Water Manag. 259, 107234. https://doi.org/10.1016/J.AGWAT.2021.107234

O'Shaughnessy, S.A., Andrade, M.A., Stone, K.C., Vories, E.D., Sui, R., Evett, S.R., 2018. Adapting a VRI Irrigation Scheduling System for Different Climates. In: Irrigation Association Show and Education Conference Technical Session Proceedings on Irrigation Association, Fairfax, VA

Radcliffe, D.E., Simunek, J., 2018. *Soil Physics with HYDRUS : Modeling and Applications*. Soil Phys. with HYDRUS. https://doi.org/10.1201/9781315275666

Rolle, M., Tamea, S., Claps, P., 2021. ERA5-based global assessment of irrigation requirement and validation. PLoS One 16. https://doi.org/10.1371/JOURNAL.PONE.0250979

Sangha, L., Lamba, J., Kumar, H., Srivastava, P., Dougherty, M., Prasad, R., 2020. An innovative approach to rainwater harvesting for irrigation based on El Niño Southern Oscillation forecasts. J. Soil Water Conserv. jswc.2020.00085. https://doi.org/10.2489/JSWC.2020.00085

Takhellambam, B.S., Srivastava, P., Lamba, J., McGehee, R.P., and Kumar, H., 2021. Potential changes in rainfall erosivity under climate change in southeastern United States. In: AGU Fall Meeting 2021.

Takhellambam, B.S., Srivastava, P., Lamba, J., Mcgehee, R.P., Kumar, H., Tian, D., 2022. Temporal disaggregation of hourly precipitation under changing climate over the Southeast United States. Sci. Data 2022 91 9, 1–14. https://doi.org/10.1038/s41597-022-01304-7

Chapter 2

Characterize the Field-Scale Spatial and Temporal Soil Water Variability in Irrigated Croplands

(*Transactions of ASABE*)

2.1 Abstract

This study investigated the spatiotemporal variability and temporal stability of soil water at various depths in two croplands sown in corn and cotton during the 2018 growing season in the Tennessee Valley Region (TVR) of northern Alabama. We use soil water instead of soil water content (vol/vol) in this paper. Classical statistics and relative difference approaches were used to analyze soil water data in this study. In the cornfield, the 30-60 cm depth showed the greatest variability, while the cotton field showed the greatest variability at 0-15 cm depth. An exponentially decreasing trend was noticed between mean soil water and coefficient of variation for all depths in the cotton field and at 30-60 cm depth in the cornfield. However, convex upward, exponentially decreasing, or no trends were found between mean soil water and standard deviation at different depths in both fields. The temporal stability analysis showed one representative soil moisture sensor (S8 in corn and S1 in cotton) for the entire soil profile in both fields. Different statistical tests, i.e., Spearman's correlation (r_s), Nash-Sutcliffe efficiency (NSE), coefficient of determination (R^2), etc., were used to reduce uncertainty or increase confidence in the performance of representative sensors. Among various field attributes, topography in corn and soil properties in cotton were determined as significant factors responsible for soil water variability. Crop evapotranspiration (ET_c) showed significant negative weak and moderate correlations with soil water in the corn and cotton fields, respectively. However, the mean air temperature showed a significant positive correlation with soil water in the cornfield and a significant negative

correlation in the cotton field. Solar radiation had a significant negative correlation with soil water in the cotton field and a non-significant correlation in the cornfield. Accumulated growing degree days (accGDD) showed a significant negative correlation with soil water in the cornfield and a positive correlation in the cotton field. This study gives insights into soil water variability, provides useful information about temporal stability, and identifies significant factors for precision uniform irrigation scheduling.

2.2 Introduction

Understanding spatial and temporal soil water dynamics in croplands is of utmost importance for irrigation scheduling and for understanding surface and subsurface transport of water, nutrients, and contaminants (Filippucci et al., 2020; Gao et al., 2020; Su et al., 2018). The spatial and temporal variations in soil water have been studied for decades around the globe at plot to watershed scales in different natural landscapes (Brocca et al., 2009; Hao et al., 2020; Shen et al., 2016). In many hydrological studies, the temporal stability concept has been used extensively to calibrate hydrological models, for flood forecasting, and for validating remote sensing data in natural landscapes (Brocca et al., 2018; Hao et al., 2020; Yetbarek and Ojha, 2020; Zaussinger et al., 2019). Knowledge of soil water variability can be helpful in erosion control and irrigation water management in crop fields during a growing season (Yetbarek and Ojha, 2020). However, plot-scale studies always have a limitation of uncertainty with upscaling to field scale (Kornelsen and Coulibaly, 2013), and studies at large scale (watershed) and small scale (plot) are of limited use to farmers. Hupet and Vanclooster (2002) suggested a need for more research at the field scale in different crop fields.

Researchers have investigated the relationship between average soil water (we use soil water instead of soil water content in vol/vol throughout chapter 1) and standard deviations to understand

spatial variability across time at various depths. However, relatively few studies are available for deeper soil profiles, as compared to those that have studied surface soil water, especially in croplands (Bauer-Marschallinger et al., 2019; Gao and Shao, 2012; She et al., 2012, 2015). There is no perfect way to explain soil water variability, and studies have shown positive, negative, and neutral correlations between average soil water and standard deviations in natural agricultural vegetation (Guber et al., 2008; Shen et al., 2016; Vereecken et al., 2014). Due to the lack of accuracy and precision in satellite data at the field scale, *in situ* soil water measurements and irrigation observations are necessary to understand soil water variability within the soil profile of croplands during the growing season (Filippucci et al., 2020). Rainfed agricultural practices are common in southeastern U.S. states such as Alabama and Tennessee. However, irrigation adoption is increasing, especially in Alabama, where irrigation has increased by 25% from 2012 to 2017 (NASS, 2017). Farmers are adopting irrigation to increase crop yields, avoid water stress, and increase water use efficiency during the growing season (FAO, 2018). Climatic variations directly influence the spatial and temporal distribution of precipitation, which challenges farmers to schedule precise and accurate irrigation. A better understanding of soil water variability in crop fields is needed to schedule precise irrigation.

Although irrigation adoption is increasing in the U.S., the main challenges to irrigation adoption are financial (NASS, 2013). Therefore, farmers schedule irrigation based on the feel of the soil and by looking at the crop at different times during the growing season (NASS, 2013, and according to a farmer survey in the TVR). Irrigation is an essential part of the hydrological cycle and food production. It accounts for 70% or more of freshwater withdrawals globally (Filippucci et al., 2020). Water withdrawals for irrigation are a concern for water availability in areas where water resources are limited. Improvements in irrigation efficiency would not reduce costs enough

to cover the soil moisture sensor installation costs and reduce uncertainty about the future availability of water (NASS, 2013), which motivated us to identify representative locations of soil water variability to install sensors in croplands.

Accurate estimation of spatial mean soil water (defined in "Methods for soil water variability analysis" section) is essential in crop fields because irrigation scheduling is often based on soil water measured at a single point or just a few points (Hao et al., 2020). Therefore, it is necessary to study soil water variability in crop fields to help farmers identify water stress, water excess, and temporally stable locations to estimate irrigation amounts and schedule precision irrigation during the growing season (Hao et al., 2020; Yetbarek and Ojha, 2020). Soil water products, such as ASCAT (Advanced Scatterometer, instruments carried on MetOp satellites, to determine information about the wind, for weather forecasting and climate research) and SMAP (Soil Moisture Active Passive, an orbiting observatory that measures the amount of water in the surface soil on Earth), have been used to produce soil water data, but they cannot be used in crop fields due to low resolution (Palombo et al., 2019). Therefore, it is important to determine soil water variability in crop fields to help farmers improve their water use efficiency and understand the significant factors for irrigation scheduling during the growing season.

Additionally, it is important to collect *in situ* soil water measurements in deeper layers to assist in hydrological modeling and validation of climate models, especially in croplands (Brocca et al., 2010; Heathman et al., 2009; Loew et al., 2013). Although *in situ* soil water measurements are expensive, time-consuming, and laborious, there is a great need in scientific and farming communities to understand the depth-dependent spatial and temporal variability of soil water in croplands, especially during growing seasons (Majdar et al., 2018). Certain locations might be temporally stable for soil water and can be used as representative locations (Vachaud et al., 1985)

for irrigation scheduling decisions. Many studies have been carried out to understand temporal stability in soil water using *in situ* measurements, remote sensing, or a combination of both methods at various depths and scales to find representative locations for hydrologic modeling purposes (Dari et al., 2019; She et al., 2015; Shen et al., 2016). According to temporal stability investigations, if a location is wet at one time, it will remain wet another time if the spatial pattern of temporal variation does not vary with time (Vachaud et al., 1985). However, a significant challenge for irrigation scheduling is the spatial variation in soil water and the difficulty in obtaining representative locations for prescribing irrigation. Efficient site-specific management of soil water with adequate irrigation requires temporal stability analysis of soil water (Yetbarek and Ojha, 2020). Irrigation scheduling using a single, temporally stable sensor that represents the field soil water can be useful and cost-effective to prescribe uniform irrigation.

Various crucial factors, including terrain attributes, soil properties, vegetation cover, and meteorological parameters, affect soil water variability (Beven and Kirkby, 1979; Mei et al., 2018; Takagi and Lin, 2012). Topographic factors have been studied more extensively than vegetation and meteorological factors. Limited research has been done at the field scale under different types of vegetation, especially in croplands (Fry and Guber, 2020; Guber et al., 2008; Rossato et al., 2017; Yetbarek and Ojha, 2020), due to the extensive work required in crop fields during a growing season. Different soil textures have shown varying degrees of temporal stability and variability of soil water. Temporal stability in soil water is defined as average soil water within a field, plot, or watershed that can be represented by a certain location. According to Mohanty and Skaggs (2001), silt loam soil has less temporal stability than sandy loam, and Choi and Jacobs (2011) found that temporal stability decreased with increasing sand content. However, it is still not clear what factors dominate soil water variability in crop fields, especially during a growing season.

The findings of this study can be useful in field-scale hydrological modeling (e.g., Soil Water Assessment Tool (SWAT) and Agricultural Policy/Environmental eXtender (APEX)), for validating remote sensing data, and for calibrating subsurface hydrology models (HYDRUS, a model to simulate soil water and solute dynamics in unsaturated soil media (PC-Progress, 2022)) in different types of vegetation (Filippucci et al., 2020; Parinussa et al., 2014; Zaussinger et al., 2019). However, many questions still need to be answered, such as: How are spatial and temporal variability affected by uniform irrigation in different croplands? What are the main factors involved in the spatial variability and temporal stability of soil water in croplands during the growing season under uniform irrigation? How can farmers adopt water use efficient uniform irrigation in crop fields during the growing season?

Different approaches, such as geostatistical analysis, have been used in many studies to understand soil water variability (Gia Pham et al., 2019; Pandey and Pandey, 2010; Vasu et al., 2017). However, a simple approach of exploratory data analysis can be useful to establish the relationship between spatial mean soil water and its variability. In this study, two crop fields (corn (*Zea mays* L.) and cotton (*Gossypium hirsutum* L.)) were studied for soil water variability using *in situ* soil water measurements to a soil depth of 60 cm under uniform irrigation management. The objectives of this study were to (1) determine the spatiotemporal variability of soil water in both croplands at different depths, (2) identify representative locations of soil water measurement for scheduling irrigation in the croplands during the growing season, and (3) identify the factors affecting the spatiotemporal variability of soil water in the croplands during the growing season.

2.3 Materials and Methods

2.3.1 Study Site Description

The study areas, which belonged to farmers, were located in the Tennessee Valley Region (TVR) of northern Alabama (fig. 2.1). The cornfield was approximately 120 ha (a 60 ha area in the middle of the field was used in this study with a slope variation of 0% to 10%), and the cotton field was 12 ha with a slope variation of 0% to 3%. The cornfield (34° 43′ 7.15″ N, 87° 23′ 9.36″ W), with minimum and maximum elevations of 168 and 178 m, respectively, above mean sea level, was located in Lawrence County, Alabama, and the cotton field (34° 43′ 18.10″ N, 87° 1′ 16.14″ W), with a minimum and maximum elevations of 181 and 185 m, respectively, above mean sea level, was located in Limestone County, Alabama. The average annual precipitation in the region (1895 to 2019) is about 1400 mm (Sangha et al., 2020a; https://sercc.com/climateinfo/monthly_seasonal). The average annual precipitation during the growing season (April to October) is 759 mm. The average annual temperature (1895 to 2019) is 17.3 °C, with a maximum temperature of 29.1 °C in August and a minimum temperature of 13.8 °C in December. The major crops grown in the TVR are corn, cotton, soybean (*Glycine max* (L.) Merr.), and winter wheat (*Triticum aestivum* L.) (Sangha et al., 2020b).

The cornfield was seeded on 10 April 2018 and harvested on 3 September 2018. The cotton field was seeded on 2 May 2018 and harvested on 24 October 2018. Both fields were under no-till management. The cotton field was planted with a cover crop (rye in previous fall) before the cotton; however, no cover crop was used in the cornfield. According to SSURGO (2020), the dominant soil types in the cornfield were Abernathy-Emory silt loams (38%), Decatur silt loam (29%), Decatur silty clay loam (20%), and Decatur silty clay (8%). In the cotton field, the dominant soil types were Guthrie silt loam (25%), Decatur silt loam (24%), Lawrence silt loam (21%), Sango

silt loam (14%), and Dickson silt loam (11%). Soil samples were collected in both fields to determine soil texture using the hydrometer method (Bouyoucos, 1962). In the cornfield, the soil texture was classified as clay loam for the upper two soil layers (0-15 cm and 15-30 cm) and clay for the deepest (30-60 cm) soil layer. Silty clay loam was the soil texture in the entire soil profile of the cotton field.

2.3.2 Field measurements

Both fields were instrumented with Watermark soil moisture sensors (Irrometer Co., Riverside, Cal.), combined into a wireless soil sensor probe, to measure soil matric potential (h) vertically at 0-15 cm, 15-30 cm, and 30-60 cm depths. Watermark sensors are electrical resistance devices that measure soil water matric potential. Watermark sensors with a similar array have been used in corn and cotton crops for irrigation scheduling at 60 cm depth in the southeastern U.S. (Lena et al., 2020; Liang et al., 2016; Vellidis et al., 2008). Therefore, we adopted a similar array in this study. In typical cornfields, greater than 50% of total roots have been found within the top 60 cm depth (Anderson, 1987; Fan et al., 2016), and the maximum root length density in a typical cotton field has been found in the top 60 cm of the soil profile (Aggarwal et al., 2017). The sensors were controlled remotely to collect data and to monitor their performance.

Sensor locations were selected based on the farmers' experience, visual conditions in the fields, soil texture, topography, and ten years of historical yield data, to capture soil water variability in crop fields and to find temporal stability in soil water measurements to determine an irrigation strategy during the growing season. Initially, 28 and 23 sensors, respectively, were installed in the corn and cotton fields. However, due to errors in measurement, bursting of sensors, and other problems, only 17 and 18 sensors, respectively, in the corn and cotton fields were considered in good condition for this study. Hourly soil water matric potential was measured from 16 May to 12

August 2018 in the cornfield and from 4 June to 18 October 2018 in the cotton field. These hourly measurements were converted to daily average data at each location for the respective depths (Kumar et al., 2020; Li et al., 2019).

The soil matric potential data were converted into soil water data using the van Genuchten model (van Genuchten, 1980). To use the van Genuchten model (eq. 1), soil water retention curves were developed for each depth (0-15 cm, 15-30 cm, and 30-60 cm) for both fields:

$$\theta(h) = \theta_r + \frac{\theta_s - \theta_r}{[1 + (\alpha|h|)^n]^{1-1/n}} \quad (2.1)$$

where $\theta(h)$ is soil water (cm^3cm^{-3}), i.e., volumetric soil water content, h is soil matric potential (cm), θ_r is residual soil water content (cm^3cm^{-3}), θ_s is saturated soil water content (cm^3cm^{-3}), α and n are shape parameters estimated from the soil water retention curve.

Undisturbed soil samples were collected at each depth to develop soil water retention curves using a hydraulic property analyzer (HYPROP 2, Meter Group, Pullman, Wash.). The intact soil cores were saturated for at least 24 h before running the experiment. Disturbed soil samples were collected to measure permanent wilting point using a dew point hygrometer (WP4C PotentiaMeter, Meter Group) (Lena et al., 2020).

The fields were equipped with remotely controlled center-pivot irrigation systems. The cornfield was equipped with a 625 m Reinke center-pivot irrigation system (Reinke Manufacturing Co., Inc., Deshler, Neb.), and the cotton field was equipped with a 195 m Valley center-pivot irrigation system (Valmont Irrigation, Valley, Neb.). Both irrigation systems had mid-elevation spray application (MESA) sprinklers equipped with pressure regulators. The center-pivots were operated by the farmers to schedule irrigation during the growing season. Although the sensors and center-

pivots were controlled remotely, the research team often visited the fields to verify the irrigation operations and to repair the sensors.

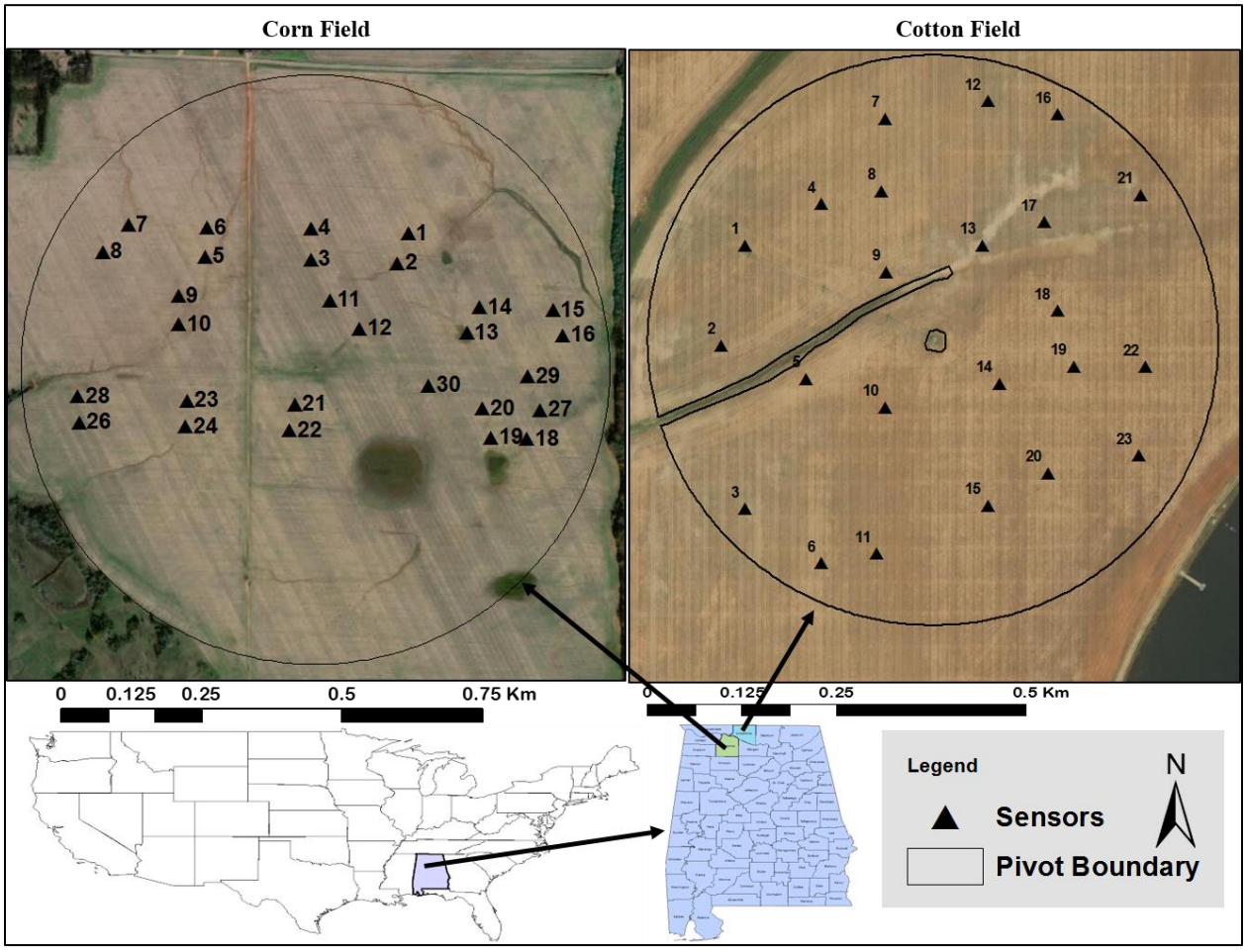

Figure 2.1 Study sites (corn and cotton fields) showing Watermark sensor locations and center-pivot irrigation boundaries during the growing season.

2.3.3 Weather Data

Due to spatial and temporal variation in precipitation (Kumar, 2016; Ridolfi et al., 2020), an automatic weather station (Vantage Pro2 Plus, Davis Instruments, Hayward, Cal.) was installed near each field to record meteorological parameters. Precipitation, temperature, and solar radiation were recorded at 15 min intervals and converted to a daily time step. Evapotranspiration (ET_o) (FAO-56 Penman-Monteith equation, Allen et al., 1998) was measured at hourly intervals and

converted to a daily time step. The annual precipitation recorded in the cornfield in 2018 was 1622 mm, with a maximum monthly precipitation of 285 mm in February and a minimum of 22 mm in July. The total precipitation recorded in the cornfield was 582 mm during the 2018 growing season (April to October). The annual precipitation recorded in the cotton field in 2018 was 1679 mm, with a maximum monthly precipitation of 249 mm in February and a minimum of 48 mm in January. The total precipitation recorded in the cotton field was 617 mm during the 2018 growing season. According to historical records (2006 to 2018) of average precipitation, the 2018 growing season was considered a wet season.

Crop evapotranspiration (ET_c) was determined using the FAO-56 method for both fields (eq. 2) (Allen et al. 1998):

$$ET_c = K_c \times ET_o \tag{2.2}$$

The growing degree days (GDD)-determined growth stages and associated crop coefficients (K_c) estimated using a smart irrigation application for cotton were used to calculate ET_c (Vellidis et al., 2016). The growth stages were assessed for corn during field visits to determine the associated K_c used to calculate ET_c (Irmak, 2017). The GDD was estimated using temperature measurements (Anandhi, 2016). Figure 2.2 shows precipitation and irrigation with ET_c data in both fields. Figure 2.3 shows cumulative water input (sum of precipitation and irrigation) and loss (ET_c) in both fields during the growing season. The total amount of irrigation applied was 66.5 mm (five irrigations) in corn and 30.5 mm (two irrigations) in cotton during the growing season.

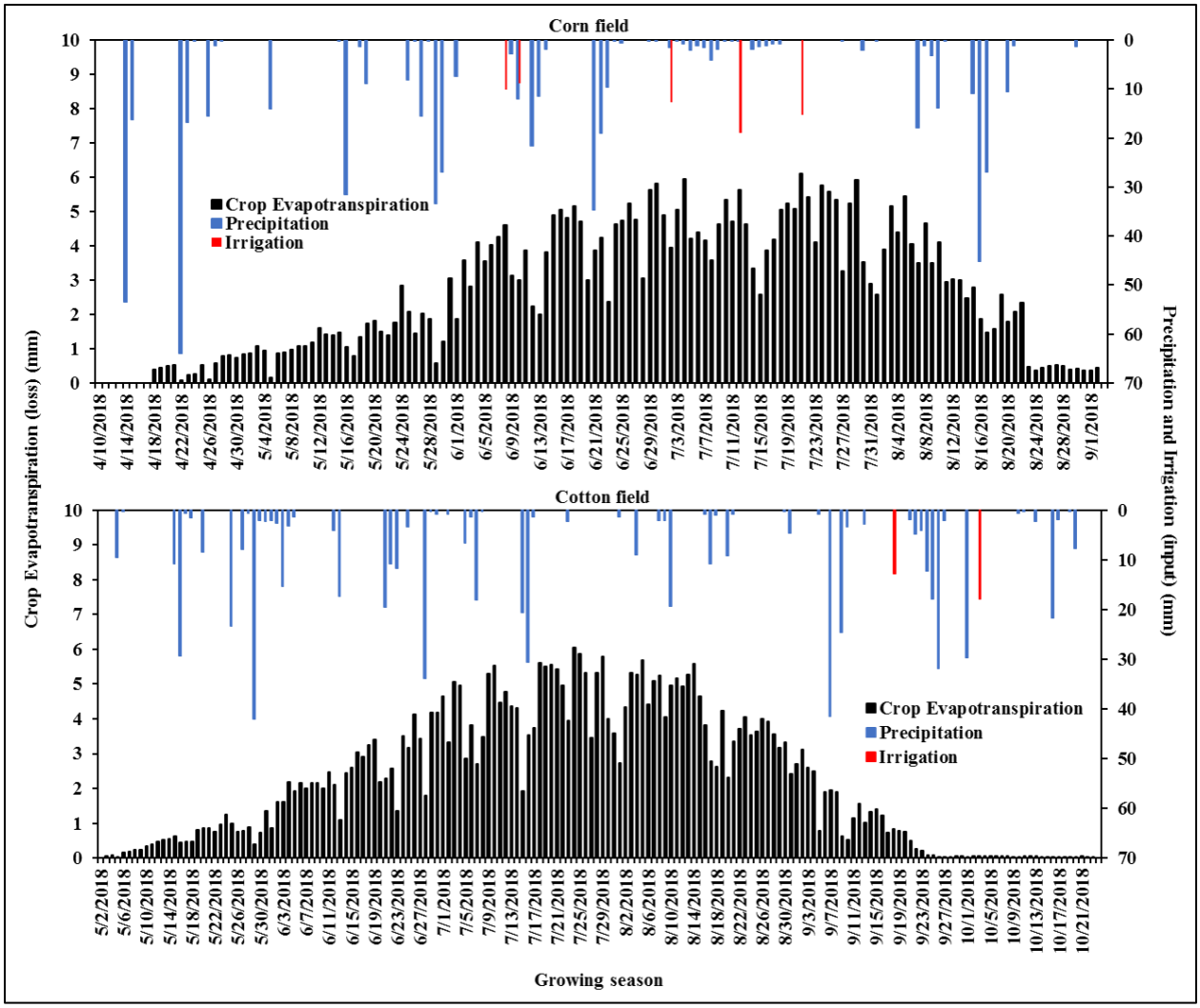

Figure 2.2 Water input (precipitation and irrigation) and loss (crop evapotranspiration) in corn and cotton fields during the growing season.

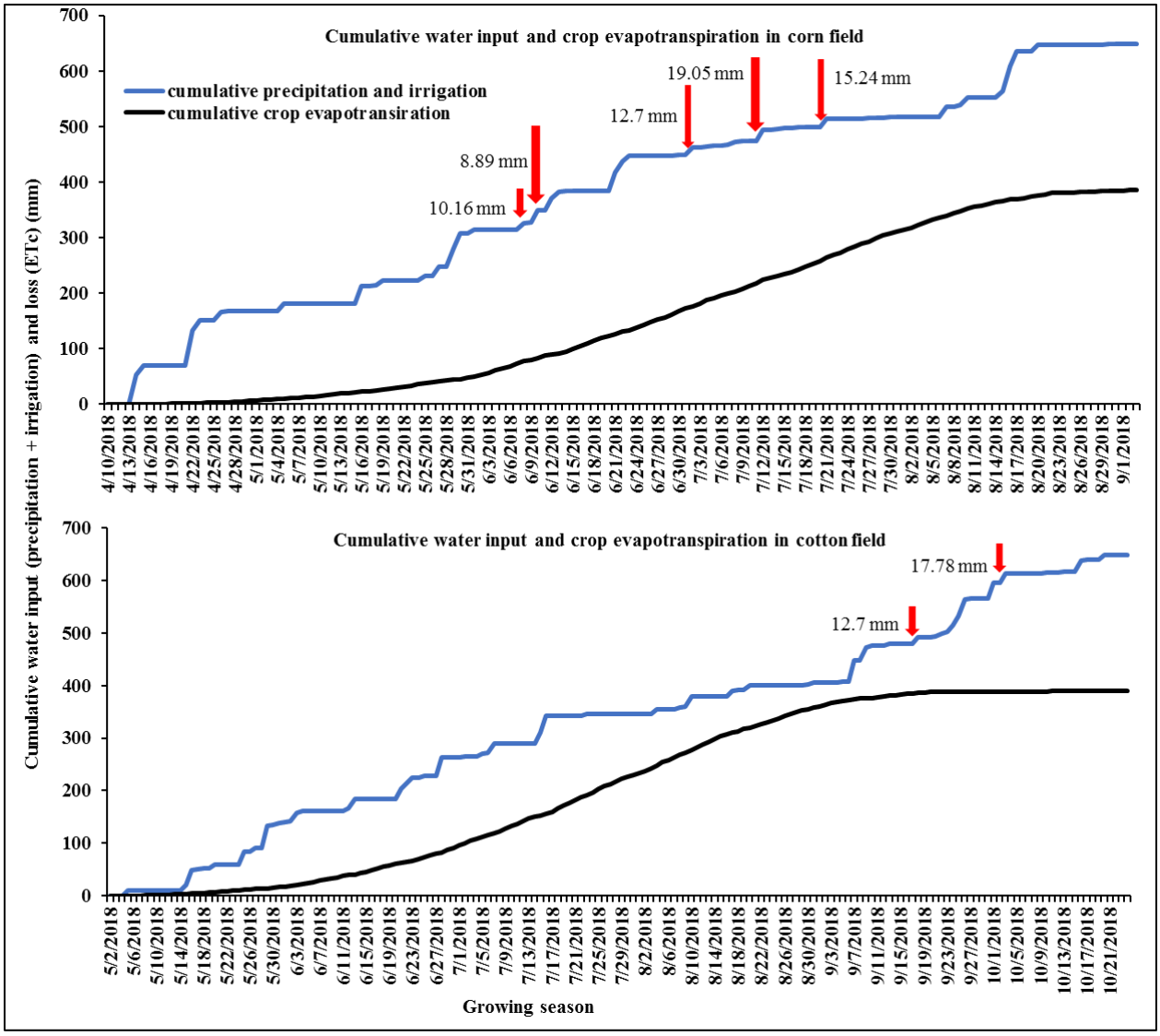

Figure 2.3 Cumulative water input (precipitation and irrigation) and cumulative crop evapotranspiration in corn and cotton fields during the growing season. Irrigations are indicated by the red arrows.

2.3.4 Methods for soil water variability analysis

2.3.4.1 Statistical Analysis

The soil water (θ) measured at each location i ($i = 1,,2, \ldots M$) and on each day j ($j = 1, 2, \ldots N$) was was used to determine various statistics for this study, where $M = 17$ and $N = 26$ for cornfield, and $M = 18$ and $N = 56$ for the cotton field. Various statistics were adopted to

minimize the uncertainty and increase confidence in the results. The spatial mean ($\bar{\theta}_j$) for each day is given by:

$$\bar{\theta}_j = \frac{\sum_{i=1}^{M} \theta_{ij}}{M} \tag{2.3}$$

The temporal mean ($\bar{\theta}_i$) for each location is given by:

$$\bar{\theta}_i = \frac{\sum_{j=1}^{N} \theta_{ij}}{N} \tag{2.4}$$

The spatial standard deviation ($\sigma(\theta_j)$) and coefficient of variation (CV(θ_j)) of soil water for each sampling day are given by:

$$\sigma(\theta_j) = \sqrt{\frac{1}{M-1}\sum_{i=1}^{M}(\theta_{ij} - \bar{\theta}_j)^2} \tag{2.5}$$

$$CV(\theta_j) = \frac{\sigma(\theta_j)}{\bar{\theta}_j} \tag{2.6}$$

In the same way, the temporal standard deviation ($\sigma(\theta_i)$) and coefficient of variation (CV(θ_i)) can be found for each location.

2.3.4.2 Temporal Stability Statistics

Vachaud et al. (1985) introduced a relative difference statistic ($\delta(\theta_{ij})$) to understand the temporal stability of measurement locations. This approach identifies representative locations for a study area based on observed soil water values. All computations are done separately for individual depths.

The relative difference $\delta(\theta_{ij})$ for each location i and each day j can be defined as:

$$\delta(\theta_{ij}) = \frac{(\theta_{ij} - \bar{\theta}_j)}{\bar{\theta}_j} \tag{2.7}$$

Based on the relative difference, the mean relative difference ($\bar{\delta}_i$) and standard deviation of relative difference ($\sigma(\bar{\delta}_i)$) for each location i can be given by:

$$\bar{\delta}_i = \frac{\sum_{j=1}^{N} \delta(\theta_{ij})}{N} \tag{2.8}$$

$$\sigma(\delta_i) = \sqrt{\frac{1}{N-1}\sum_{j=1}^{N}\left(\delta_{ij} - \bar{\delta}_i\right)^2} \tag{2.9}$$

The mean relative difference ($\bar{\delta}_i$) quantifies the departure of soil water at a specific location from the field mean soil water and distinguishes whether the location is drier or wetter than the field mean during a growing period. A representative location shows a mean relative difference of zero and a small standard deviation ($\sigma(\delta_i)$). Values of ($\bar{\delta}_i$) greater or less than zero indicate over- or under-estimation of field mean soil water and indicate wetter and drier conditions, respectively (Jacobs et al., 2004). A location with a small value of $\left|\bar{\delta}_i\right|$ and $\sigma(\delta_i)$ is considered representative, or temporally stable. The mean relative difference is also defined as an index of the temporal variability of soil water.

A single statistic introduced by Jacobs et al. (2004), called the index of time stability (ITS), was used to identify the best sampling location during a growing season. A low ITS value indicates a representative, or temporally stable, location for soil water in a field during the growing season. The ITS for each location is given by:

$$ITS_i = \sqrt{\left(\bar{\delta}_i^{\,2} + \sigma(\delta_i)^2\right)} \tag{2.10}$$

Spearman's rank correlation (r_s) has also been widely used to explain the temporal stability of soil water in croplands. Spearman's rank correlation was computed between the soil water at each location i and the spatial mean soil water on day j during the growing season:

$$r_{s,j} = 1 + \frac{6\sum_{j=1}^{N}\left(R(\theta_{ij}) - R(\bar{\theta}_j)\right)^2}{n(n^2-1)} \tag{2.11}$$

where $R(\theta_{ij})$ is the rank of soil water at location i varying in time j, and $R(\bar{\theta}_j)$ is the rank of mean spatial soil water during time j.

The index of agreement (IA) is a standardized measurement index that was developed by Willmott et al. (1985), also known as the Willmott index, to measure the degree of performance of any statistical analysis used here for temporal stability representation. It varies from 0 to 1, where 0 indicates no agreement, and 1 indicates perfect agreement with the data:

$$IA_i = 1 - \frac{\sum_{j=1}^{N}(\bar{\theta}_j - \theta_{ij})^2}{\sum_{j=1}^{N}\left(|\theta_{ij} - mean(\bar{\theta}_j)| + |\bar{\theta}_j - mean(\bar{\theta}_j)|\right)^2} \tag{2.12}$$

Additional criteria widely used in hydrologic simulations were also adopted to test the temporal stability of soil water and to test if the spatial mean soil water can be represented by one sensor. The goal was to see if these adopted statistics could also provide similar conclusions using coefficient of determination (R^2), root mean square error (RMSE), Kling-Gupta efficiency (KGE) (Gupta et al., 2009; Knoben et al., 2019), and Nash-Sutcliffe efficiency (NSE) (Nash and Sutcliffe, 1970):

$$NSE = 1 - \frac{\sum_{j=1}^{N}(\bar{\theta}_j - \theta_{ij})^2}{\sum_{j=1}^{N}\left(\bar{\theta}_j - mean(\bar{\theta}_j)\right)^2} \tag{2.13}$$

$$KGE = 1 - \sqrt{(r-1) + (\alpha-1) + (\beta-1)} \tag{2.14}$$

$$\alpha = \frac{\sigma_{\theta_i}}{\sigma_{\bar{\theta}_j}}, \alpha = \frac{\mu_{\theta_i}}{\mu_{\bar{\theta}_j}}$$

where r is the correlation coefficient between the temporally stable sensor and field mean soil water, α is the variability ratio between the standard deviation of each location (σ_{θ_i}) and the standard deviation of spatial mean soil water ($\sigma_{\bar{\theta}_j}$), and β is the ratio between average soil water at each location (μ_{θ_i}) and the average of spatial mean soil water ($\mu_{\bar{\theta}_j}$). The values of KGE and NSE range from -∞ to 1. A value close to 1 indicates a perfect association between the data.

Coefficient of determination, R^2, and RMSE, are common and widely used statistics in hydrology; therefore, the equations are not shown here. The statistics were evaluated between the soil water at each location *i* and the spatial mean soil water on day *j* in both crop fields during the growing season. This provided another method to verify the temporal stability of the sensor used to represent the field mean soil water in each field. The closer r_s, R^2, KGE, and NSE are to 1 and the closer RMSE is to zero, the greater the accuracy of the representative sensor for estimating field mean soil water.

The number of sensors required to estimate average soil water within a certain absolute error limit can be determined for the maximum soil water variability through implicit relationships developed by Wang et al. (2008):

$$NRS = t^2_{1-\alpha/2,NRS-1} \times \left(\frac{\sigma(\delta_j)^2}{AE^2}\right) \quad (2.15)$$

where $t^2_{1-\alpha/2,NRS-1}$ is value of t-distribution of α significance and AE is absolute error.

2.3.4.3 Factors Responsible for Soil Water Variability

Meteorological parameters were used in this study to find correlations with field mean soil water during the growing season. These meteorological parameters were recorded for both fields. Topographic and soil parameters, including elevation, slope, electrical conductivity (EC, measured with a V3100 meter, Veris Technologies, Salina, Kans.) at shallow (0-30 cm) and deep (0-90 cm) depths in the soil profile, and sand, silt, and clay percentages were also used to investigate correlations with mean soil water. The elevation data were collected using a John Deere StarFire 6000 system (Deere and Company, Moline, IL, USA) (a real-time kinematic GPS with horizontal) installed on the harvesters. The slopes of both fields were estimated using ArcGIS (ver. 10.3.1) (Esri, Redlands, Cal.). Spearman's rank correlation was used to find significant correlations between the parameters and mean soil water in both fields (Majdar et al., 2018) to evaluate the significant factors that need to be considered in irrigation scheduling.

2.4 Results and Discussion

2.4.1 Spatial Variability in Soil Water

Figure 2.4 shows the soil water in both fields at different depths at various locations during the growing season. The box and whisker plots show variations in soil water at each sensor location with maximum, minimum, median, and upper and lower quartiles. Soil water varied from location to location within each field, and sensor 30 (S30) indicated the minimum average soil water in the entire soil profile in the cornfield (fig. 2.4a to 2.4c). This variation in soil water from one location to another could be due to differences in soil properties, such as hydraulic conductivity (Heathman et al., 2012). However, due to precipitation and irrigation (Heathman et al., 2012; Shen et al., 2016), the deepest soil layer (30-60 cm) held greater mean soil water, followed by the 15-30 cm and 0-15 cm soil depths in the cornfield (fig. 4a to 4c and 5a). In the cotton field, sensor 3 (S3) indicated the minimum average soil water at the 0-15 cm and 30-60 cm depths (fig. 2.4d to 2.4f).

Sensor 18 (S18) indicated the maximum average soil water at the 0-15 cm and 15-30 cm depths (fig. 2.4d to 2.4f). The variation in soil water with location might be due to differences in soil properties and cover crops in the cotton field (Yetbarek and Ojha, 2020). The least variation in soil water (fig. 2.4b and 2.4e) was observed at the 15-30 cm depth in both fields.

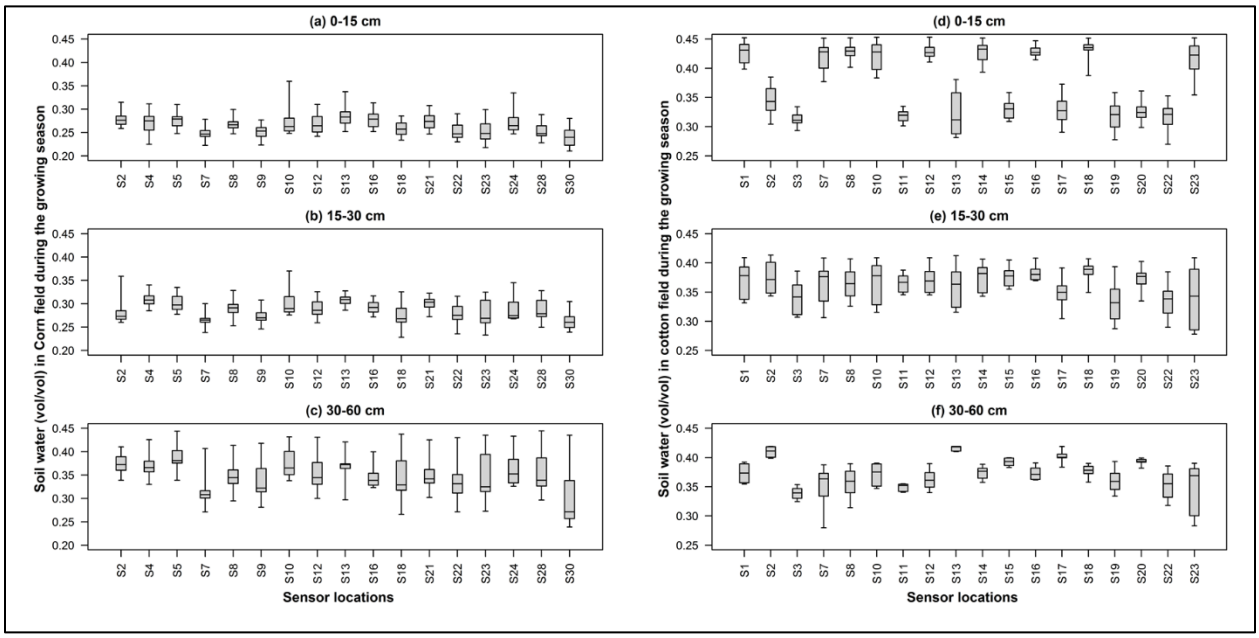

Figure 2.4 Box plots of soil water variability in the (a-c) cornfield and (d-f) cotton field during the 2018 growing season.

The variation in spatial mean soil water (fig. 2.5) at different depths could be linked to the changes in daily precipitation, irrigation, and (ET_c) in both fields during the growing season. The fluctuations in standard deviation (fig. 2.6) at different depths were due to variation in soil water caused by water input and losses. For example, in the cornfield on June 15, an increase in soil water (fig. 2.5a) at the 0-15 cm and 15-30 cm depths can be observed due to rainfall events (fig. 2.2a, 12 to 14 June), but a decrease occurred at the 30-60 cm depth. The change in standard deviation (fig. 2.6a) can be seen at the 30-60 cm depth, but not in the other two soil depths. Likewise, the effects of rainfall or irrigation on soil water and standard deviation were noticed in

both fields during the growing season. It is somewhat complicated to understand the trends in soil water and standard deviation separately (fig. 2.5 and 2.6). Therefore, we developed relationships between soil water and standard deviation in soil water at separate depths (fig. 2.7).

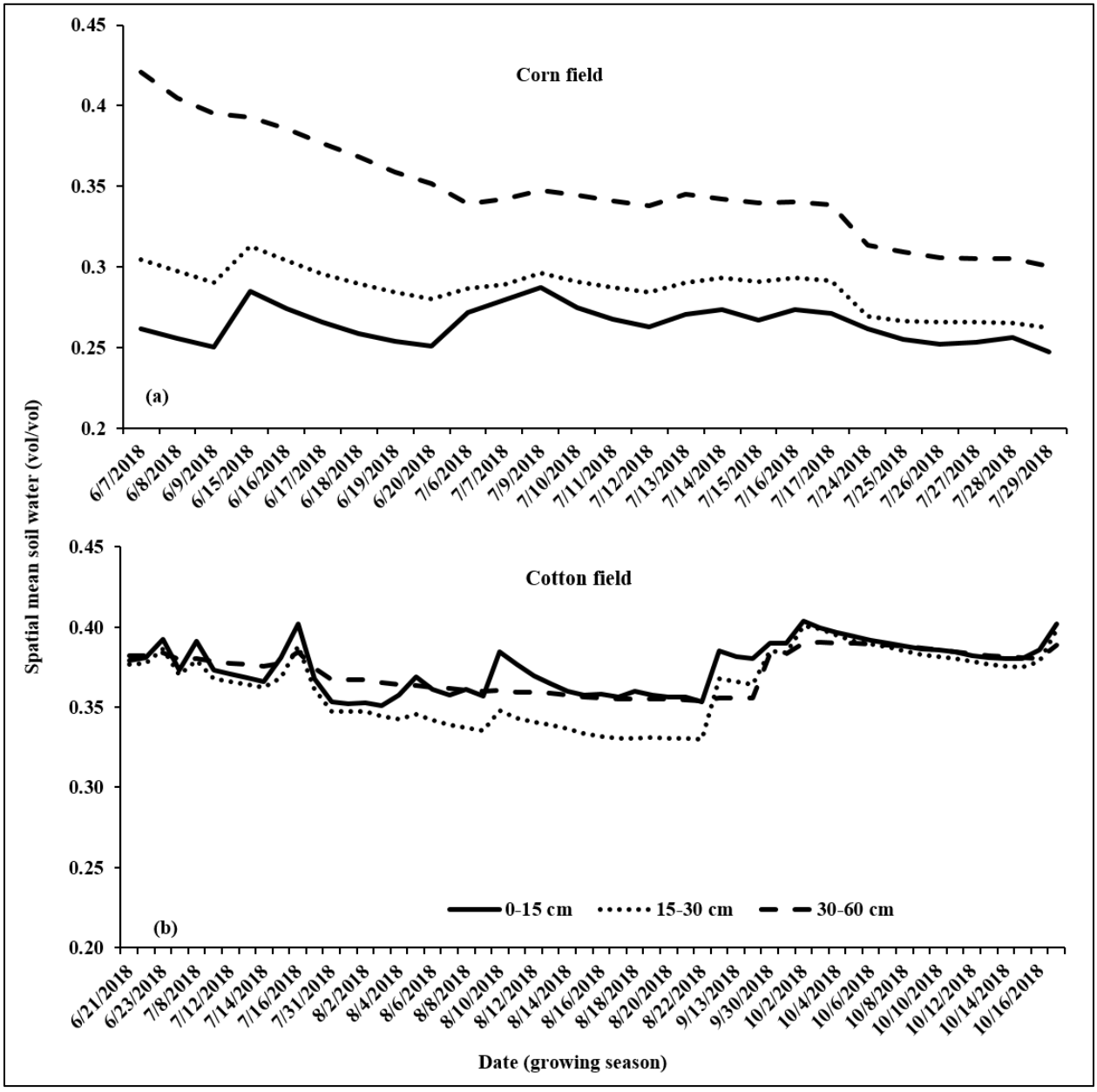

Figure 2.5 Spatial mean soil water distribution in the (a) cornfield and (b) cotton field during the 2018 growing season.

In the cornfield, a convex upward trend with a threshold of 0.345 (vol/vol) was detected between $\sigma(\theta_j)$ and $\bar{\theta}_j$ at the 30-60 cm depth. An exponentially decreasing trend between $\mathrm{CV}(\theta_j)$ and $\bar{\theta}_j$ at the same depth (fig. 2.7c for $\mathrm{CV}(\theta_j)$ vs $\bar{\theta}_j$) showed consistency with previous studies at 0-15 cm depth with different land uses (Brocca et al., 2012; Dari et al., 2019). A convex trend explains that the variability in soil water increases and decreases, respectively, before and after a threshold value of soil water. An exponential relationship explains that the variability parameters decrease with increasing soil water. However, no trends in $\mathrm{CV}(\theta_j)$ and $\sigma(\theta_j)$ with soil water ($\bar{\theta}_j$) were detected at the 0-15 cm and 15-30 cm depths in the cornfield (fig. 2.7a and 2.7b for $\mathrm{CV}(\theta_j)$ vs $\bar{\theta}_j$). Similar trends were observed by Brocca et al. (2010). These patterns have not been reported in previous studies for any croplands.

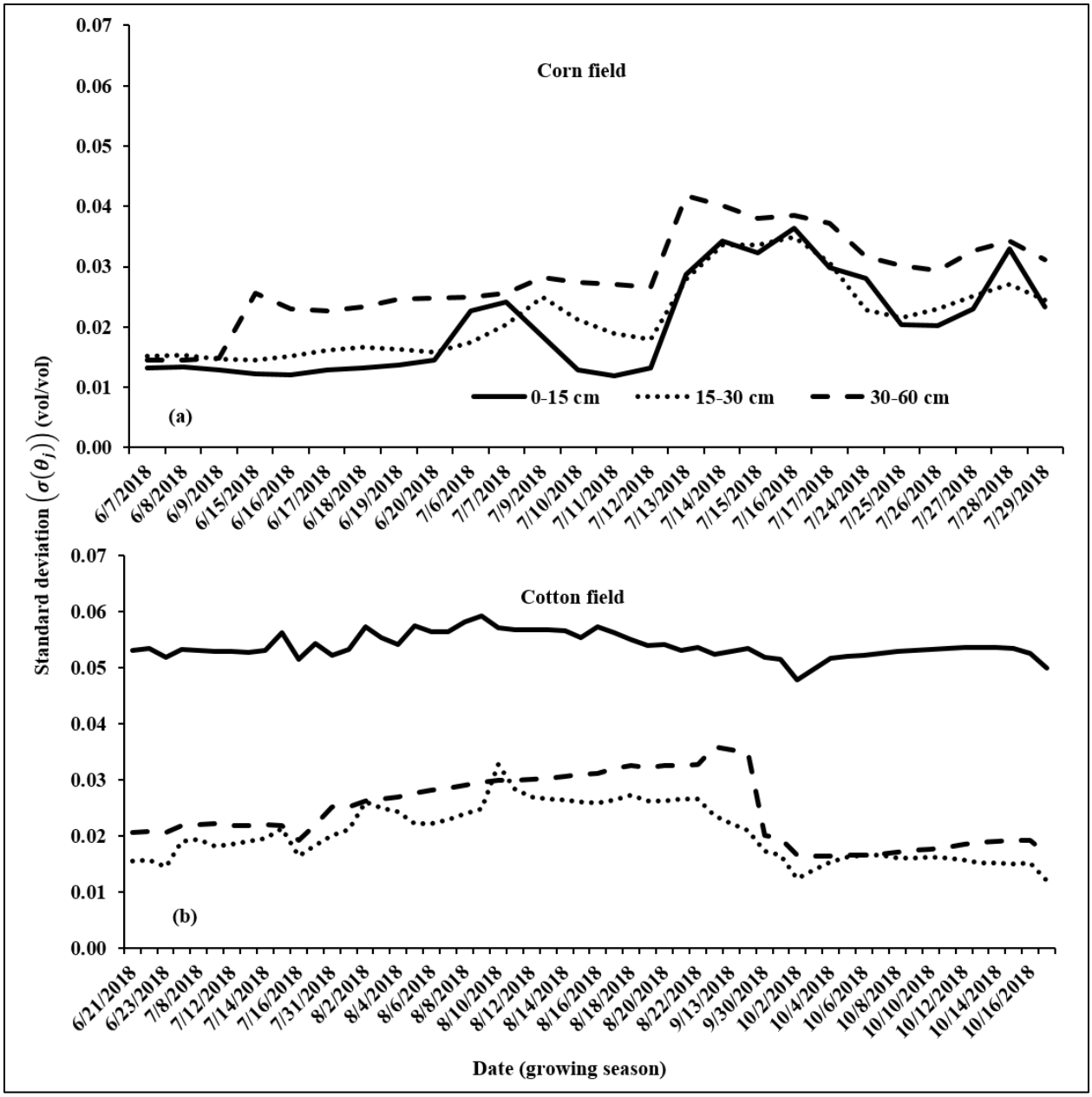

Figure 2.6 Distribution of standard deviation in the (a) cornfield and (b) cotton field at different depths during the 2018 growing season.

In the cotton field, a convex upward pattern with a threshold of 0.357 (vol/vol) was detected between $\sigma(\theta_j)$ and $\bar{\theta}_j$ at the 0-15 cm depth, while an exponentially decreasing trend was detected between $\mathrm{CV}(\theta_j)$ and $\bar{\theta}_j$ (fig. 2.7). For the 15-30 cm and 30-60 cm depths, an exponentially decreasing trend of $\mathrm{CV}(\theta_j)$ and $\sigma(\theta_j)$ with soil water $(\bar{\theta}_j)$ was detected. Similar results regarding

the trends in of CV(θ_j) and $\sigma(\theta_j)$ with $\bar{\theta}_j$ were obtained in previous studies with various land uses in the watershed (Brocca et al., 2010; Dari et al., 2019) but not in croplands.

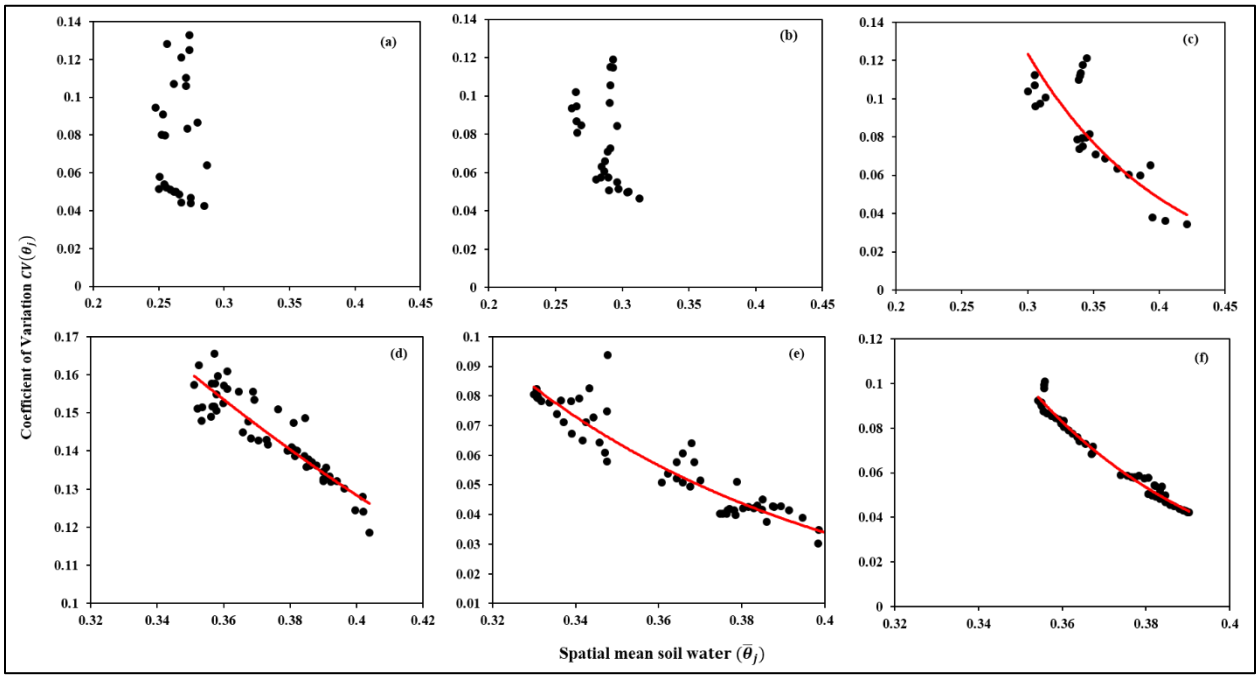

Figure 2.7 Trendline (red lines) between coefficient of variation of soil water and spatial mean soil water in the cornfield at (a) 0-15 cm, (b) 15-30 cm, and (c) 30-60 cm (exponential) depths and in the cotton field (exponential) at (d) 0-15 cm, (e) 15-30 cm, and (f) 30-60 cm depths during the 2018 growing season. These trend lines are the regression lines.

However, some of the trends in this study did not follow previous studies. For example, a convex trend between CV(θ_j) and $\bar{\theta}_j$ in the cornfield and an exponential trend between $\sigma(\theta_j)$ and $\bar{\theta}_j$ in the cotton field were detected during the growing season. The relationships detected between $\sigma(\theta_j)$ and $\bar{\theta}_j$ in this study did not align with Shen et al. (2016), who showed an increasing trend at different depths in cropland in an arid watershed-scale study with a shallow groundwater table during the growing season. This contradiction in the relationship between watershed and field-scale studies has been noted by others (Brocca et al., 2007, 2010). We found that the cotton field showed a higher standard deviation in soil water than the cornfield at the 0-15 cm depth during the

growing season. We also found that the maximum standard deviation was in the top layer (0-15 cm) in the cotton field and in the deepest layer (30-60 cm) in the cornfield (fig. 2.6). This might be a result of different factors, including differences in precipitation and irrigation, topographic and climatic factors, root distribution, water uptake, management practices, and soil hydraulic properties in the fields (Heathman et al., 2012; Liu et al., 2018; Shen et al., 2016).

The variation in soil water between the two fields could be due to differences in soil hydraulic properties (Heathman et al., 2012), topography, climate, root distribution, and water uptake within the soil profiles (Wang et al., 2010). For example, topography significantly affected soil water in the cornfield, but not in the cotton field (table 2.1). The silt percentage, however, significantly affected soil water in the cotton field, but not in the cornfield.

Table 2.1 Spearman's rank correlation of temporal mean soil water with topographic attributes and soil parameters.[a]

Factor	Cornfield			Cotton Field		
	0-15 cm	15-30 cm	30-60 cm	0-15 cm	15-30 cm	30-60 cm
Elevation (m)	-0.39	-0.31	-0.45*	0.18	-0.15	-0.23
Slope (%)	-0.20	-0.25	-0.32	0.32	-0.04	-0.10
Sand (%)	0.23	-0.13	-0.25	-0.27	-0.35	-0.08
Silt (%)	-0.06	0.03	0.32	0.50*	0.27	-0.18
Clay (%)	-0.30	0.10	-0.25	-0.01	-0.06	0.16
EC	NA	NA	NA	NA	-0.54*	-0.47*

[a] Asterisks (*) indicate significance at the 0.1 level, NA = not available.

The corn and cotton fields exhibited maximum spatial variation at the 30-60 cm and 0-15 cm depths, respectively, during the growing season. This might be due to topographic differences in the cornfield and the cover crop in the cotton field. Cover crops help to retain water in the surface soil layer while minimizing soil evaporation (Heathman et al., 2012). Furthermore, topography had a significant effect on soil water at the 30-60 cm depth in the cornfield (table 2.1) but no significant effect in the cotton field. Likewise, silt percentage in the cotton field had a significant

effect on soil water at the 0-15 cm depth. Silt holds more water than sand due to its finer texture. Hence, it can be concluded that the standard deviation was substantially dependent on soil water rather than soil depth during the growing season.

Furthermore, the impacts of different canopy structures, crop types, root water uptake, and atmospheric exposure of the surface, as well as precipitation and irrigation, help to strengthen the spatial homogeneity and reduce the standard deviation (Liu and Shao, 2014; Vereecken et al., 2014; Wang et al., 2015; Zucco et al., 2014). One of the reasons for the spatial variability in both fields could be the no-tillage management in both fields, and the cover crop in the cotton field (Heathman et al., 2012). This is discussed in more detail later.

2.4.2 Temporal Stability of Soil Water

A representative of the mean soil water is required to understand the temporal stability of soil water in the two crop fields during the growing season. A relative difference approach was used to study the temporal stability. Therefore, statistics including $\bar{\delta}_i$, $\sigma(\delta_i)$, and ITS_i were evaluated and compared for all sensor locations in both fields. The $\bar{\delta}_i$ and $\sigma(\delta_i)$ values for each sensor location were ranked in ascending order with their respective depths (fig. 2.8). The $|\bar{\delta}_i|$ value ranged from 0.001 to 0.155 in the cornfield and from 0 to 0.164 in the cotton field. The $\sigma(\delta_i)$ value ranged from 0.015 to 0.128 in the cornfield and from 0.009 to 0.083 in the cotton field. The ITS_i value ranged from 0.018 to 0.180 in the cornfield and from 0.010 to 0.165 in the cotton field. The $\bar{\delta}_i$ and ITS_i value agree in identifying the most representative sensor in both the fields.

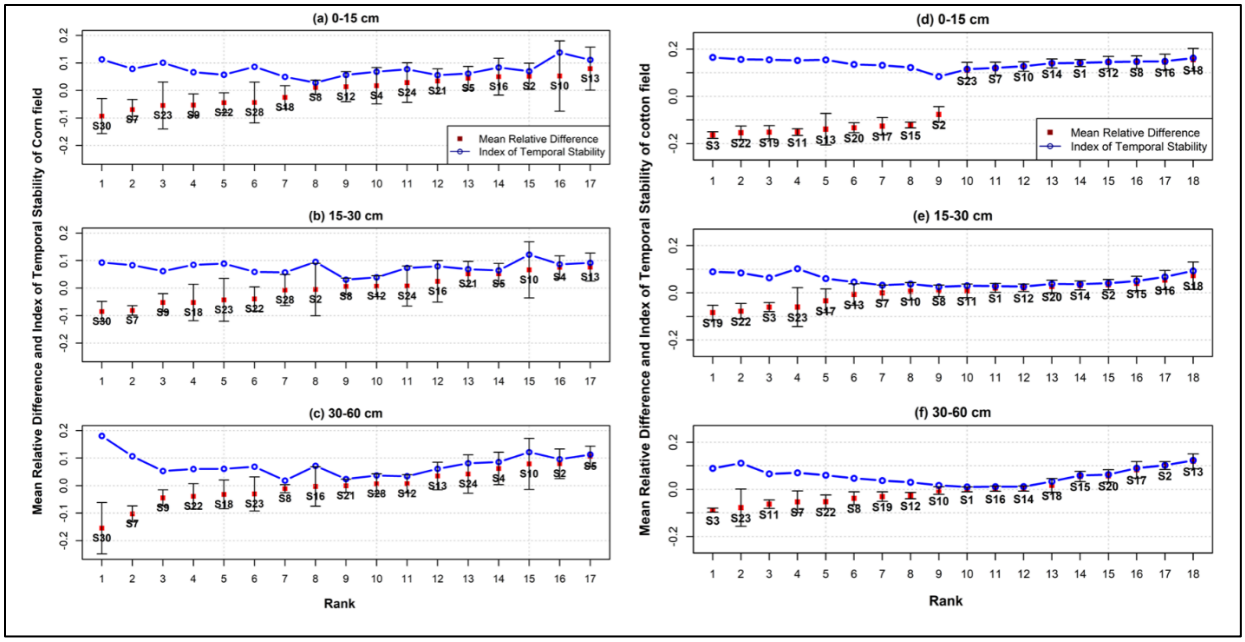

Figure 2.8 Rank ordered mean relative difference and index of temporal stability of soil water in the (a-c) cornfield and (d-f) cotton field. Error bars show standard deviations in relative difference.

Tables 2.2 and 2.3 list the Spearman's rank correlation (r_s) values between different soil depths to evaluate the spatial correlations for $\bar{\delta}_i$, $\sigma(\delta_i)$, and ITS_i. Table 2.2 shows that r_s was significant between all soil depths at a significance level of 0.05 in the cornfield. It showed that the spatial pattern in soil water was correlated between among all soil layers. However, in the cotton field, r_s was not significant between the 0-15 cm and 30-60 cm depths for $\bar{\delta}_i$ and between all soil depths for ITS_i. All the significant correlations were positive for all soil depths. Although the spatial patterns were not consistent with soil depth in both fields, the 0-15 cm and 15-30 cm depths showed stronger correlations compared to other depths in the cornfield.

Table 2.2 Matrix of Spearman's rank correlation coefficients between soil depths in cornfield. All correlations are significant at the 0.05 level.

	Soil Depth (cm)		
Statistics		**15-30**	**30-60**
$\bar{\delta}_i$	0-15	0.87	0.82

	15-30	-	0.81
$\sigma(\delta_i)$	0-15	0.68	0.65
	15-30	-	0.61
ITS_i	0-15	0.65	0.58
	15-30	-	0.72

Table 2.3 Matrix of Spearman's rank correlation coefficients between soil depths in cotton field. Asterisks (*) indicate significance at the 0.05 level.

		Soil Depth (cm)	
Statistics		**15-30**	**30-60**
$\bar{\delta}_i$	0-15	0.66*	0.17
	15-30	-	0.50*
$\sigma(\delta_i)$	0-15	0.70*	0.60*
	15-30	-	0.69*
ITS_i	0-15	0.23	-0.19
	15-30	-	0.26

Values of $\bar{\delta}_i$ that are close to zero and relatively small values of $\sigma(\delta_i)$ and ITS_i indicate temporal stability of soil water. These ranges sometimes mislead the results to define a location as temporally stable that could represent the spatial mean soil water (Dari et al., 2019). Therefore, to verify if a representative location was temporally stable, additional statistical criteria were adopted, including r_s, R^2, RMSE, IA, KGE, and NSE, between a representative location and the spatial mean soil water (table 2.4). In the cornfield, sensor 8 (S8) was found to be temporally stable at all soil depths (fig. 2.8a to 2.8c) and can therefore be used as a representative sensor location to estimate mean soil water in the cornfield during the growing season (fig. 2.9a to 2.9c). This may be due to soil hydraulic properties at S8 that are similar to the mean soil hydraulic properties, combined with soil homogeneity and soil water in the field (Yetbarek and Ojha, 2020). The adopted statistics verify that S8 is the best representative sensor and also support the relative difference approach (table 2.4). Sensors S7, S9, S18, S22, S23, and S30 were always dry, while sensors S4, S5, S10, S12, S13, S21, and S24 were always wet for the entire soil profile. This variation in dryness and wetness indicated soil heterogeneity from location to location and

homogeneity within the entire soil profile at particular locations. Topographic differences can also cause such variations in the dryness and wetness of sensors. However, the rest of the sensors were in a transitioning phase of dry and wet at different depths. Sensor S30 was the driest at all soil depths, while sensor S13 was the wettest in the upper two soil layers during the growing season.

Table 2.4 Summary of temporal stability statistics between field mean soil water and representative sensor.

Statistics	Cornfield (S8)			Cotton Field (S1)		
	0-15 cm	15-30 cm	30-60 cm	0-15 cm	15-30 cm	30-60 cm
r_s	0.84	0.75	0.95	0.95	0.98	0.96
R^2	0.76	0.85	0.97	0.9	0.97	0.94
RMSE	0.007	0.009	0.007	0.053	0.011	0.004
IA	0.9	0.93	0.99	0.42	0.96	0.98
KGE	0.76	0.68	0.94	0.84	0.8	0.89
NSE	0.7	0.79	0.95	-9.07	0.85	0.93

In the cotton field, sensor S1 was temporally stable at all depths during the growing season (fig. 2.8d to 2.8f), and it can be used as a representative sensor location to estimate the mean soil water in the cotton field (fig. 2.9d to 2.9f). Although S1 had $\bar{\delta}_i$ and ITS_i values of 0.14 at the 0-15 cm depth (fig 2.8d), it provided the most accurate spatial mean soil water at all depths. Sensor S1 showed temporal stability at deeper soil layers in the cotton field (table 2.4). However, according to the relative difference approach, no sensor showed a perfect zero value for $\bar{\delta}_i$ in the top soil layer (fig. 2.8d), which suggests that no sensor was temporally stable at the 0-15 cm depth. The IA and NSE values confirmed this lack of temporal stability at the 0-15 cm depth (table 2.4). However, r_s, R^2, RMSE, and KGE presented convincing evidence to consider S1 a representative sensor at the 0-15 cm depth. Therefore, S1 can be considered a temporally stable location at all soil depths, and it can be used as a representative sensor location to estimate mean soil water in the cotton field during the growing season. Sensors S3, S19, and S22 were always dry, while sensor S18 was always wet for the entire soil profile during the growing season. Sensor S3 was the driest

at the 0-15 and 30-60 cm depths, while sensor S18 was the wettest in the upper two soil depths in the cotton field during the growing season (fig. 2.8d to 2.8f). Other sensors similar to S1 were also able to produce the mean soil water (fig. 2.9d to 2.9f), but the statistical parameters were not as good as for S1.

Table 2.5 Soil silt content and soil electrical conductivity (EC) at a representative sensors (S1) in cotton field with respect to field average.

Soil Depth	Sensor S1		Field	
(cm)	Silt (%)	EC	Silt (%)	EC
0-15	53.8	NA	54.4	NA
15-30	52.65	18	47.55	16
30-60	49.48	44.54	54	51

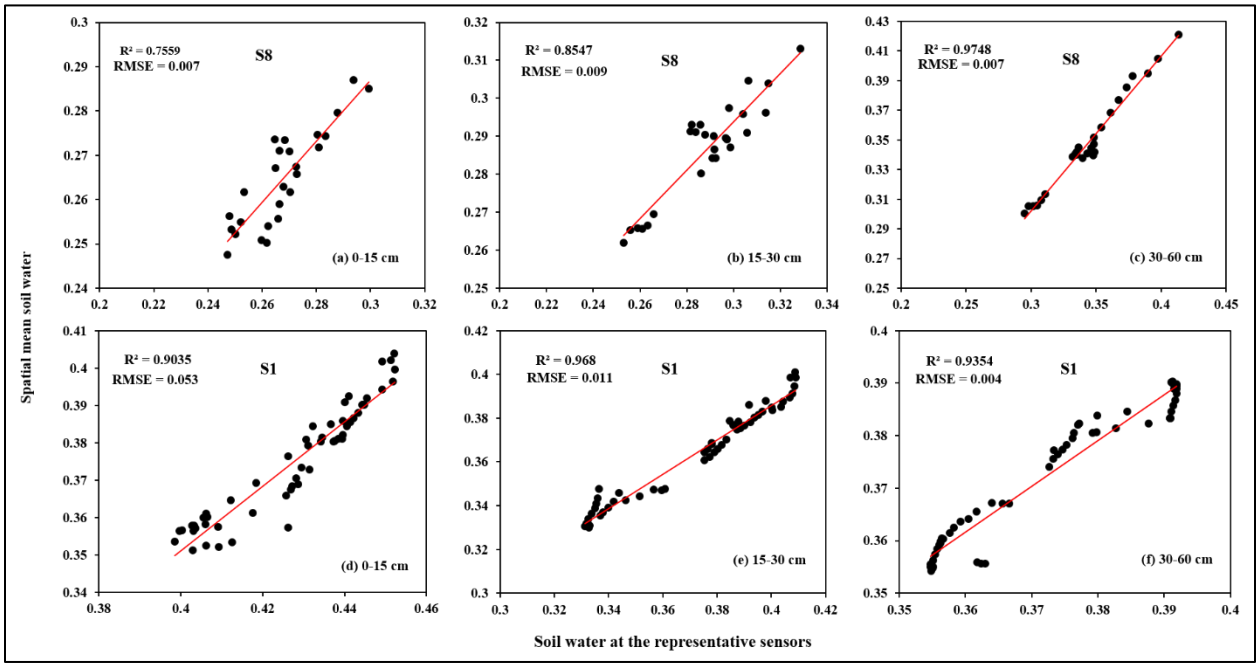

Figure 2.9 Relation between spatial mean soil water and representative sensors in the cornfield (sensor S8) at (a) 0-15 cm, (b) 15-30 cm, (c) 30-60 cm depths, and in the cotton field (sensor S1) at (d) 0-15 cm, (e) 15-30 cm, and (f) 30-60 cm depths during the growing season. The red lines are regression lines.

Any sensor that has statistics similar to S8 in the cornfield and similar to S1 in the cotton field, or a sensor that can estimate mean soil water, can be used to represent mean soil water using an offset

correction to serve as a temporally stable sensor (Heathman et al., 2012; Martínez-Fernández and Ceballos, 2005; She et al., 2012, 2015). Therefore, according to the $\bar{\delta_i}$, $\sigma(\delta_i)$, ITS_i, r_s, R^2, RMSE, IA, KGE, and NSE values, because the goal was to find the best representative sensor location to estimate mean soil water in crop fields, S8 in the cornfield and S1 in the cotton field were selected as temporally stable sensors during the growing season. This decision might help the farmers in making decisions to reduce costs and labor during the growing season. The temporal stability increased with soil depth in the crop fields (table 2.4), therefore, an intermediate soil layer can play significant role for farmers to track soil water during the growing season due to irrigation from the upper layer and suction from bottom layer. Sensor S8 in the cornfield was located at an elevation of 173 m. The properties of the representative locations (S8 in corn and S1 in cotton) are shown in fig. 2.10 and table 2.5.

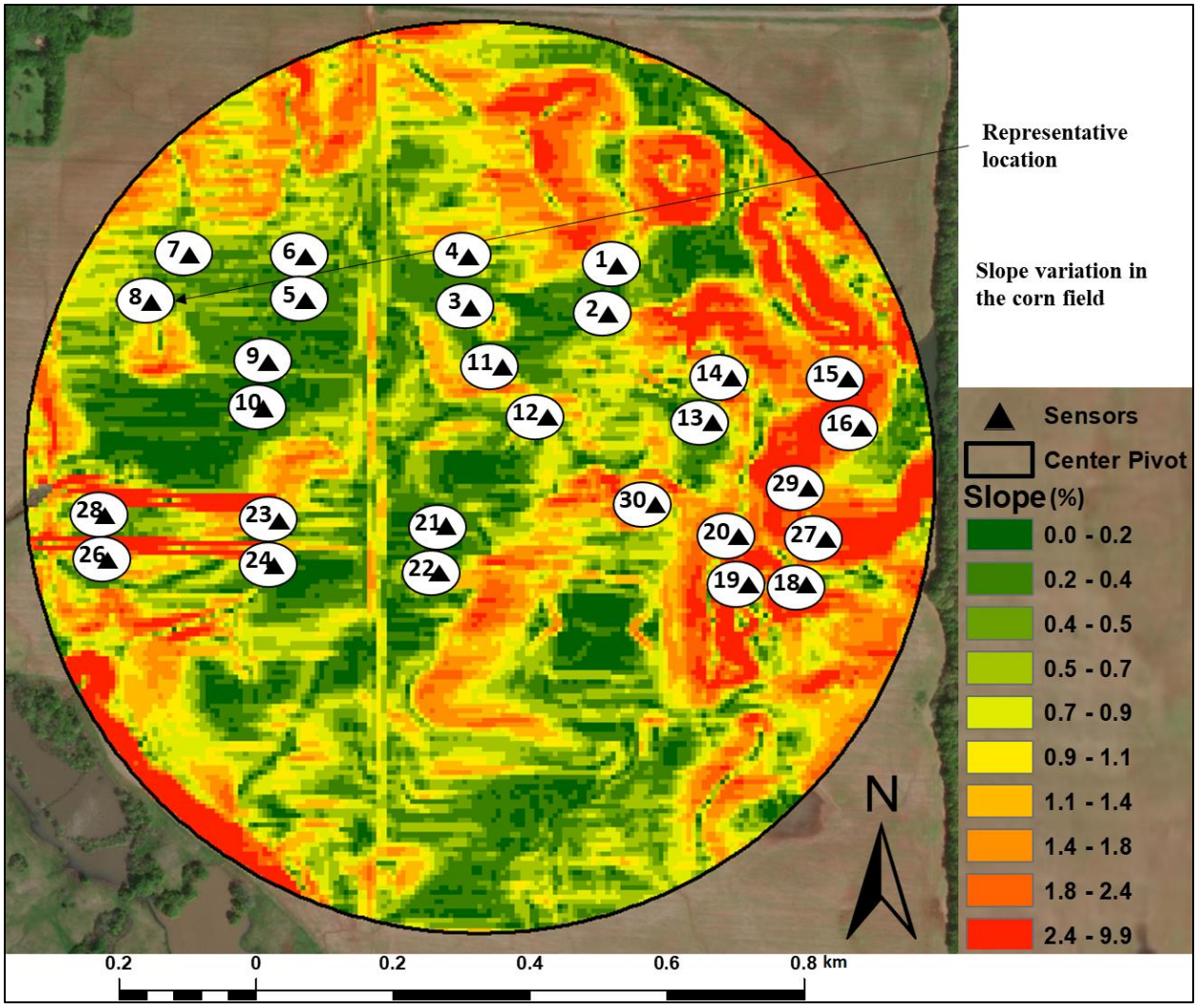

Figure 2.10 Location of representative sensor (S8) in cornfield with respect to slope and other sensors in the field.

2.4.3 Factors Responsible for Soil Water Variability

The mean soil water was affected differently in the two crop fields. Spearman's rank correlation was estimated between soil water and the parameters considered responsible for the soil water variability. The topographic variation in a crop field can be a factor responsible for soil water variability, especially in deep soil layers. A high slope causes flow in a lateral direction, as surface or subsurface runoff, and reduces infiltration (Huat et al., 2006). The topographic attributes in the cornfield showed an impact on soil water variation during the growing season. Sensor S30 was

located on a high slope that could have led to surface or subsurface runoff and reduced infiltration, resulting in a relatively dry 30-60 cm soil layer. However, sensor S5 was located on a low slope, which could have resulted in the wettest 30-60 soil layer in the cornfield. Most of the weather variables (ET_c, Mean air temperature, etc..) showed a significant positive correlation with soil water in the cornfield but a significant negative correlation with soil water in the cotton field. This difference might be due to differences in the plant canopies during the growing season, in addition to variation in topography, climate, root system, soil properties, and size of the fields.

The ET_c was significantly poorly correlated (-0.33) with soil water at the 15-30 cm depth in the cornfield (table 2.6). However, ET_c showed a significant moderate correlation (-0.60 to -0.67) with soil water at all soil depths in the cotton field. The ET_c showed a significantly higher correlation with soil water at the 15-30 cm depth in both fields, which suggests a great influence of ET_c on soil water at the 15-30 cm depth as compared to the other soil depths. This could be because cotton has a deeper root system (>90 cm) for water uptake as compared to corn (50 cm) (Wang et al., 2010). Studies have shown that corn and cotton have shallow and deep root systems, respectively, for water uptake (Wang et al., 2010). Root water uptake can be described using the root depths for both crops during the growing season, which affects the soil water variation. It has been determined that root water uptake increases with root depths greater than 90 cm during the growth stages in cotton. However, in corn, the depth of root water uptake increases to 50 cm from the jointing stage to flowering but decreases in the full maturity stage. Therefore, the soil water variation between the two crops could be due to different root water uptake in the fields during the growing season. In addition to the root system, cotton has a small and light canopy during the growing stages as compared to corn, which has a long and dense canopy during the growing stages.

Table 2.6 Spearman's rank correlation between spatial mean soil water and meteorological parameters.[a]

Factor	Cornfield			Cotton Field		
	0-15 cm	15-30 cm	30-60 cm	0-15 cm	15-30 cm	30-60 cm
ET (cm)	-0.08	-0.33*	-0.31	-0.63*	-0.67*	-0.60*
Mean air temperature (°C)	0.35*	0.41*	0.42*	-0.46*	-0.55*	-0.53*
Solar radiation (W m^{-2})	0.03	0.24	0.29	-0.37*	-0.42*	-0.39*
accGDD (°C)	-0.19	-0.67*	-0.95*	0.39*	0.31*	0.27*

[a] Asterisks (*) indicate significance at the 0.1 level

It has also been observed that no-till and cover crops help restore soil water in the soil (Heathman et al., 2012). Both fields were under no-till management before seeding. However, the cotton field was planted with a cover crop before the growing season, and no cover crop was planted in the cornfield. Therefore, the variation in soil water in the fields can also be due to cover crop management practices (Heathman et al., 2012). The mean air temperature and solar radiation showed stronger correlations in deeper soil layers in both fields. The accumulated growing degree days (accGDD) showed an increasing negative correlation with increasing depth in the cornfield and a decreasing positive correlation in the cotton field. This was due to the different root distributions of the crops, as mentioned previously.

Different topographic attributes, such as elevation and slope, were considered to evaluate the effects of these parameters on soil water variations in both fields during the growing season. The sand, silt, and clay percentages and the soil EC were also considered for their effect on soil water. In the cornfield, elevation was significantly correlated with soil water at the 30-60 cm depth (table 2.1), which shows the impact of topography on soil water variation in the deepest soil layer. No other field attributes (slope and sand, silt, and clay percentages) were significantly correlated with soil water at any soil depth in the cornfield. However, the silt percentage at 0-15 cm, EC at 15-30 cm, and EC at 30-60 cm showed significant correlations with soil water in the cotton field. This might be due to the cover crop in the cotton field, which held water at the surface, along with the

silt. No other field attributes (elevation, slope, sand, and clay) were significant in the cotton field. The variation in r_s was found to be due to difference in elevation in the cornfield and to soil properties in the cotton field (table 2.1).

2.5 Summary and Conclusions

This study of spatiotemporal variability in soil water at three depths (0-15 cm, 15-30 cm, and 30-60 cm) was performed in two crop fields (corn and cotton) during the 2018 growing season in the TVR in northern Alabama. It can be concluded that soil water can be a key variable for determining uniform rate irrigation in different croplands. Soil water can be used to optimize the amount, time, and rate of irrigation in crop fields during the growing season. The standard deviation did not increase with increasing soil water, and same was found by Shen et al. (2016) for all soil depths in croplands in their research. The soil water variability in the two fields was substantially dependent on soil water in the different soil layers. Therefore, soil water in the intermediate soil layer can play a vital role in soil water variability in crop fields due to irrigation from the upper soil layer and suction from the bottom soil layer.

Farmers can reduce the number of sensors installed in their fields to save time, cost, and labor during the growing season, and farmers can schedule precise uniform irrigation (right amount and right time) considering the entire soil profile. The temporal stability increased with soil depth in the crop fields irrespective of the irrigation application and the factors affecting soil water variation during the growing season. However, dry, wet, and temporally stable locations need to be monitored to understand the spatial variation in soil water in the entire field. After knowing the soil water variability, farmers need to decide the number of sensors based on their budget. The number of sensors can also be determined based on statistical criteria. Statistical techniques can

reduce the number of sensors, but the cost has to be paid by the farmer for sensors. Therefore, we suggest that farmers decide the number of sensors based on their budget.

Using the standard deviation through implicit relationships at absolute errors of 5% and 10%, the number of sensors was estimated for both crop fields. Figure 2.11 shows that a maximum of ten sensors in the cornfield and six sensors in the cotton field would be required to determine the mean soil water with 5% absolute error. Topography can be an influential factor in a field similar to the cornfield (topographic variations), which needs to be considered, but not in a field similar to the cotton field which was almost level. The number of sensors can also be related to crop types with similar root distributions and canopy structures.

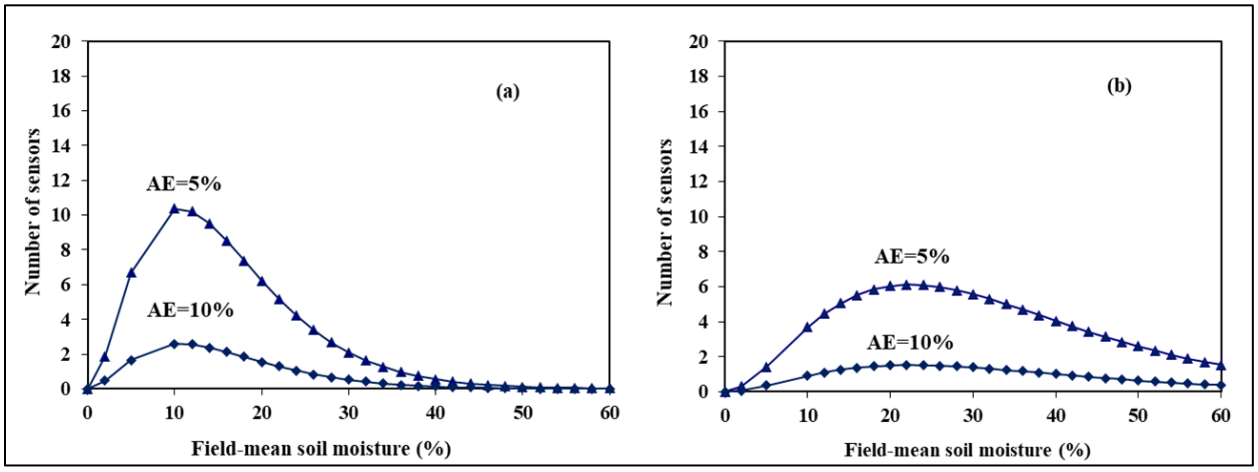

Figure 2.11 Number of sensors required in the (a) corn and (b) cotton fields.

This study was conducted at various depths in two crop fields during a wet season, based on the historical average precipitation. Irrigation is expensive. Therefore, we need to investigate the spatiotemporal variability of soil water in different growing seasons and in different crops over multiple years to help farmers adopt irrigation while reducing the associated cost. We focused on 60 cm of soil depth in this study. However, to determine the full soil water balance based on the entire root depth of a crop, sensors should be installed in soil layers deeper than 60 cm to determine

if the measurement of soil water in deeper soil layers (below 60 cm) can improve water use efficiency.

Acknowledgement

The authors would like to express their gratitude to the following individuals and agencies for their support and funding for this project: Dr. George Vellidis of the University of Georgia, Posey Farms, Haney Farms, the USDA Natural Resources Conservation Service (NRCS), and the Alabama Cooperative Extension System (ACES). This research was supported by the USDA-NRCS CIG (69-3A75-17-273) and the AAES PAR program, the USDA-NIFA Hatch Project (ALA014-1-19052), and the Alabama Agricultural Experiment Station. We also thank Dr. Prem Parajuli, Associate Editor of the NRES Technical Community of ASABE, and the three anonymous reviewers whose scrupulous reviews greatly improved the manuscript.

2.6 References

Aggarwal, P., Bhattacharyya, R., Mishra, A.K., Das, T.K., Šimůnek, J., Pramanik, P., Sudhishri, S., Vashisth, A., Krishnan, P., Chakraborty, D., Kamble, K.H., 2017. Modelling soil water balance and root water uptake in cotton grown under different soil conservation practices in the Indo-Gangetic Plain. Agric. Ecosyst. Environ. 240, 287–299. https://doi.org/10.1016/j.agee.2017.02.028

Allen, R. G., Pereira, L. S., Raes, D., & Smith, M., 1998. FAO Irrigation and drainage paper No. 56. Rome: Food and Agriculture Organization of the United Nations, 56(97), e156.

Anandhi, A., 2016. Growing degree days - Ecosystem indicator for changing diurnal temperatures and their impact on corn growth stages in Kansas. Ecol. Indic. 61, 149–158. https://doi.org/10.1016/j.ecolind.2015.08.023

Anderson, E.L., 1987. Corn root Ggrowth and distribution as influenced by tillage and nitrogen Fertilization. Agron. J. 79, 544–549. https://doi.org/10.2134/agronj1987.00021962007900030029x

Bauer-Marschallinger, B., Freeman, V., Cao, S., Paulik, C., Schaufler, S., Stachl, T., Modanesi, S., Massari, C., Ciabatta, L., Brocca, L., Wagner, W., 2019. Toward global soil moisture monitoring with sentinel-1: harnessing assets and overcoming obstacles. IEEE Trans. Geosci. Remote Sens. 57, 520–539. https://doi.org/10.1109/TGRS.2018.2858004

Beven, K. J., & Kirkby, M. J., 1979. A physically based, variable contributing area model of basin hydrology / Un modèle à base physique de zone d'appel variable de l'hydrologie du bassin versant. Hydrol. Sci. Bull. 24, 43–69. https://doi.org/10.1080/02626667909491834

Bouyoucos, G.J., 1962. Hydrometer Method Improved for Making Particle Size Analyses of Soils1. Agron. J. 54, 464–465. https://doi.org/10.2134/agronj1962.00021962005400050028x

Brocca, L., Melone, F., Moramarco, T., Morbidelli, R., 2010. Spatial-temporal variability of soil moisture and its estimation across scales. Water Resour. Res. 46. https://doi.org/10.1029/2009WR008016

Brocca, L., Melone, F., Moramarco, T., Morbidelli, R., 2009. Soil moisture temporal stability over experimental areas in Central Italy. Geoderma 148, 364–374. https://doi.org/10.1016/j.geoderma.2008.11.004

Brocca, L., Morbidelli, R., Melone, F., Moramarco, T., 2007. Soil moisture spatial variability in experimental areas of central Italy. J. Hydrol. 333, 356–373. https://doi.org/10.1016/j.jhydrol.2006.09.004

Brocca, L., Tarpanelli, A., Filippucci, P., Dorigo, W., Zaussinger, F., Gruber, A., Fernández-Prieto, D., 2018. How much water is used for irrigation? A new approach exploiting coarse resolution satellite soil moisture products. Int. J. Appl. Earth Obs. Geoinf. 73, 752–766. https://doi.org/10.1016/j.jag.2018.08.023

Brocca, L., Tullo, T., Melone, F., Moramarco, T., Morbidelli, R., 2012. Catchment scale soil moisture spatial–temporal variability. J. Hydrol. 422–423, 63–75. https://doi.org/10.1016/j.jhydrol.2011.12.039

Dari, J., Morbidelli, R., Saltalippi, C., Massari, C., Brocca, L., 2019. Spatial-temporal variability of soil moisture: Addressing the monitoring at the catchment scale. J. Hydrol. 570, 436–444. https://doi.org/10.1016/j.jhydrol.2019.01.014

Fan, J., McConkey, B., Wang, H., Janzen, H., 2016. Root distribution by depth for temperate agricultural crops. F. Crop. Res. 189, 68–74. https://doi.org/10.1016/j.fcr.2016.02.013

FAO., 2018. The future of food and agriculture: Alternative pathways to 2050. Rome, Italy: United Nations FAO.

Filippucci, P., Tarpanelli, A., Massari, C., Serafini, A., Strati, V., Alberi, M., Raptis, K.G.C., Mantovani, F., Brocca, L., 2020. Soil moisture as a potential variable for tracking and quantifying irrigation: A case study with proximal gamma-ray spectroscopy data. Adv. Water Resour. 136, 103502. https://doi.org/10.1016/j.advwatres.2019.103502

Fry, J.E., Guber, A.K., 2020. Temporal stability of field-scale patterns in soil water content across topographically diverse agricultural landscapes. J. Hydrol. 580, 124260. https://doi.org/10.1016/j.jhydrol.2019.124260

Gao, L., Shao, M., 2012. Temporal stability of soil water storage in diverse soil layers. Catena 95, 24–32. https://doi.org/10.1016/j.catena.2012.02.020

Gao, X., Xiao, Y., Deng, L., Li, Q., Wang, C., Li, B., Deng, O., Zeng, M., 2019. Spatial variability of soil total nitrogen, phosphorus and potassium in Renshou County of Sichuan Basin, China. J. Integr. Agric. 18, 279–289. https://doi.org/10.1016/S2095-3119(18)62069-6

Gia Pham, T., Kappas, M., Van Huynh, C., Hoang Khanh Nguyen, L., 2019. Application of Ordinary Kriging and Regression Kriging Method for Soil Properties Mapping in Hilly Region of Central Vietnam. ISPRS Int. J. Geo-Information 8, 147. https://doi.org/10.3390/ijgi8030147

Guber, A.K., Gish, T.J., Pachepsky, Y.A., van Genuchten, M.T., Daughtry, C.S.T., Nicholson, T.J., Cady, R.E., 2008. Temporal stability in soil water content patterns across agricultural fields. CATENA 73, 125–133. https://doi.org/10.1016/j.catena.2007.09.010

Gupta, H. V, Kling, H., Yilmaz, K.K., Martinez, G.F., 2009. Decomposition of the mean squared error and NSE performance criteria: Implications for improving hydrological modelling. J. Hydrol. 377, 80–91. https://doi.org/10.1016/j.jhydrol.2009.08.003

Hao, X., Qiu, Y., Fan, Y., Li, T., Leng, D., Li, S., Kang, S., 2020. Applicability of temporal stability analysis in predicting field mean of soil moisture in multiple soil depths and different seasons in an irrigated vineyard. J. Hydrol. 588, 125059. https://doi.org/10.1016/j.jhydrol.2020.125059

Heathman, G.C., Cosh, M.H., Han, E., Jackson, T.J., McKee, L., McAfee, S., 2012. Field scale spatiotemporal analysis of surface soil moisture for evaluating point-scale in situ networks. Geoderma 170, 195–205. https://doi.org/10.1016/j.geoderma.2011.11.004

Heathman, G.C., Larose, M., Cosh, M.H., Bindlish, R., 2009. Surface and profile soil moisture spatio-temporal analysis during an excessive rainfall period in the Southern Great Plains, USA. CATENA 78, 159–169. https://doi.org/10.1016/j.catena.2009.04.002

Huat, B. B., Ali, F. H., & Low, T. H., 2006. Water infiltration characteristics of unsaturated soil slope and its effect on suction and stability. Geotechnical & Geological Engineering, 24(5), 1293-1306. https://doi.org/10.1007/s10706-005-1881-8

Hupet, F., Vanclooster, M., 2002. Intraseasonal dynamics of soil moisture variability within a small agricultural maize cropped field. J. Hydrol. 261, 86–101. https://doi.org/10.1016/S0022-1694(02)00016-1

Irmak, S., 2017. Evapotranspiration Basics and Estimating Actual Crop Evapotranspiration from Reference Evapotranspiration and Crop-Specific Coefficients. Nebraska Extension NebGuide G1994.

Jacobs, J.M., Mohanty, B.P., Hsu, E.-C., Miller, D., 2004. SMEX02: Field scale variability, time stability and similarity of soil moisture. Remote Sens. Environ., 2002 Soil Moisture Experiment (SMEX02) 92, 436–446. https://doi.org/10.1016/j.rse.2004.02.017

Knoben, W.J.M., Freer, J.E., Woods, R.A., 2019. Technical note: Inherent benchmark or not? Comparing Nash–Sutcliffe and Kling–Gupta efficiency scores. Hydrol. Earth Syst. Sci. 23, 4323–4331. https://doi.org/10.5194/hess-23-4323-2019

Kornelsen, K.C., Coulibaly, P., 2013. Advances in soil moisture retrieval from synthetic aperture radar and hydrological applications. J. Hydrol. https://doi.org/10.1016/j.jhydrol.2012.10.044

Kumar, H., Srivastava, P., Ortiz, B.V., Takhellambam, B.S., Morata, G., Bondesan, L. and Lamba, J., 2020. Spatiotemporal Soil Moisture Variability in Corn and Cotton Fields with Uniform Irrigation During the Growing Season. In: AGU Fall Meeting Abstracts (Vol. 2020, pp. H209-05).

Kumar, H., 2016. Regionalization of flow duration curves of meso-scale catchments. MS thesis. Roorkee, India: Indian Institute of Technology Roorkee, Department of Hydrology.

Lena, B.P., Ortiz, B. V., Jiménez-López, A.F., Sanz-Sáez, Á., O'Shaughnessy, S.A., Durstock, M.K., Pate, G., 2020. Evaluation of infrared canopy temperature data in relation to soil water-based irrigation scheduling in a humid subtropical climate. Trans. ASABE 65, 1217–1231. https://doi.org/10.13031/Trans.13912

Li, Q., Peng, C., Wu, H., Wang, Y., 2019. Study on temporal and spatial variation of soil moisture based on sensing data of internet of things. AIP Conf. Proc. 2122, 20006. https://doi.org/10.1063/1.5116445

Liang, X., Liakos, V., Wendroth, O., Vellidis, G., 2016. Scheduling irrigation using an approach based on the van Genuchten model. Agric. Water Manag. 176, 170–179. https://doi.org/10.1016/j.agwat.2016.05.030

Liu, B., Shao, M., 2014. Estimation of soil water storage using temporal stability in four land uses over 10 years on the Loess Plateau, China. J. Hydrol. 517, 974–984. https://doi.org/10.1016/j.jhydrol.2014.06.003

Liu, Z., Wang, Yanhui, Yu, P., Tian, A., Wang, Yarui, Xiong, W., Xu, L., 2018. Spatial Pattern and Temporal Stability of Root-Zone Soil Moisture during Growing Season on a Larch Plantation Hillslope in Northwest China. Forests 9, 68. https://doi.org/10.3390/f9020068

Loew, A., Stacke, T., Dorigo, W., De Jeu, R., Hagemann, S., 2013. Potential and limitations of multidecadal satellite soil moisture observations for selected climate model evaluation studies. Hydrol. Earth Syst. Sci 17, 3523–3542. https://doi.org/10.5194/hess-17-3523-2013

Majdar, H.A., Vafakhah, M., Sharifikia, M., Ghorbani, A., 2018. Spatial and temporal variability of soil moisture in relation with topographic and meteorological factors in south of Ardabil Province, Iran. Environ. Monit. Assess. 190, 500. https://doi.org/10.1007/s10661-018-6887-9

Martínez-Fernández, J., Ceballos, A., 2005. Mean soil moisture estimation using temporal stability analysis. J. Hydrol. 312, 28–38. https://doi.org/10.1016/j.jhydrol.2005.02.007

Mei, X., Zhu, Q., Ma, L., Zhang, D., Liu, H., Xue, M., 2018. The spatial variability of soil water storage and its controlling factors during dry and wet periods on loess hillslopes. Catena 162, 333–344. https://doi.org/10.1016/j.catena.2017.10.029

Mohanty, B. P., & Skaggs, T. H., 2001. Spatio-temporal evolution and time-stable characteristics of soil moisture within remote sensing footprints with varying soil, slope, and vegetation. Adv. Water Resour., 24(9), 1051-1067. https://doi.org/10.1016/S0309-1708(01)00034-3

Nash, J.E., Sutcliffe, J. V, 1970. River flow forecasting through conceptual models part I. A discussion of principles. J. Hydrol. 10, 282–290. https://doi.org/10.1016/0022-1694(70)90255-6

NASS., 2013. Farm and ranch irrigation survey. In Census of agriculture (Vol. 3). Washington, DC: USDA National Agricultural Statistics Service. Retrieved from https://www.nass.usda.gov/Publications/AgCensus/2012/Online_Resources/Farm_and_Ranch_Irrigation_Survey/fris13.pdf

NASS., 2017. United States Summary and State Data. In Census of Agriculture. Washington, DC: USDA National Agricultural Statistics Service.

Palombo, A., Pascucci, S., Loperte, A., Lettino, A., Castaldi, F., Muolo, M.R., Santini, F., 2019. Soil moisture retrieval by integrating tasi-600 airborne thermal data, worldview 2 satellite data and field measurements: petacciato case study. Sensors 19, 1515. https://doi.org/10.3390/s19071515

Pandey, V., Pandey, P.K., 2010. Spatial and temporal variability of soil moisture. Int. J. Geosci. 01, 87–98. https://doi.org/10.4236/ijg.2010.12012

Parinussa, R.M., Yilmaz, M.T., Anderson, M.C., Hain, C.R., de Jeu, R.A.M., 2014. An intercomparison of remotely sensed soil moisture products at various spatial scales over the Iberian Peninsula. Hydrol. Process. 28, 4865–4876. https://doi.org/10.1002/hyp.9975

Ridolfi, E., Kumar, H., Bárdossy, A., 2020. A methodology to estimate flow duration curves at partially ungauged basins. Hydrol. Earth Syst. Sci. 24, 2043–2060. https://doi.org/https://doi.org/10.5194/hess-24-2043-2020

Rossato, L., Alvalá, R.C. dos S., Marengo, J.A., Zeri, M., Cunha, A.P.M. do A., Pires, L.B.M., Barbosa, H.A., 2017. Impact of Soil Moisture on Crop Yields over Brazilian Semiarid. Front. Environ. Sci. 5, 73. https://doi.org/10.3389/fenvs.2017.00073

Sangha, L., Lamba, J., Kumar, H., 2020a. Effect of ENSO-based upstream water withdrawals for irrigation on downstream water withdrawals. Hydrol. Res. https://doi.org/https://doi.org/10.2166/nh.2020.156

Sangha, L., Lamba, J., Kumar, H., Srivastava, P., Dougherty, M., Prasad, R., 2020b. An innovative approach to rainwater harvesting for irrigation based on El Niño Southern Oscillation forecasts. J. Soil Water Conserv. jswc.2020.00085. https://doi.org/10.2489/JSWC.2020.00085

She, D., Liu, Y., Shao, M., Carlos, T.L., Yu, S., 2012. Temporal stability of soil water content for a shallow and deep soil profile at a small catchment scale. Aust. J. Crop Sci. 6, 1192.

She, D., Zhang, W., Hopmans, J.W., Timm, L.C., 2015. Area representative soil water content estimations from limited measurements at time-stable locations or depths. J. Hydrol. 530, 580–590. https://doi.org/10.1016/j.jhydrol.2015.10.016

Shen, Q., Gao, G., Hu, W., Fu, B., 2016. Spatial-temporal variability of soil water content in a cropland-shelterbelt-desert site in an arid inland river basin of Northwest China. J. Hydrol. 540, 873–885. https://doi.org/10.1016/j.jhydrol.2016.07.005

SSURGO, 2020. Soil Survey Geographic (SSURGO) database. Washington, DC: USDA Natural Resources Conservation Service. Retrieved from https://sdmdataaccess.sc.egov.usda.gov/

Su, B., Zhao, G., Dong, C., 2018. Spatiotemporal variability of soil nutrients and the responses of growth during growth stages of winter wheat in northern China. PLoS One 13, e0203509. https://doi.org/10.1371/journal.pone.0203509

Takagi, K., Lin, H.S., 2012. Changing controls of soil moisture spatial organization in the Shale Hills Catchment. Geoderma 173–174, 289–302. https://doi.org/10.1016/j.geoderma.2011.11.003

Thorburn, P.J., Ehleringer, J.R., 1995. Root water uptake of field-growing plants indicated by measurements of natural-abundance deuterium. Plant Soil 177, 225–233. https://doi.org/10.1007/BF00010129

Vachaud, G., Silans, A.P. De, Balabanis, P., Vauclin, M., 1985. Temporal Stability of Spatially Measured Soil Water Probability Density Function. Soil Sci. Soc. Am. J. 49, 822–828. https://doi.org/10.2136/sssaj1985.03615995004900040006x

van Genuchten, M.T., 1980. A Closed-form Equation for Predicting the Hydraulic Conductivity of Unsaturated Soils. Soil Sci. Soc. Am. J. 44, 892–898. https://doi.org/10.2136/sssaj1980.03615995004400050002x

Vasu, D., Singh, S.K., Sahu, N., Tiwary, P., Chandran, P., Duraisami, V.P., Ramamurthy, V., Lalitha, M., Kalaiselvi, B., 2017. Assessment of spatial variability of soil properties using geospatial techniques for farm level nutrient management. Soil Tillage Res. 169, 25–34. https://doi.org/10.1016/j.still.2017.01.006

Vellidis, G., Liakos, V., Andreis, J.H., Perry, C.D., Porter, W.M., Barnes, E.M., Morgan, K.T., Fraisse, C., Migliaccio, K.W., 2016. Development and assessment of a smartphone application for irrigation scheduling in cotton. Comput. Electron. Agric. 127, 249–259. https://doi.org/10.1016/j.compag.2016.06.021

Vellidis, G., Tucker, M., Perry, C., Kvien, C., Bednarz, C., 2008. A real-time wireless smart sensor array for scheduling irrigation. Comput. Electron. Agric. 61, 44–50. https://doi.org/10.1016/j.compag.2007.05.009

Vereecken, H., Huisman, J.A., Pachepsky, Y., Montzka, C., van der Kruk, J., Bogena, H., Weihermüller, L., Herbst, M., Martinez, G., Vanderborght, J., 2014. On the spatio-temporal dynamics of soil moisture at the field scale. J. Hydrol., Determination of soil moisture: Measurements and theoretical approaches 516, 76–96. https://doi.org/10.1016/j.jhydrol.2013.11.061

Wang, C., Zuo, Q., Zhang, R., 2008. Estimating the necessary sampling size of surface soil moisture at different scales using a random combination method. J. Hydrol. 352, 309–321. https://doi.org/10.1016/j.jhydrol.2008.01.011

Wang, P., Song, X., Han, D., Zhang, Y., Liu, X., 2010. A study of root water uptake of crops indicated by hydrogen and oxygen stable isotopes: A case in Shanxi Province, China. Agric. Water Manag. 97, 475–482. https://doi.org/10.1016/j.agwat.2009.11.008

Wang, T., Wedin, D.A., Franz, T.E., Hiller, J., 2015. Effect of vegetation on the temporal stability of soil moisture in grass-stabilized semi-arid sand dunes. J. Hydrol. 521, 447–459. https://doi.org/10.1016/j.jhydrol.2014.12.037

Willmott, C.J., Ackleson, S.G., Davis, R.E., Feddema, J.J., Klink, K.M., Legates, D.R., O'Donnell, J., Rowe, C.M., 1985. Statistics for the evaluation and comparison of models. J. Geophys. Res. Ocean. 90, 8995–9005. https://doi.org/10.1029/JC090iC05p08995

Yetbarek, E., Ojha, R., 2020. Spatio-temporal variability of soil moisture in a cropped agricultural plot within the Ganga Basin, India. Agric. Water Manag. 234, 106108. https://doi.org/10.1016/j.agwat.2020.106108

Zaussinger, F., Dorigo, W., Gruber, A., Tarpanelli, A., Filippucci, P., Brocca, L., 2019. Estimating irrigation water use over the contiguous United States by combining satellite and reanalysis soil moisture data. Hydrol. Earth Syst. Sci. 23, 897–923. https://doi.org/https://doi.org/10.5194/hess-23-897-2019

Zucco, G., Brocca, L., Moramarco, T., Morbidelli, R., 2014. Influence of land use on soil moisture spatial–temporal variability and monitoring. J. Hydrol., Determination of soil moisture: Measurements and theoretical approaches 516, 193–199. https://doi.org/10.1016/j.jhydrol.2014.01.043

Chapter 3

Understand Within-Field Variability in Soil Nutrients for Site-Specific Agricultural Management in an Irrigated Cornfield

(*Journal of ASABE*)

3.1 Abstract

The adoption of precision agricultural practices in Alabama has been increasing in recent years. Although challenging, understanding nutrient variability in agricultural fields is important for site-specific management. This study investigated soil phosphorus (P) and nitrogen (N) variability in an irrigated cornfield located in the Town Creek Watershed of the Tennessee Valley Region of Alabama, USA during the 2019 growing season. Three different irrigation management zones (high yield-HY, moderate yield-MY, and low yield-LY) were delineated based on ten years of historical records of corn grain yield, soil texture, and measured topography using the Management Zone Analyst (MZA) software. The soil samples at 0-15 cm, 15-30 cm, and 30-60 cm depths were collected five different times during the 2019 growing season. Both manure and inorganic fertilizer were uniformly applied during the growing season. At all soil depths, the HY and MY zones had higher soil nutrient concentrations than the field average nutrient concentration. However, the LY zone had below field average soil nutrient concentration in the entire soil profile. The whole above-ground plants without grain in HY and MY zones had higher than average and the plants in the LY zone had lower than average nutrient concentrations throughout the cornfield. This site-specific nutrient variation in these zones was due to within-field terrain attributes, differences in soil properties, and surface runoff losses. A significant difference was recorded in the corn grain yield in the HY and LY zones of the field. Two extreme groups of nutrients were found in the cornfield similar to irrigation management zones (HY and LY). A zone with a higher yield also

had higher soil and plant nutrients in the zone (HY), and a zone with a lower yield had lower soil and plant nutrients in the zone (LY). Incorporating soil nutrient variability for site-specific management in management zone delineation can help with reducing nutrient application and nutrient loss, and improving yield. This study supports adoption of precision agricultural management practices based on in-field nutrient variability across the cornfield during the growing season.

3.2 Introduction

The world population is approximately 7.9 billion in 2022 with an average population growth rate of 0.9% annually (United States Census Bureau, 2022). Increasing population necessitates increasing crop grain yield. Precision management of agricultural practices, importantly nutrient and water management, during a growing season can help increase crop yield. Site-specific crop management is an important element of precision agriculture, which aims to manage within-field variability, increase crop productivity, reduce average production costs while optimizing resources, and foster environmental sustainability, thus improving land-use efficiency (Serrano et al., 2011). Farmers have been conventionally adopting a single rate for fertilizer or manure and irrigation application within a field. However, this uniform application leads to excessive nutrients or water in some areas and inadequate nutrients and water in others due to variability within the field (Mallarino and Wittry, 2004). Although farmers have been adopting uniform applications for irrigation and nutrients, they have been facing the issue of crop yield variability across the field and inadequate productivity in some parts compared to others. Such agricultural systems are inefficient and need to be improved with the aim of precision agricultural management. The irrigated land area has expanded by 5% in the last 15 years in the United States (USDA-NASS, 2019). However, the southeastern USA represents only 10% of the total irrigated land in the United

States. Although Alabama has a relatively small amount of irrigated land, irrigation adoption has increased by 25% from 2012 to 2017 (USDA-NASS, 2019). The future forecast of precipitation data showed the 14% increment in the annual average of precipitation by 2059, which would alter the time, erosivity characteristics, and distribution of the precipitation events (Takhellambam et al., 2021, 2022). The distribution of precipitation over the growing season is important to avoid water stress and meet crop water demand (Kumar et al., 2020, 2021b). Therefore, irrigation adoption has been increasing to help farmers to improve water use efficiency, avoid water stress, maintain adequate soil moisture, and reduce nutrient loss. Thus, knowing the within-field variability in soil nutrients, the adopting nutrient management practices (Serrano et al., 2011), and appropriate irrigation practices can help with improving nutrient availability to plants, reducing contamination of surface water due to surface runoff, and reducing pressure on freshwater availability during the growing season (Yost et al., 2019).

Soil nutrients are significant elements that support plant growth and crop productivity. Macronutrients (P, N, and K) are required in large quantities and are the focus of many interventions, unlike micronutrients (Fe, Mn, and Zn, etc.) that are required in small quantities. The deficiency of micronutrients can result in severe crop failure, while excess levels can lead to health hazards (Mathew et al., 2016). Inadequate management of macronutrients limits crop yield and causes loss of soil productivity. Proper and effective management of macronutrients and assessment of their effects on crop yield and environmental quality requires an understanding of their variability in concentration across the field (Morales et al., 2014). Phosphorus (P) and nitrogen (N) are essential macronutrients for plant growth, which affect crop yield. However, excess application of these nutrients in agricultural fields leads to contamination of surface and groundwater (Hanrahan et al., 2019) locally, regionally, and globally. Several factors are

responsible for nutrient loss from agricultural fields, including fertilizer application method, rate, and timing; irrigation rate; field topography; and soil properties (Hanrahan et al., 2019; Umali et al., 2012; Williams et al., 2018). To reduce nutrient loss in surface runoff, it is recommended not to irrigate soon after fertilizer application, and not to apply fertilizer or manure in any form before an impending rain event (Schröder et al., 2004; Sharpley, 1997; Smith et al., 2007). For surface application of manure, however, it is important to move these nutrients further into the soil where, for example, ammonia volatilization would be minimized. The longer the time between fertilizer or manure application and rainfall or irrigation, the smaller the nutrient loss in surface runoff (Schroeder et al., 2004). Therefore, understanding nutrient variability is key for site-specific management to help minimize nutrient input, and discourage constant rate application throughout the field without considering variability in crop yield, which can benefit farmers by decreasing production costs with the added advantage of environmental protection.

The levels of P and N vary temporally and spatially within a field (Bogunovic et al. 2014; Gao et al., 2019; Su et al. 2018; Umali et al. 2012). Many studies have investigated spatial variation in nutrient levels in cropland, but few studies have focused on spatiotemporal variations within the same cropland during a growing season (Su et al., 2018). Therefore, more studies on variability in soil nutrients in cropland at various growth stages during a growing season are needed to help farmers to increase crop yield and reduce nutrient losses. Nutrient uptake for plant growth depends on nutrient availability in soil across the field (Gallardo and Paramá, 2007; Su et al., 2018). The accumulation of nutrient proportion in the plants depends on their availability in the soil (Razaq et al., 2017; Tewolde et al., 2019). If fertilizer application is not managed properly, the plant's ability to take other nutrients from soils is reduced, and water quality is degraded due to surface runoff loss (Harmel et al., 2009). Also, inadequate P and N concentration in the plants negatively affects

the plant and root growth development, and consequently crop yield (Malhotra et al., 2018; Razaq et al., 2017). The leaching of nutrients in agricultural fields depends on soil physical characteristics, (Chakraborty et al., 2020) and the strength of binding forces between nutrients and soil (King et al., 2015). Understanding site-specific management of soil nutrients in agricultural fields has been a hot topic but challenging to study around the globe (Su et al., 2018) for adopting precision management practices. Various experiments have been performed to study nutrient variability from plot to watershed scales to compare nutrient levels between plots, fields, and watersheds. However, studies on temporal variability with implications on crop yield variability are still scarce, and the results from controlled experiments have limited applicability to the actual field. It is important to understand the within-field variation of nutrients at different depths and at different times and stages during a growing season (Bogunovic et al., 2014; Su et al., 2018). The nutrient uptake in plants varies according to the growth stage of a crop during the growing season (Su et al., 2018). The tasseling and silking stages in the corn, for example, are high nutrient demanding periods during a growing season. Knowing the nutrient level in the soil at different times can help to reduce yield loss or improve yield management. Therefore, it is important to investigate temporal variations in soil nutrients in crop fields during the growing season. Due to spatial variability in crop yield, it is important to optimize the agricultural systems to achieve the food demands by reducing the yield losses or improving yield management. Precision agriculture aims to improve site-specific yield management and identify the factors responsible for within-field variability that reduce the crop yield across the field (Jiang et al., 2021; McEntee et al., 2019). Therefore, studies need to investigate the significance of prevailing factors (field attributes, soil properties) influencing the nutrient variability, which is necessary for enhancing site-specific recommendations in farming practices, improving yield management, delineating management

zones, and contributing to the refinement of existing decision support tools. Precision farming studies need to fill the gap of inefficient yield productivity in some areas within the field due to poorly or uniformly managed agricultural systems.

Previous studies have focused on nutrient budgeting (quantification of nutrients before and after the crop) and variation in different agricultural fields (Bundy and Sturgul, 2001; Hanrahan et al., 2019). However, less is known about the nutrient variation during the growing season (at various stages of the crops) within the same cropland (Su et al., 2018). Therefore, this study investigated within-field nutrient (P and N) variability at different soil depths and its impact on crop yield in a 120 ha cornfield located in Alabama, USA during the 2019 growing season. We quantified levels of soil P and N at various times during the growing season to understand spatiotemporal variability across the field. The first objective of this study was to determine within-field soil nutrient variability at different times and depths in a crop growing period. We hypothesized that soil P and N vary greatly within a field even after adopting the same best management practice (BMP) throughout the field. The second objective was to identify the factors significantly affecting nutrient and crop yield variability. We hypothesized that crop yield is significantly correlated with nutrient variability during a growing season.

3.3 Materials and Methods

3.3.1 Study Area Description

This research was conducted in Town Creek (34°43'7.15"N, 87°23'9.36"W) Watershed of Lawrence County in the Tennessee Valley Region (TVR) of North Alabama, USA (fig. 3.1). The study region is classified as subtropical humid with average annual precipitation of 140 cm ("Monthly and Seasonal Climate Information | Southeast Regional Climate Center," 2020; Kumar et al., 2021b). The study was conducted in a 120 ha area of a cornfield during the 2019 growing

season. The growing season usually occurs from April to October and the distribution of total monthly precipitation over the 2019 growing season is shown in fig. 3.2. Dekalb® DKC 66-97, corn hybrid (Dekalb Genetics Corporation, DeKalb, IL, USA) was seeded with a seeding rate of 84,000 seeds per ha. The plant and row spacing in the field were 15 cm and 76 cm, respectively. Both manure and inorganic fertilizers were uniformly applied in the field during the growing season. Poultry litter was broadcasted uniformly on the soil surface at a rate of 4.5 Mg ha^{-1} using a mechanical spreader before the seeding and inorganic fertilizer was applied uniformly two times during the crop growing period (table 3.1). The application rate of nitrogen and phosphorus in the poultry litter was 105 kg ha^{-1} and 116 kg ha^{-1}, respectively. The first inorganic fertilizer application was applied at the rate of 67 kg ha^{-1} for nitrogen and 45 kg ha^{-1} for phosphorus and potassium at the time of seeding (table 3.1). The side-dress application was conducted at the rate of 201 kg ha^{-1} for nitrogen. The study area was equipped with a remotely controlled 625 m long Reinke center pivot irrigation system (Reinke Manufacturing Co., Inc., Deshler, NE, USA) with a mid-elevation spray application (MESA) sprinklers fitted with pressure regulators. With the uniform irrigation system, Kumar et al. (2020, 2021b) found soil moisture variability in the study field during the 2018 growing season. Therefore, the center pivot was retrofitted with variable-rate irrigation (VRI) technology with solenoid valves to control water application during the 2019 growing season. Uniformity testing of the center pivot irrigation system was performed before the growing season with the catch can test (Dukes and Perry, 2006; Irmak et al., 2011; Ortiz et al., 2021). Readers can follow Ortiz et al. (2021) for detailed and stepwise information. The field was under no-till management practices.

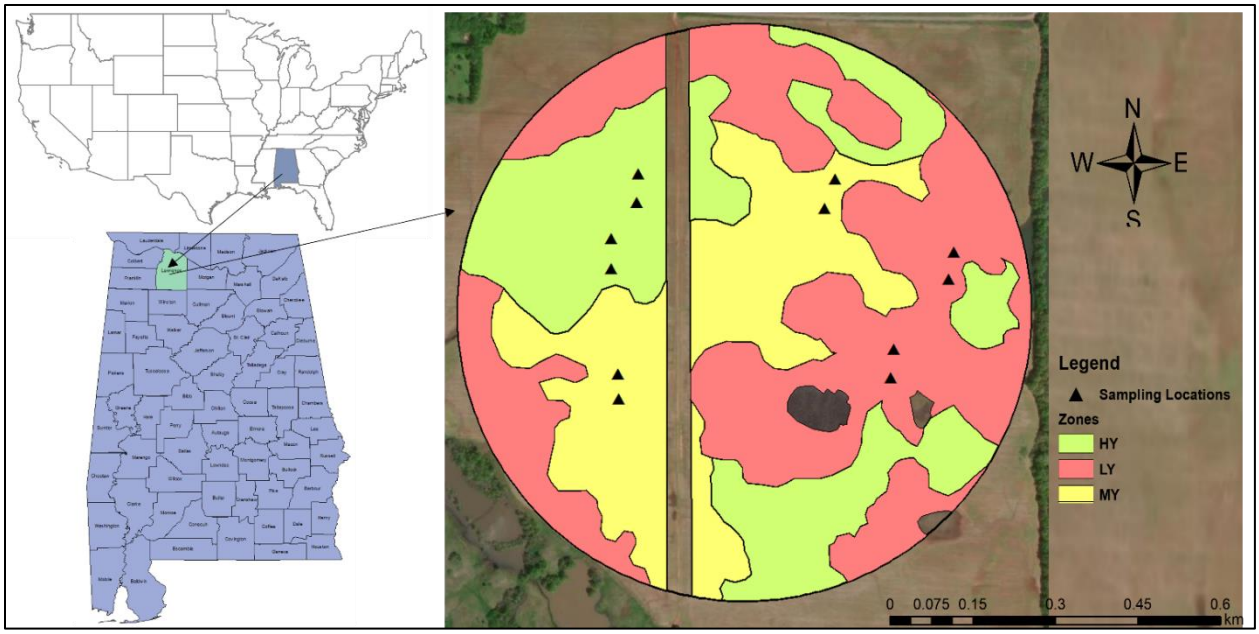

Figure 3.1 Cornfield with soil sampling locations for nutrient analysis during the growing season. HY is high yield zone, LY is low yield, and MY is moderate yield zone.

3.3.2 Field Measurements and Data Collection

Due to spatial and temporal variation in precipitation (Ridolfi et al., 2020), a weather station was installed near the field to measure precipitation locally during the growing season. Before soil sampling for nutrient analysis during the 2019 growing season, the field was delineated in different irrigation management zones based on topography, historical yield data, and soil texture (Kumar et al., 2021a) (fig. 3.1) using the Management Zone Analyst software (MZA, USDA-ARS, Columbia, MO, USA). A similar approach to delineating management zones was adopted by Jiménez et al. (2020) in South Alabama and Filho et al. (2020) in Central Alabama. This software uses unsupervised fuzzy classification to find homogenous areas with similar attributes using the input provided and creates boundaries at transitory areas between the zones (Fridgen et al., 2004). After processing the data through MZA software, three zones (namely, high yield-HY, moderate yield-MY, and low yield-LY) were identified. The areas covered by HY, MY, and LY zones were 34 ha, 30 ha, and 50 ha, respectively. To provide the information in the MZA software, elevation

data were collected using a John Deere StarFire^{TM} 6000 real-time kinematic GPS receiver (Deere and Company, Moline, IL, USA) mounted to the farmer's grain combine. The field varied in elevation from 168 m to 178 m above the mean sea level. The corn grain yield was collected using a yield monitor mounted on a combine with a differentially corrected real-time kinematic (RTK) GPS system. Based on historical yield data collected by the farmers, we found substantial yield variability across the field. Also, the corn grain yield for the 2019 growing season varied from 10125 kg ha^{-1} to 18829 kg ha^{-1} with an average (corresponding to each GPS point value) of 14258 kg ha^{-1} in the HY zone, from 9450 kg ha^{-1} to 17317 kg ha^{-1} with an average of 13941 kg ha^{-1} in the MY zone, and from 3139 kg ha^{-1} to 14301 kg ha^{-1} with an average of 10575 kg ha^{-1} in the LY zone. This corn grain yield was adjusted to 15.5 % moisture. Soil samples from several locations at 0-15 cm, 15-30 cm, and 30-60 cm soil depths were collected in the field to determine soil texture using the hydrometer method (Bouyoucos, 1962). The soil properties were determined for each depth. Average soil properties for each zone are summarized in table 3.2.

Table 3.1 Timeline of the 2019 corn growing season in the crop field.

SN	Task	Date	Remarks
1	1st soil sampling	March 21, 2019	Pre-plant soil sampling
2	Poultry litter application	March 21, 2019	4.5 Mg ha^{-1}
3	NPK application	March 28, 2019	67 kg ha^{-1} N, 45 kg ha^{-1} P_2O_5, and 45 kg ha^{-1} K_2O
4	Corn sowing	March 28, 2019	
5	2nd soil sampling	April 28, 2019	Post-plant soil sampling
6	Side dressing	May 5, 2019	201 kg ha^{-1} a N
7	3rd soil sampling	June 22, 2019	Silking stage soil sampling
8	4th soil sampling	August 1, 2019	Pre-harvest soil sampling
9	Corn harvesting	August 30, 2019	
10	5th soil sampling	September 11, 2019	Post-harvest soil sampling

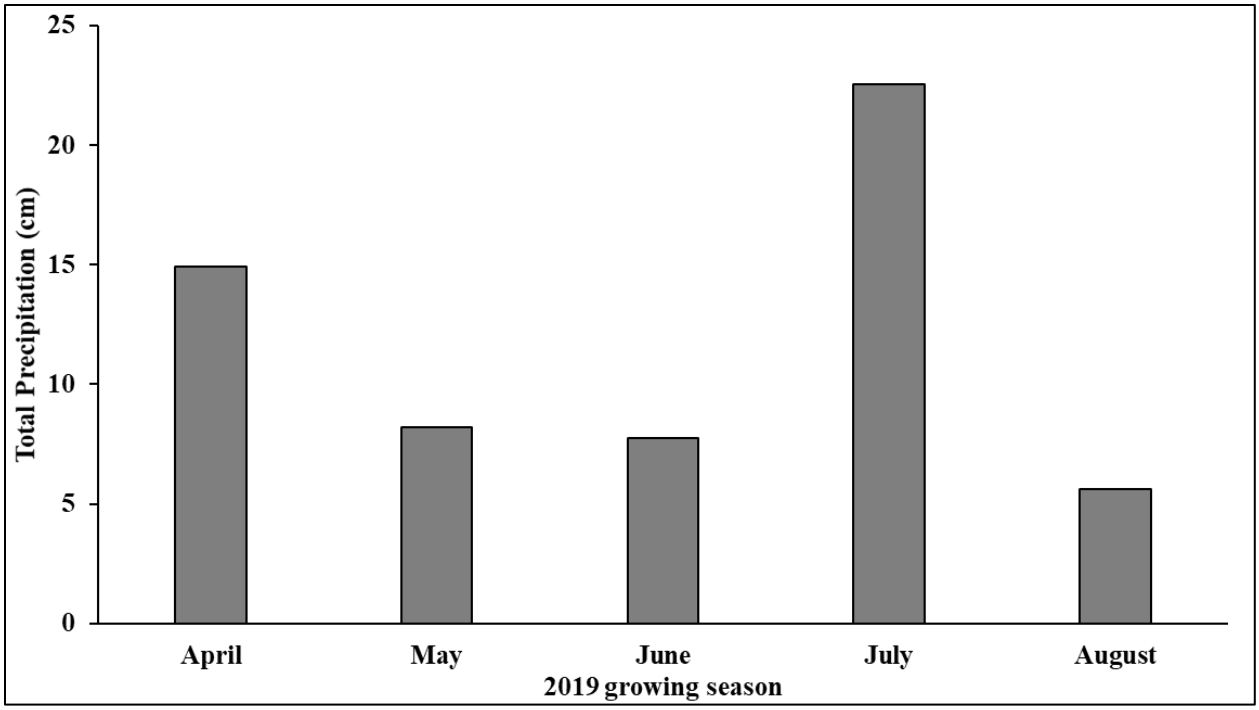

Figure 3.2 Total monthly precipitation received over the 2019 growing season.

Watermark soil moisture sensors (Irrometer Co., Riverside, CA, USA) were installed to monitor soil matric potential at 0-15 cm, 15-30 cm, and 30-60 cm depths. Site-specific deficit irrigation was prescribed within the field during the growing season. Irrigation was triggered when there was a deficit of about 2.54 cm (as the upper limit) of irrigation depth in the root zone as compared to field capacity in any zone within the field. Each zone received a deficit irrigation amount indicated by the sensor data in each zone. The reason to use 2.54 cm as the upper limit is that this was the maximum capacity of the center pivot irrigation system for applying irrigation in the field. The variability in precipitation and irrigation amount received in each zone was captured in soil matric potential data, which were used to determine irrigation depth to schedule irrigation. The field capacity and permanent wilting point were assumed at soil matric potentials of 33 kPa and 1500 kPa, respectively, as these are characteristic of the texture category of the soils. A total of four irrigations were scheduled on the cropland during the growing season. Although the total water

requirement for corn in Alabama is about 64 cm (Butler and Srivastava, 2007), the total amount of water received in the HY, MY, and LY zones was 69.72 cm, 70.10 cm, and 68.78 cm, respectively. The distribution of precipitation is very important over the growing season and has an impact on irrigation frequency and consequently on crop yield. Therefore, if the precipitation is received during a high water demand period, irrigation amount and frequency will be decreased, but if the precipitation is received at the beginning or near the end of the growing season, it does not have much impact on irrigation. According to Lee (2019), tasseling and silking are the highest daily water demand periods for corn during a growing season. In our field, the high water demand period (tasseling and silking) occurred from mid-May to mid-June during the 2019 growing season, and only 3 cm of precipitation was received during this interval of high water demand. The maximum precipitation was received at the beginning (April) and towards the end (July) of the growing season. Therefore, irrigation was required to meet the crop water demands. All irrigation events happened from May through June in the cornfield. However, no substantial differences were observed in the total water received by the HY, MY, and LY zones. Similar conditions have been observed by Filho et al. (2020) in Alabama and Irmak et al. (2012) in Nebraska, USA, and they triggered irrigation during such periods too.

After delineating the zones, soil samples were collected in the proximity of the Watermark sensors for nutrient analysis (fig. 3.1). A total of 540 soil samples (3 depths x 3 replicates x 3 zones x 4 locations x 5 sampling times) was collected for analysis before sowing to after harvesting the corn. The rationale behind the multiple locations was to capture maximum variability and reduce the uncertainty in soil nutrient data. Three replicates of collected soil samples were composited to attain a relatively homogenous sample for each individual depth at each location. Above ground plant samples (above-ground) were also collected at different corn growth stages in each

management zone for nutrient analysis of the plants (Geisseler et al., 2017; Jones and Case, 2018). A grid of 1 m x 1 m, which covered two rows, was used in each zone for plant sampling for nutrient analysis. According to the guidelines recommended by Geisseler et al. (2017) and Jones and Case (2018) for nutrient analysis in corn plant samples, the whole plants in the grid at the V4 stage were collected as the first plant sampling. For second and third plant sampling at the tasseling and silking stages, leaves opposite and below primary ears were collected. The plant heights and leaf area index (LAI) were also recorded in both zones at the silking stage of corn during the growing season. The LAI was measured using an LAI-2200 Plant Canopy Analyzer (LI-COR Environmental, Lincoln, NE, USA). Undisturbed soil samples were collected in each zone to develop soil water retention curves using an HYPROP measurement system (Meter Group Inc., Pullman, WA, USA) (Peters et al., 2015). These undisturbed soil samples were collected using 5 cm deep and 8 cm diameter stainless-steel rings. A detailed procedure for developing soil water retention curves is shown in Lena et al. (2021, 2022).

Table 3.2 Soil properties, sand (%), silt (%), clay (%), soil organic matter (SOM, %), bulk density (g cm^{-3}), and pH in each zone. Within each zone, mean values (± standard deviation) of various soil properties followed by the identical letter are not significantly different at the 0.05 significance level.

Zone	Sand (%)	Silt (%)	Clay (%)	Soil texture	SOM (%)	Bulk density (g cm^{-3})[bd]	pH
HY	16 ± 9.06 a	47.93 ± 10.65 a	36.07 ± 15 a	Silty clay loam	3.94 ± 0.40 a	1.60 ± 08 a	5.82 ± 0.60 a
MY	22.31 ± 6.55 a	40.67 ± 8.06 a	37.02 ± 9.52 a	Clay loam	4.18 ± 0.69 a	1.60 ± 06 a	5.13 ± 0.55 b
LY	30.36 ± 7.86 b	28.87 ± 9.27 b	40.78 ± 8.78 a	Clay	4.50 ± 0.78 b	1.67 ± 08 a	5.35 ± 0.68 b

[bd] Dry bulk density, calculated as mass of oven-dried soil / volume of soil sample.

3.3.3 Sample Processing

In the next step, the composited soil samples were oven-dried and ground using a soil grinder and passed through a 2-mm sieve for chemical analysis. The grinder was cleaned with a vacuum cleaner between the samples. The soil samples were analyzed for total P, total N, ortho-phosphorus (OP), and soil organic matter (SOM). The SOM was determined using the loss-on-ignition method (Wright et al., 2008) in the Soil and Water laboratory of the Department of Biosystems Engineering at Auburn University. For OP determination, colorimetric analysis (ammonium-molybdate-ascorbic method) was used (Ahmad et al., 2020; Harmel et al., 2009). The OP ions react with ammonium molybdate and antimony potassium tartrate under acidic conditions to form a molybdate-phosphate complex. The samples were extracted using distilled water (DI, pH = 6.95) for OP analysis with 3 g soil in a 50 mL centrifuge tube. The centrifuge tube was filled with DI water up to 30 mL solution of soil and water (1:10::soil:solution). After centrifuging each sample at 4600 rpm for 30 minutes at 10 °C or less, samples were filtered through Whatman no. 42 filter paper in scintillation vials. The scintillation vials were stored in a refrigerator at 4 °C and analyzed within 24 hours for OP. Total P and total N in soil samples were determined by acid digestion using persulfate Kjeldahl digesting solution (Dayton et al., 2017, American Public Health Association, 1998). All the standard solutions including blanks were also digested to keep a similar matrix for the analysis. A 0.5 g sample was digested in a 6 mL digesting solution and centrifuged before the analysis. A Lachat automated flow injection analyzer (Quikchem series 2) (Hach Company, Loveland, CO, USA) was used to analyze these nutrients in the soil samples. To ensure the accuracy of analyses and avoid discrepancies, we ran standard and blank solutions after every 15 samples. The plant samples were analyzed for total P using ICAP-Open vessel wet digestion Digi Block 3000 and for total N using LECO-Nitrogen gas analyzer by Waters Agricultural

Laboratories, Inc. (Camilla, GA). Plant samples were oven-dried at 80 °C. The dried samples were ground in a Wiley model 4 mill to pass through a 20 mesh (1.0 mm) screen before lab analyses. The mill was cleaned with a vacuum cleaner between the samples.

3.3.4 Hydrological Properties Analysis of the Field

To understand nutrient variability for site-specific management, the knowledge of within-field hydrology is important. Different terrain analyses using collected elevation data were conducted to evaluate the significant factors that can affect site-specific nutrient variability and that need to be considered in precision nutrient management. The slopes and topographical wetness index (TWI) (Beven and Kirkby, 1979) were determined using ArcGIS (version 10.3.1) (Esri, Redlands, CA, USA). Maps of TWI and slope were developed to understand the topographical variation in these three different zones (fig. 3.3a and 3.3b). TWI explains the potential high and low water accumulation areas within the landscape. A low TWI value represents a low water accumulation and high slope area, and a high TWI value represents a high water accumulation and relatively level area with a low slope (Qin et al., 2011). Maestrini and Basso (2018) found the areas that allow water accumulation without runoff and waterlogging exhibits large TWI values. The surface drainage lines (fig. 3.3b) were also delineated to understand the direction of the surface water flow within the field.

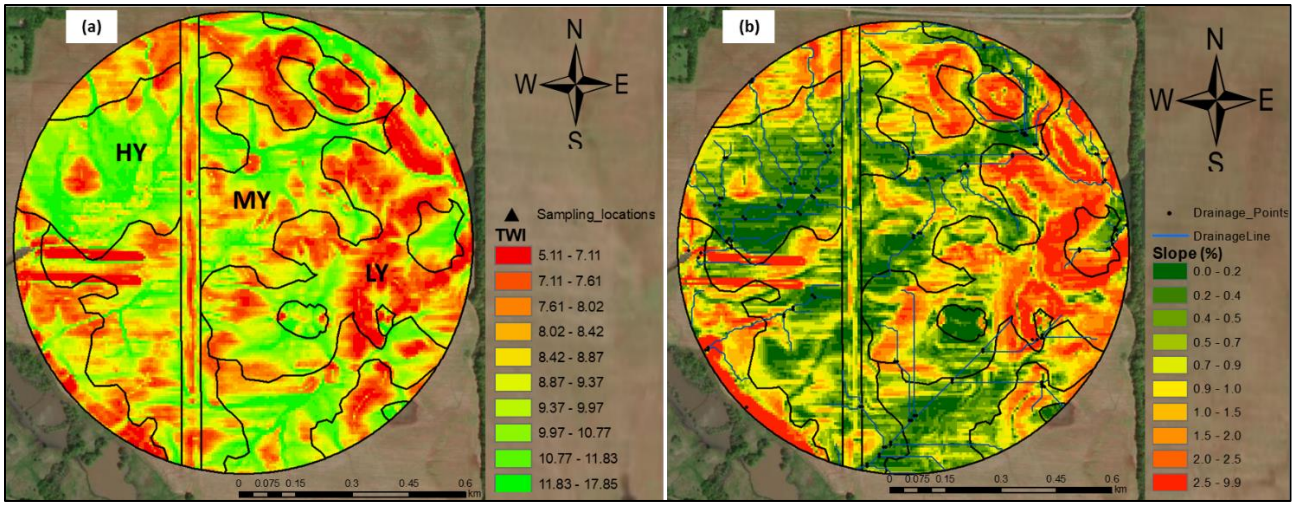

Figure 3.3 Terrain maps showing (a) Topographic wetness index (TWI) variation and (b) Slope and surface drainage pattern in the cornfield.

3.4 Statistical Analysis

In this section, we will use the following indices for notation:

- The sampling time is indexed by j, with $j = 1,2,\ldots.N$ (where N = 5, number of sampling times);
- The sampling zone is indexed by k, with $k = 1,2,3$, and the specific sampling location is indexed by i, with $i = 1,2,\ldots.M$ (where M = 12, number of sampling locations);
- The sampling depth is indexed by l, with $l = 1,2,3$.

Considering these notations, it is assumed that the samples analyzed for nutrients are independent of each other at the same depth (for example, 0-15 cm soil samples are independent between all locations). This assumption is valid because any two sampling locations were at least approximately 100 m apart. In addition, we used C as a common symbol for nutrient concentration in this study. The nutrient concentration C_{ijl} at each sampling location i, each day j, and each depth l was used to calculate different statistical features to understand the variability in nutrients during the growing season. The spatial mean ($\bar{C}_{jl}$) for each sampling time was calculated

$$\bar{C}_{jl} = \frac{\sum_{i=1}^{M} C_{ijl}}{M} \tag{3.1}$$

The temporal mean ($\bar{C}_{il}$) was calculated as

$$\bar{C}_{il} = \frac{\sum_{j=1}^{N} C_{ijl}}{N} \tag{3.2}$$

The spatial standard deviation $\left(\sigma(C_{jl})\right)$ and coefficient of variation $\left(CV(C_{jl})\right)$ of nutrients for each sampling time is given by

$$\sigma(C_{jl}) = \sqrt{\frac{1}{M-1}\sum_{i=1}^{M}\left(C_{ijl} - \bar{C}_{jl}\right)^2} \tag{3.3}$$

$$CV(C_{jl}) = \frac{\sigma(C_{jl})}{\bar{C}_{jl}} \tag{3.4}$$

In the same way, the temporal standard deviation $\sigma(C_{il})$ and coefficient of variation $CV(C_{il})$ can be calculated for each location. The nutrient data were normalized based on the average concentration to understand the variation at different sampling locations and at different sampling times in the cropland during the growing season. The relative difference, $\delta(C_{ijl})$, for each location and time was defined as

$$\delta(C_{ijl}) = \frac{\left(C_{ijl} - \bar{C}_{jl}\right)}{\bar{C}_{jl}} \tag{3.5}$$

Based on the relative difference, the mean relative difference ($\bar{\delta}_{c,il}$) and standard deviation of relative difference $\left(\sigma(\bar{\delta}_{c,il})\right)$ for each location (i) and each depth (l) can be given by

$$\bar{\delta}_{c,il} = \frac{\sum_{j=1}^{N} \delta(C_{ijl})}{N} \tag{3.6}$$

$$\sigma(\bar{\delta}_{c,il}) = \sqrt{\frac{1}{N-1}\sum_{j=1}^{N}\left(\delta(C_{ijl}) - \bar{\delta}_{c,il}\right)^2} \tag{3.7}$$

To understand the zone-wise nutrient variation within the field during the growing season, the results were clustered according to zones based on sampling locations in the respective zones. The mean relative difference quantifies the departure of a nutrient in a zone from the average field nutrient and distinguishes whether the zone was lower or higher than the mean field nutrient during the growing period. A value of the mean relative difference in a zone at a certain depth greater or less than zero indicates adequate or inadequate conditions of nutrients concentration in the field, respectively. The analyses were carried out at each depth (l) independently. The Spearman's rank correlation (r_s) was computed to understand the association between the variables during the growing season.

Finally, in order to consider all effects jointly, and the repeated observations over time, we employed a mixed linear model with nested random effects to assess nutrient variation between different zones and depths during the growing season. Since all effects are factors that can be represented by their respective indices, the model can be written as

$$C_{ijkl} = \beta_0 + \beta_j + \beta_k + \beta_l + \beta_{kl} + \gamma_k + \gamma_{k(i)} + \gamma_{k(i(l))} + \epsilon_{ijkl} \tag{3.8}$$

where β_m is the coefficient of the fixed effect for a general level m ($m\ is\ general\ level\ for\ all\ \beta\ and\ \gamma\ coefficients\ such\ as\ 0, j, k, l$), γ_m is the random effect for a general level m, and ϵ is the error term. More specifically, β_{kl} represents the fixed effect interaction between zone and depth while $\gamma_{k(i)}$ and $\gamma_{k(i(l))}$, respectively, represent the

random effect of location (nested in the zone k) and depth (nested in the zone k and location i). Aside from taking into account the sampling time through the coefficient β_j, this mixed linear model aims to account for and isolate the dependence in the data due to the repeated measurements over time for each depth, location, and zone. By doing so, it is possible to obtain more precise and reliable testing for the fixed effects of interest which relate to the effect of time, zone, and depth on the nutrient concentration during the growing season. This approach has been adopted and promoted in other soil science studies dealing with data collected over different locations in space (Slaets et al., 2021). All the statistical analyses were performed using R software (R Project for Statistical Computing software (https://www.r-project.org/)) at a 0.05 significance level. Also, Moran's I test (Plant, 2018) was conducted on the residuals of the model to evaluate the spatial autocorrelation among them. This test led us to state that the observations have no spatial autocorrelation among them. The p-values (0.26, 0.29, and 0.49, for total P, OP, and total N, respectively) obtained were too high as compared to 0.05 to reject the null hypothesis of no-autocorrelation for each nutrient. The Bonferroni correction was used for multiple comparisons (Plant, 2018). From now onwards, the corresponding nutrient symbols will replace general notation C. For example, if we discuss soil total P, we will use TP in place of C to explain our results.

3.5 Results and Discussion

3.5.1 Soil P Variability During the Growing Season

The mean relative difference oin P at three soil layers (0-15 cm, 015-30 cm, and 30-60 cm) of each zone, were computed during the growing season, to understand the variation in the entire soil profile. Based on the relative difference approach and mixed-linear model, the spatiotemporal patterns in total P between the zones across the cornfield were significantly different. According

to $\bar{\delta}_{TP}$ in soil, total P, HY and MY zones had a positive value, and the LY zone had a negative value at all three soil depths. For an average condition of soil total P in any zone, $\bar{\delta}_{TP}$ should be zero. Therefore, it explained the adequate condition of soil total P in the HY and MY zones and inadequate conditions of soil total P in the LY zone compared to the average soil total P within the field during the 2019 growing season (fig. 3.4). The $\bar{\delta}_{TP}$was +0.17, +0.29, and +0.37 in the HY zone in 0-15 cm, 15-30 cm, and 30-60 cm soil profiles, respectively, during the growing season. However, in the LY zone, $\bar{\delta}_{TP}$ was -0.46 in 0-15 cm, -0.53 in 15-30 cm, and -0.38 in 30-60 cm soil profile. This pattern of total P variability indicated that the LY zone was low in soil total P relative to the average total P concentration in the field during the growing season. The mixed model explained a similar pattern of variability in total P during the growing season. The significant differences in total P were noticed between HY and LY, and MY and LY zones; however, there was no significant difference between HY and MY zones during the growing season. The effects of depth, time, zone, and interaction between zone and depth were significant for soil total P in the study. The variation in the field topography, soil physical and hydraulic properties, and field hydrology (Plach et al. 2019; Reid et al. 2019) resulted in the variable soil P levels across the cropland field, which are discussed in the following sections.

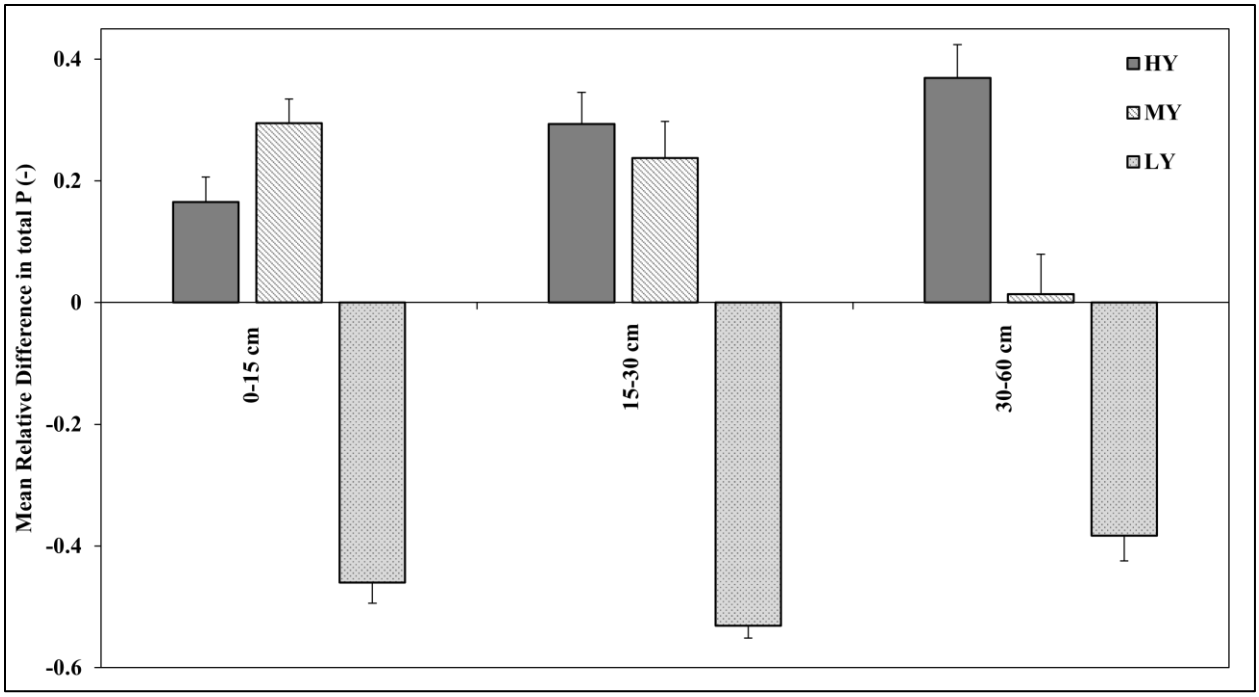

Figure 3.4 Mean relative difference in soil total P in zones at varying soil profiles during the growing season. Error bars represent standard deviation in relative difference.

The total P data showed that the spatiotemporal mean of total P varied during the 2019 growing season, with the mean (CV) of 553 (0.13) mg kg^{-1}, 617 (0.13) mg kg^{-1}, and 257 (0.20) mg kg^{-1} in the 0-15 cm soil profile of HY, MY, and LY zones, respectively. In 15-30 cm soil profile, soil total P was 510 (0.10) mg kg^{-1} in HY, 489 (0.16) mg kg^{-1} in MY, and 185 (0.14) mg kg^{-1} in LY zones. In 30-60 cm soil profile, soil total P was 467 (0.10) mg kg^{-1} in HY, 342 (0.27) mg kg^{-1} in MY, and 208 (0.23) mg kg^{-1} in LY zones. Based on descriptive analysis, huge differences in within-field variability of soil total P were found across the zones during the growing season. The baseline (pre-plant sample) total P concentrations in the 0-15 cm soil profile before the planting were 550 (0.14) mg kg^{-1}, 601 (0.13) mg kg^{-1}, and 234 (0.24) mg kg^{-1} in the HY, MY, and LY zones, respectively. At the end of the growing season (post-harvest) in the 0-15 cm soil profile, the total P concentration were 534 (0.12) mg kg^{-1}, 544 (0.16) mg kg^{-1}, and 236 (0.26) mg kg^{-1} in the HY, MY, and LY zones, respectively. In the middle soil profile (15-30 cm), total P varied from 487

(0.12) mg kg^{-1} at baseline to 530 (0.08) mg kg^{-1} at end of the growing season in the HY zone. However, in the LY zone, the total P varied from 188 (0.13) mg kg^{-1} at baseline to 180 (0.06) mg kg^{-1} at end of the growing season. At the deepest soil profile (30-60 cm), total P varied from 488 (0.08) mg kg^{-1} at baseline to 455 (0.16) mg kg^{-1} at end of the growing season in the HY zone, from 331 (0.26) mg kg^{-1} at baseline to 313 (0.29) mg kg^{-1} at end of the growing season in the MY zone, and 212 (0.25) mg kg^{-1} at baseline to 214 (0.25) mg kg^{-1} at end of the growing season in the LY zone. The variability in soil total P showed that the HY zone had a greater and LY zone had a lower soil total P concentration than the average concentration of soil total P in all depths during the growing season, which means soil total P had different spatial variability between the HY and LY zones, and this needs to be considered in management zone delineation. It will help farmers to make decision with precision farming practices in terms of variable nutrient management of zones within a field. Availability of P is rarely adequate for optimum growth and development of plants due to soil fixation (Malhotra et al., 2018). Soil OP also had similar spatial variability within HY and LY zones. Therefore, according to our analysis, lower soil total P than average in the LY zone might have restricted the release of soil total P to OP and limited the supply to the plants in a similar proportion as the HY zone. Plants in the HY and LY zones did not accumulate nutrients in the same proportion due to differences in the availability of nutrients in soils, which affected the growth of the plants. Plants in the LY zone were smaller and had lower total P concentration compared to the HY zone due to lower P concentrations available in the LY zone, which impacted the crop yield. Serrano et al. (2011) also found the similar pattern of variability in phosphate greater and lower than average in a pasture field.

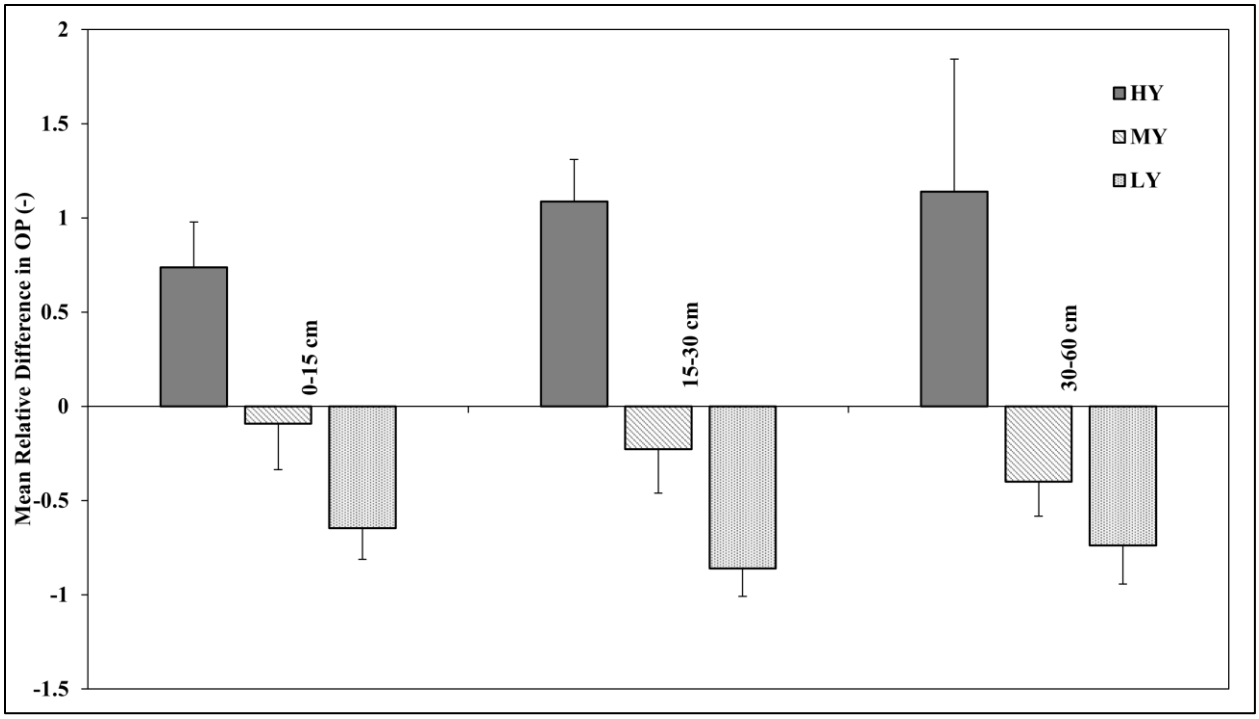

Figure 3.5 Mean relative difference in soil OP during the growing season. Error bars represent standard deviation in relative difference.

A similar trend of the mean relative difference in soil total P was also followed by soil OP (fig. 3.5). The HY zone had maximum, and the LY zone had minimum soil OP within the field. However, the MY zone was held between HY and LY zones. It explained the adequate condition of soil OP in the HY zone and inadequate conditions in the LY zone compared to average soil OP during the growing season (fig. 3.5). The mixed model also explained a similar pattern of variability in soil OP during the growing season. The HY zone was significantly higher in soil OP as compared to the LY zone. The deeper soil profiles were significantly lower in soil OP as compared to the topsoil profile (0-15 cm) in the HY zone. The effects of zone, depth, and time were significant for soil OP in the cropland. However, the depth did not have any interaction effect with the zones during the growing season. The mean relative difference showed an increasing pattern in soil total P and OP with soil depths in the HY zone. It showed the difference in soil P concentration increased with increasing soil depth as compared to average soil P concentration

within the field corresponding to respective soil profiles during the growing season. However, the LY zone always had below average soil P concentrations during the growing season. Differences in soil physical and chemical properties across the zones may have caused soil P variability during the growing season. The HY zone had a saturated hydraulic conductivity of 63 cm day^{-1}, and the LY zone had 9 cm day^{-1}. Within-field hydraulic conductivity variability in the HY and LY zones can help explain this variability. The downward movement of nutrients depends on water movement, i.e., infiltration and percolation (Defterdarović et al., 2021). A slow rate of water movement in the LY zone decreased the flow of nutrients and more opportunity for P fixation. Therefore, soil OP differences increase with increasing soil depth in the LY zone compared to the HY zone. Lower soil OP in the root zone reduced the nutrient uptake by plant roots, which affected the plant and root growth. The concentration of P affects plant reproduction, plant stalk strength, plant growth, and crop yield (Beegle and Durst, 2014). It was noticed that the plants in the LY zone were smaller in height than in the HY and MY zones. According to the average plant height measurements at the silking stage, the plant height in the HY and LY zones were 225 cm and 195 cm, respectively. Also, the LAI was 4.13 $cm^2\ cm^{-2}$ and 3.34 $cm^2\ cm^{-2}$ in the HY and LY zones, respectively. Phosphorus is required for the growth and development of plants (Dhillon et al., 2017). It is also necessary for energy transfer produced through photosynthesis to be used for reproduction (Malhotra et al., 2018). Availability of P in soil affects plant uptake and consequently plant and root growth (Razaq et al., 2017). This showed that an inadequate amount of P decreased the plant growth, and energy transfer for photosynthesis, and increased plant stress in the LY zone, which ultimately affected crop productivity. Similar results have been reported by Dhillon et al. (2017) and Malhotra et al. (2018). The applied fertilizers and manures were washed away due to the surface runoff during the growing season since erosion patterns were observed in the LY zone.

3.5.2 Soil N Variability During the Growing Season

The HY and MY zones had positive values of $\bar{\delta}_{TN}$ at all three depths (0-15 cm, 15-30 cm, and 30-60 cm) during the growing season. However, the LY zone had negative values for $\bar{\delta}_{TN}$ in the entire soil profile. The positive values describe the adequate condition of soil total N in the HY and MY zones and inadequate conditions of soil total N in the LY zone compared to the average soil total N within the field during the 2019 growing season, since the plant height and LAI were smaller in the LY zone as compared to the HY zone. In the HY zone, the $\bar{\delta}_{TN}$ was +0.01, +0.03, and +0.04, respectively, in 0-15 cm, 15-30 cm, and 30-60 cm soil profiles during the growing season. However, in the LY zone, $\bar{\delta}_{TN}$ was -0.04, -0.05, and -0.07, respectively, in 0-15 cm 15-30 cm, and 30-60 cm soil profiles during the growing season.

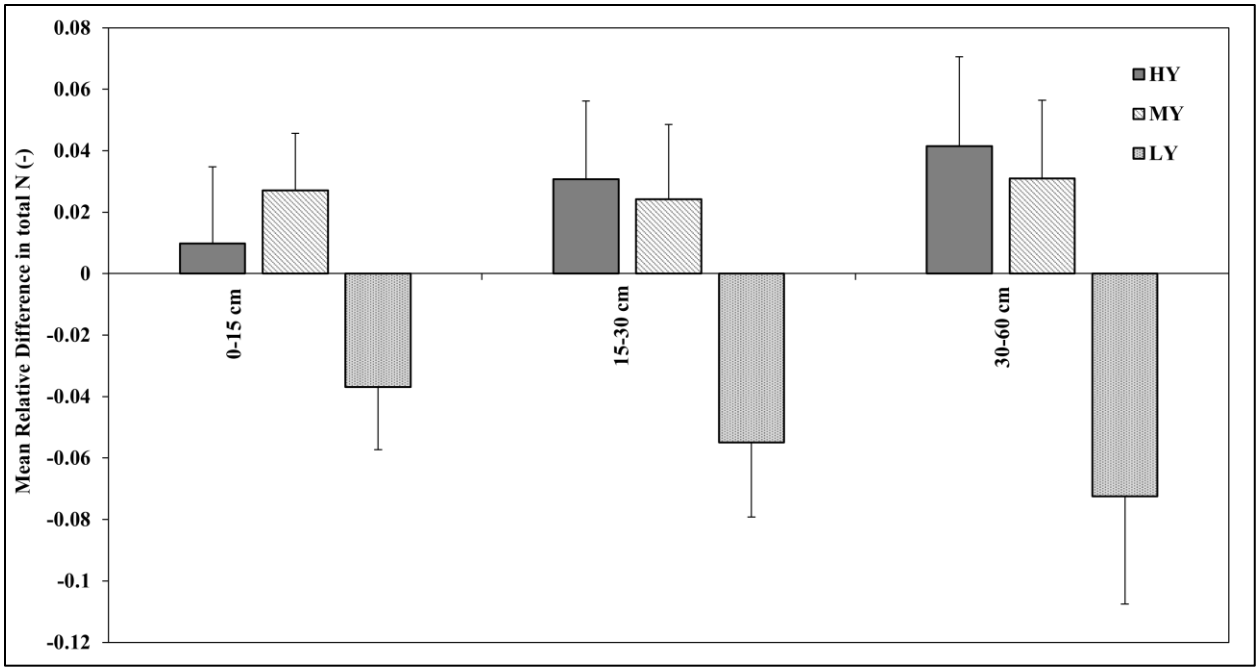

Figure 3.6 Mean relative difference in soil total N during the growing season. Error bars represent standard deviation in relative difference.

A $\bar{\delta}_{TN}$ value close to zero represents the average soil total N concentration within the field during the growing season. The trend in total N variability showed that the soil total N was lower in the

LY zone and greater in the HY zone compared to the average total N concentration within the field during the growing season. Tewolde et al. (2019) found that N accumulation in the plants in proportion highly depends on N availability in the soil. Our analysis showed that soil total N was not uniformly available throughout the field during the growing season. The HY zone had a higher proportion available as compared to the LY zone, which revealed that N also had the corresponding spatial variability in these zones similar to P. According to Tewolde et al. (2021), N becomes approximately 35% available after applying poultry litter in the same season and enhances the crop yield. In our study field, farmers uniformly applied poultry litter first and inorganic fertilizer afterward. Levels of N and crop yield were greater in the HY zone as compared to the LY zone in all samplings. It was inferred from this analysis that the LY zone always had lower soil total N than the HY zone throughout the season, and variable management practices need to be adopted in such conditions for precision farming. Similar to P, N is also an important component for supporting plant and root growth (Razaq et al., 2017). Plant height and LAI at the silking stage were lower in the LY zone than in the HY zone, which revealed that N availability was lower in the LY zone for plant uptake and deceased plant growth and development as compared to the HY zone. The linear mixed model of soil total N also explained a similar trend across the field during the growing season. The linear-mixed model resulted in a lower soil total N in the LY zone than in the HY and MY zones during the growing season. It was also found that deep soil layers were significantly lower in soil total N than the topsoil profile across the crop field. However, no interaction between zones and soil profiles was reported in soil total N. The effects of the zone, depth, and time were significant for soil total N in the cropland. However, the depth did not have any interaction effect with the zones during the growing season. A significant effect of sampling time was observed in soil total N when the sampling was done during post-plant, silking, and pre-

harvest times. Time as a fixed effect showed a significant effect on soil total N during the growing season. This was caused by additional nitrogen application by the farmers as the conventional application of inorganic fertilizer during the growing season. The spatiotemporal mean of soil total N concentration in the soil profile of 0-15 cm was 3.75 (0.05) g kg^{-1} in the HY zone, 3.81 (0.04) g kg^{-1} in the MY zone, and 3.57 (0.05) g kg^{-1} in the LY zone during the 2019 growing season. In the 15-30 cm soil profile, the total N concentrations were 3.52 (0.05) g kg^{-1} in HY zone, 3.50 (0.05) g kg^{-1} in the MY zone, and 3.23 (0.06) g kg^{-1} in LY zone. In the 30-60 cm soil profile, total N was 3.45 (0.05) g kg^{-1} in the HY zone, 3.45 (0.05) g kg^{-1} in the MY zone, and 3.10 (0.08) g kg^{-1} in the LY zone. The positive increasing trend of the mean relative difference in soil total N with increasing soil depths was observed in the HY zone. However, a negative increasing trend of the mean relative difference in soil total N with increasing soil depth was found in the LY zone during the growing season. This trend explained the high soil total N in the HY zone and low total N in the LY zone concerning the average soil total N within the field at the corresponding soil depths (fig. 3.6).

3.5.3 Variability in Nutrients Retained in the Plants During the Growing Season

Levels of soil nutrients provide major guidelines for fertilizer management in current and future growing seasons. However, the status of nutrients retained in the plants can be a complementary guideline to adopting BMPs for nutrient management and for comprehending the spatial variability in the corn grain yield. We investigated the plant total N and total P for variability in nutrients retained in the plants at different stages during the 2019 growing season. According to the mean relative difference in plant total N and total P, the HY and MY zones had a positive value, and the LY zone had a negative value (fig. 3.7). Nutrients which accumulated in the plants had a greater concentration in the HY zone and a lower concentration in the LY zone compared to the average

concentration of plant nutrients within the field. Nitrogen and P are critical nutrients for plant growth and root development, which are important components useful in evaluating the effect of nutrients on both plant and root growth. Razaq et al. (2017) found that higher N and P concentrations in the plant tissue and application of nutrients in the field significantly affected the plant height and root growth. Similarly, we found that plant growth and nutrients in plant tissue were lower in the LY zone and greater in the HY zone due to lower soil nutrient concentrations available within the LY zone than HY zone. Mean plant heights were 225 cm in the HY zone and 195 cm in the LY zone. The observed LAI was 4.13 $cm^2\ cm^{-2}$ in the HY zone and 3.34 $cm^2\ cm^{-2}$ in the LY zone at silking stage. The plants in the LY zone had a lower possibility of nutrient uptake due to lower nutrient concentration available in the soil as found in previous studies (Pereira et al., 2020; Razaq et al., 2017; Tewolde et al., 2021), which affected the plant height, growth, and productivity in the LY zone. Therefore, plants in the HY zone had adequate nutrients and the LY zone had inadequate nutrients during the growing season (fig. 3.7). The plant nutrients had a similar pattern of variability as in the soil nutrients obtained across the field. This revealed the negative impact of nutrient loss in the LY zone on plant growth and crop yield (fig. 3.8). Therefore, the results of this study showed that yield in the HY zone was related to adequate soil and plant nutrients in the HY zone, and yield in the LY zone was related to inadequate soil and plant nutrients in the LY zone during the growing season.

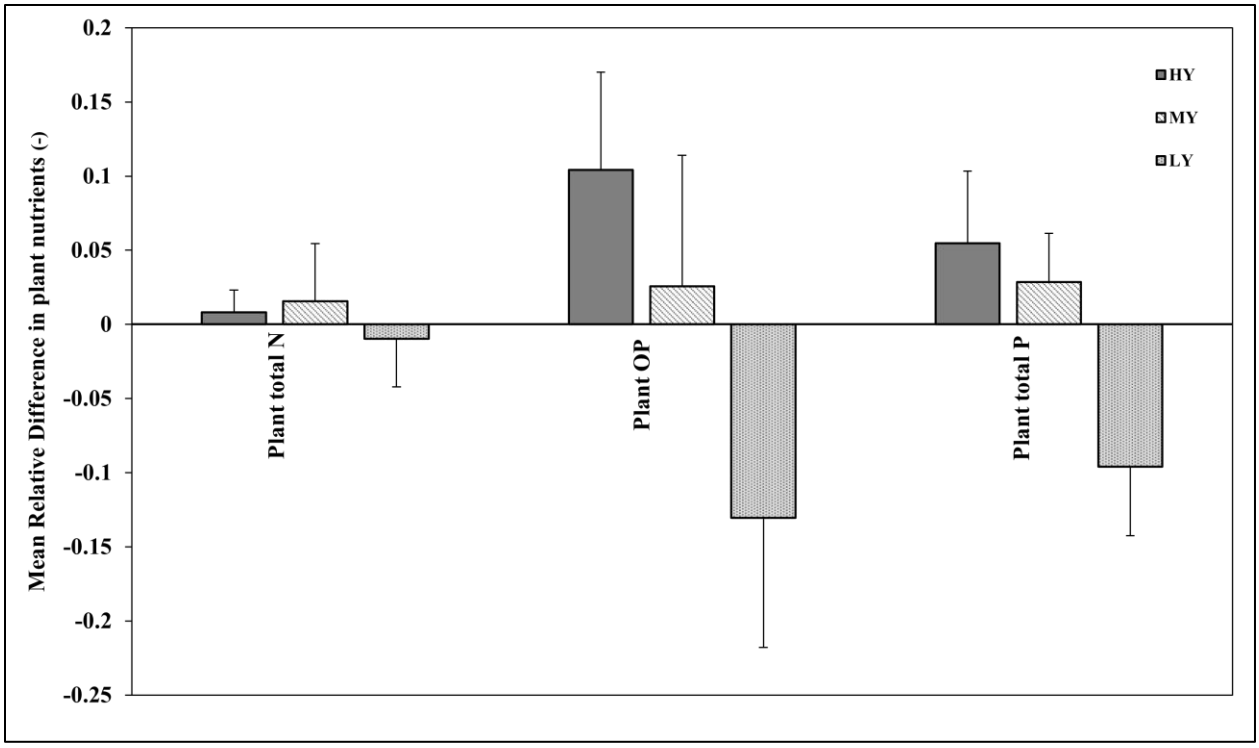

Figure 3.7 Mean relative difference in plant nutrients during the growing season. Error bars represent standard deviation in relative difference.

3.5.4 Factors Responsible for Site-Specific Nutrient Variability

The above-mentioned nutrient variability in different management zones led to the investigation of different factors (e.g., topography, soil properties, and hydrology of the field) that caused variation within the field. The TWI map (fig. 3.3a) showed lower values of TWI in the LY zone which led to a lower concentration of OP (slow conversion of total P into OP due to lower wetness for the mineralization process) during the growing season. Also, lower TWI in the LY zone led to lower total P and total N concentration in LY and higher TWI in HY led to high total P and total N in the zone. This lower TWI affected the mineralization process that is affected by biotic and abiotic factors, including organic P substrate availability and the geochemical properties of soil (Shaw and Cleveland, 2020). Mineralization is a slow process, and this could have been an issue for a decade in the field, which resulted in low plant-available P and N in the LY zone. Ultimately,

these long-term processes reduced the productivity in this part of the field. We also calculated r_s between TWI and the temporal average of soil nutrients to understand the relationship with TWI across the crop field (table 3.3). The correlation coefficients were significant in the soil profiles for soil nutrients during the growing season. Based on a positive correlation between TWI and nutrient concentrations, a higher TWI value in the HY zone was correlated with the higher nutrient concentrations in HY, and a lower value of TWI in LY was correlated with the lower nutrient concentrations in the LY zone. The soil P had a stronger correlation in upper soil layers than in the deep soil layer. This explained the stronger soil P dependency on topographic wetness index (TWI) at the upper soil layer than in the deep soil layers. However, soil total N had a stronger correlation with TWI in the deep soil layers than in the upper soil layers. This implied the strong soil N dependency on TWI in deep soil layers.

Table 3.3 Correlation coefficients between terrain attributes and soil nutrients in the cornfield. Asterisks (*) indicate significance at the 0.05 level.

	TWI			Slope		
	0-15 cm	**15-30 cm**	**30-60 cm**	**0-15 cm**	**15-30 cm**	**30-60 cm**
Soil TP	0.74*	0.82*	0.76*	-0.84*	-0.78*	-0.56*
Soil OP	0.80*	0.76*	0.34	-0.71*	-0.52*	-0.18
Soil TN	0.64*	0.78*	0.81*	-0.68*	-0.78*	-0.80*

Erosion gullies were observed in the LY zone during the growth stages and after harvesting, which revealed nutrient loss due to surface runoff and topographical variations in the field. The topographical variations can be understood using the slope variations in the field (fig. 3.3b). A high slope area increases the chance of lateral water movement and reduces infiltration (Huat et al., 2006). In our study field, the LY zone had a higher elevation and slope than the HY zone. Previous studies have found that higher elevation and steep fields tend to have higher erosion and runoff, lower infiltration, and lower soil productivity (Jiang and Thelen, 2004). We found similar results in our study, that slope was greater and hydraulic conductivity was lower in the LY zone

as compared to the HY zone. The lower hydraulic conductivity and greater slope contributed towards the generation of surface runoff in the LY zone. The runoff generation was one of the dominant factors for lower nutrient concentration in the LY zone; also reported by Plach et al. (2018) and Smith et al. (2007) in their studies. Greater slope and lower TWI values in the LY zone did not create the conditions for water accumulation, so greater slope and lower TWI this caused loss of nutrients with generated surface runoff. However, the HY zone with greater TWI and lower slope had a greater water accumulation condition, which allowed the nutrients to be retained in the zone. This lack of surface runoff reduced the loss of nutrients in the HY zone. Therefore, the HY zone behaved as a pool for nutrients due to no surface runoff and high water accumulation, and no erosion patterns were observed during and after the growing season.

We also computed r_s between slope and the temporal mean of soil nutrient concentrations to explain the relationship of soil nutrients with slope across the cropland. The r_s values were significant for all nutrients except soil OP at 30-60 cm soil layer (table 3.3). A negative correlation between nutrient concentrations and slope explained that a lower slope in the HY zone had higher nutrient concentrations in the HY zone, and a higher slope in the LY zone had lower nutrient concentrations in the LY zone. Similar relationships were obtained in earlier studies conducted in Michigan, USA (Jiang and Thelen, 2004). Less availability of soil nutrients in certain areas of the field reduced the crop yield. The weak binding of nutrients with soils due to dominant hydrological characteristics (TWI, slope, runoff) and soil physical properties in the LY zone enhanced losses. The surface runoff, TWI, erodibility, and slope across the field induced nutrient loss during the growing season. The hydrologic perspective also suggests that soil profile with higher hydraulic conductivity will have a high infiltration rate and reduced runoff and vice versa (Cai and Ugai, 2004; Duong et al., 2019; Qi and Vanapalli, 2015). According to soil hydraulic properties in all

three zones, the LY zone had lower hydraulic conductivity, higher slope, and lower TWI. Based on water input data, the entire field received the same precipitation events and the LY zone received the least irrigation amount during the growing season; however, no significant differences were found in irrigation amount at the end of the growing season. When the rainfall intensity is greater than the saturated hydraulic conductivity of the soil, surface runoff occurs along the slope (Huat et al., 2006). A saturated hydraulic conductivity for the LY zone of 9 cm day^{-1} induced surface runoff, thereby, causing nutrient loss during the growing season. Djodjic et al. (2004) also found that higher water movement down and laterally through the soil profile leads to leaching faster, compared to slow water movement. It can also be seen from the drainage pattern within irrigation zones of the field (fig. 3.3b). We also computed r_s between total P and OP in each of the zones during the growing season. The correlation coefficients were significant with 0.52 ($p<0.0001$) in the HY zone and 0.42 ($p<0.0001$) in the LY zone. It was noticed from the correlation that HY had a better association between soil total P and soil OP than the LY zone during the growing season. Low water accumulation, an outward drainage pattern, surface runoff, and lower hydraulic conductivity limited water movement in the LY zone as compared to the HY zone, which had greater hydraulic conductivity, an inward drainage pattern, and no runoff. Leaching of nutrients within the soil layers happens due to surface water infiltration. However, the field hydrological characteristics were not conducive to infiltration in the LY zone, which resulted in surface runoff with eroded nutrients from the LY zone. A lack of nutrients within the root zone reduced nutrient uptake, which negatively affected the plant height and growth during the growing season. The inward drainage pattern did not allow water to flow out as overland flow and retained the nutrients in the HY zone and worked as a nutrient pool. Therefore, lower slope and higher hydraulic conductivity in the HY zone resulted in greater infiltration and nutrient leaching (fig.

3.3b) as compared to the LY zone. This increased the nutrient uptake in the root zone and the plants in the HY zone had greater nutrient concentration, which enhanced the plant growth in the HY zone relative to the LY zone. The effect of nutrient uptake in plants was observed, affecting plant height and LAI during the growing season. Plants in the LY zone did not develop (plant growth, height and LAI) as fully as in the HY zone, which ultimately caused the variability in nutrients and affected the crop yield This will be discussed in following section.

3.5.5 Impact of Soil Nutrient Variability on Crop Yield

The soil nutrients varied across the zones. Also, there was spatial variation in crop yield at the end of the season. The corn grain yield produced within the field during the 2019 growing season, as measured by the combine yield monitor, varied from 3,139 kg ha^{-1} to 18,829 kg ha^{-1}. The average yields (standard deviation) of 14258 (872) kg ha^{-1} 1 in the HY zone was significantly greater than the 10575 (2022) kg ha^{-1} in the LY zone ($p < 0.001$). The least yield was produced in the LY zone (red) and a higher yield was produced in the other two zones (HY and MY) of the field (green) (fig. 3.8). The availability of soil nutrients increases and decreases the nutrient uptake by plants and adequate nutrient concentration in the plants helps with plant height, growth, and productivity (Malhotra et al., 2018; Pereira et al., 2020; Tewolde et al., 2019). In our study, we found that the average plant heights at the silking stage of corn were 225 cm and 195 cm with corresponding LAI of 4.13 cm^2 cm^{-2} and 3.34 cm^2 cm^{-2} in the HY and LY zones, respectively. Lack of nutrient availability in the LY zone limited the plant uptake and reduced the crop growth in the LY zone, which caused the corn grain yield differences across the field.

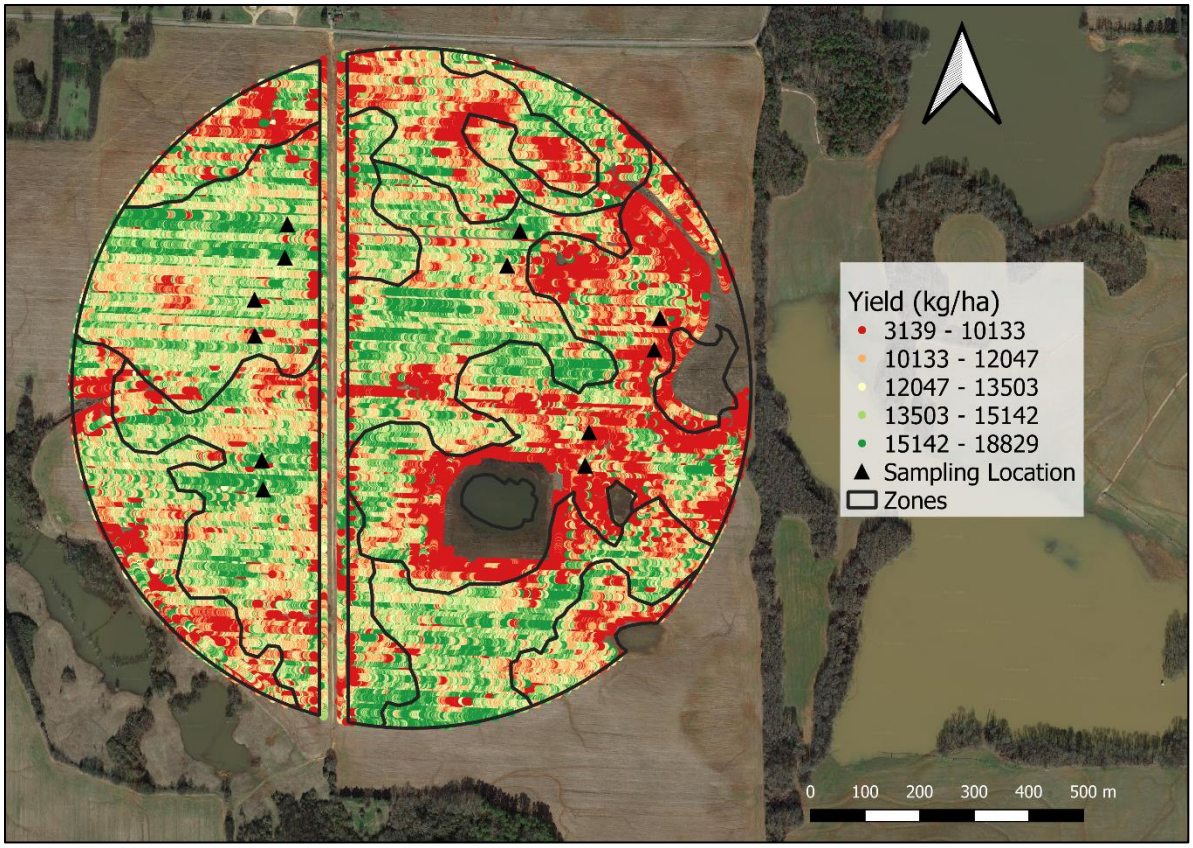

Figure 3.8 Corn grain yield variation in the field during the 2019 growing season. The corn grain yield was adjusted to 15.5% moisture. The gray areas indicate relatively low land areas in the field.

3.5.5.1 Plant Nutrients and Crop Yield

We also calculated r_s between corn grain yield and plant total P and plant total N during the growing season. The tasseling and silking stages of corn are high nutrient demand period in a growing season. The plant total P at silking stage had a positive significant correlation of +0.63 ($p<0.0001$), which indicated that increasing P increase crop yield. However, the correlation was not significant at the V4 and tasseling stages. The plant total N had a positive significant correlation of +0.85 ($p<0.0001$) at the tasseling stage, however, a negative correlation of -0.63 ($p<0.0001$) was at the V4 stage of the corn. This explained that yield had a positive correlation with the nutrient uptake by the plants during the growing season. The r_s between yield and plant nutrients indicated

that higher nutrients retained in the plants at the tasseling and silking stages can increase corn grain yield.

3.5.5.2 Topographical Attributes and Crop Yield

We also investigated TWI and slope as responsible factors for corn grain yield variability in the field. Maestrini and Basso (2018) investigated corn, soybean, wheat, and cotton in the US Midwest, and found that areas with higher TWI values resulted in a higher crop yield. We found a strong r_s of +0.66 ($p < 0.02$) between the TWI and grain yield in the field. This indicated grain yield was affected by topographical wetness in the field. Lower TWI led to low corn grain yield, while a higher TWI led to higher corn grain yield in the field. Slope and corn grain yield had a negative correlation of -0.85 ($p<0.0005$), which explained that a higher slope in the field led to a lower corn grain yield. Similar results have been found in a study conducted by Jiang and Thelen (2004) in a cornfield. Based on the above discussion, the LY zone had a greater slope and lower yield than the HY zone. A lower elevation and slope have greater water accumulation and greater yield productivity (Jiang and Thelen, 2004; Serrano et al., 2011). In our study field, TWI was lower and the slope was greater in the LY zone. The LY zone did not have enough water accumulation conditions to release soil nutrients for plant uptake unlike in the HY zone with its lower slope and greater TWI, which ultimately had an impact on plant height, LAI, and corn grain yield. The whole above-ground plants without grain in the HY zone had greater nutrient concentrations, and plants in the LY zone can have the same potential of soil nutrients available to plants if the LY zone can be managed in a different way to increase the nutrient concentrations in the soil and reduce the losses during the growing season

3.6 Summary and Conclusions

It can be concluded from the study that the soil nutrient availability and nutrient retained in the whole above-ground plants without grain did not occur uniformly across the crop field, although fertilizers and manure were uniformly applied during the 2019 growing season. The crop growth data showed that plants grew proportionally to the soil nutrient availability throughout the field. The soil nutrients (P and N) had within-field variability across the cornfield during the growing season. Nutrients retained in the plant had a similar pattern of within-field variability in soil nutrients during the growing season. Soil nutrients and nutrients in the whole above-ground plants variability was correlated with crop yield variability across the cornfield. The HY and MY zones had higher nutrients in soil and plants compared to the LY zone. The zone with greater nutrient concentrations compared to field average nutrient concentrations had a higher corn grain yield, and the zone with a lower nutrient concentration compared to the field average nutrient concentrations had a lower corn grain yield. Consistent management practices (irrigation, fertilizer application, and manure application) were applied across the field. However, different topographic attributes affected soil nutrient availability, soil nutrient loss, nutrient uptake, crop growth and development, and corn grain yield across the field. The TWI, slope, and soil hydraulic properties were found as factors responsible for within-field nutrient and corn grain yield variability across the crop field. Considering nutrient variability in management zone delineation can be an effective way to improve precision agriculture adoption during the growing season. Mainly, two extreme groups of nutrient variability (HY zone and LY zone) in soil and plants were identified, which can play an important role in the site-specific management of nutrients to improve crop yield. Therefore, it is of utmost importance to study nutrient variability across crop fields to increase crop yield, reduce loss of nutrients, and reduce negative environmental aspects. Improving and

optimizing the lower crop yield areas similar to high yield areas can increase productivity from the same crop field during the same growing season.

3.7 Implications for Site-Specific Management

Certain areas of a field may be more susceptible to nutrient loss (surface runoff loss in our study), lower nutrient availability for plant uptake, and, thus, reduce crop yield. For large cropland areas, executing uniform BMPs throughout the field fails to obtain uniform nutrient variability and yield across the crop field during the growing season. Implementation of different BMPs can improve nutrient variability and availability and can also help to improve crop yield. Farmers need to use different fertilizer rates and strategies within zones of the field during the growing season. As a recommendation, to minimize nutrient losses, improve crop and root growth, reduce negative environmental aspects, and increase crop productivity, farmers can use one or multiple conservation practices described below.

- Apply nutrients to meet the agronomic requirements of the crop fields. The surface application of nutrient sources needs to be in the zones with a low potential for surface runoff.

- Subsurface application of fertilizers or manures can help nutrients to be held in the soil for a longer period during the growing season, especially in runoff-susceptible areas. This can include subsurface band application of poultry litter and knifing-in the side-dress application of N.

- The use of multiple irrigation events with lower water application rates might help reduce nutrient losses in the zones which have high nutrient loss potential caused by surface runoff

during a growing season. This can promote plant health and the field may have the same crop maturity time, so crop productivity may be increased.

- Drip irrigation can be a good irrigation practice in areas that have high nutrient loss potential through surface runoff.

- Fertigation can also be a good option for farmers to reduce energy consumption and increase nutrient availability and nutrient use efficiency.

- Cover crops in the lower nutrient and higher runoff-generating areas may help enhance the soil water-holding capacity, increase adsorption of nutrients to soil particles, and improve field hydrologic and hydraulic properties.

- Conservation tillage with cover crops in the LY areas can reduce soil erosion and loss of sediment-bound nutrients, conserve soil water, build the soil structure, and improve water infiltration. However, tillage with no cover crop increases the disruption in soil structure, accelerating the surface runoff and soil erosion, which increase nutrient loss and decrease crop yield.

- No-tillage with cover crops in the lower nutrient and higher runoff generating areas can help enhance the soil water-holding capacity, increase adsorption of nutrients to soil particles, and improve field hydrologic and hydraulic properties (such as water retention, infiltration, and hydraulic conductivity). In Alabama, cover crop residue left in the field reduced surface runoff and increased water infiltration by 50 to 800% (SARE, 2007).

3.8 References

American Public Health Association., 1998. Standard methods for the examination of water and wastewater: Washington. DC, American Public Health Association, American Water Works Association, and Water Environment Federation.

Ahmad, A., Arif, M.S., Yasmeen, T., Riaz, M., Rizwan, M., Shahzad, S.M., Ali, S., Riaz, M.A., Sarosh, M., 2020. Seasonal variations of soil phosphorus and associated fertility indicators in wastewater-irrigated urban aridisol. Chemosphere 239, 124725. https://doi.org/10.1016/J.CHEMOSPHERE.2019.124725

Beegle, D., Durst, P.T., 2002. Managing Phosphorus for Crop Production. Agronomy Facts, 13, 035, Penn State Extension.

Beven, K.J., Kirkby, M.J., 1979. A physically based, variable contributing area model of basin hydrology / Un modèle à base physique de zone d'appel variable de l'hydrologie du bassin versant. Hydrol. Sci. Bull. 24, 43–69. https://doi.org/10.1080/02626667909491834

Bogunovic, I., Mesic, M., Zgorelec, Z., Jurisic, A., Bilandzija, D., 2014. Spatial variation of soil nutrients on sandy-loam soil. Soil Tillage Res. 144, 174–183. https://doi.org/10.1016/j.still.2014.07.020

Bouyoucos, G.J., 1962. Hydrometer Method Improved for Making Particle Size Analyses of Soils. Agron. J. 54, 464–465. https://doi.org/10.2134/agronj1962.00021962005400050028x

Bundy, L.G., Sturgul, S.J., 2001. A phosphorus budget for Wisconsin cropland. J of Soil Water Conserv. 56, 243-249.

Butler, G.B., Srivastava, P., 2007. An Alabama BMP Database for Evaluating Water Quality Impacts of Alternative Management Practices. Appl. Eng. Agric. 23, 727–736. https://doi.org/10.13031/2013.24056

Cai, F., Ugai, K., 2004. Numerical Analysis of Rainfall Effects on Slope Stability. Int. J. Geomech. 4, 69–78. https://doi.org/10.1061/(asce)1532-3641(2004)4:2(69)

Chakraborty, D., Prasad, R., Brantley, E., 2020. Phosphorus Basics : Understanding Pathways of Soil Phosphorus Loss. Alabama Coop. Ext. Syst.

Dayton, E.A., Whitacre, S., Holloman, C., 2017. Comparison of three persulfate digestion methods for total phosphorus analysis and estimation of suspended sediments. Appl. Geochemistry 78, 357–362. https://doi.org/10.1016/j.apgeochem.2017.01.011

Defterdarović, J., Filipović, L., Kranjčec, F., Ondrašek, G., Kikić, D., Novosel, A., Mustać, I., Krevh, V., Magdić, I., Rubinić, V., Bogunović, I., Dugan, I., Čopec, K., He, H., Filipović, V., 2021. Determination of Soil Hydraulic Parameters and Evaluation of Water Dynamics and Nitrate Leaching in the Unsaturated Layered Zone: A Modeling Case Study in Central Croatia. Sustain. 2021, Vol. 13, Page 6688 13, 6688. https://doi.org/10.3390/SU13126688

Dhillon, J., Torres, G., Driver, E., Figueiredo, B., Raun, W.R., 2017. World Phosphorus Use Efficiency in Cereal Crops. Agron. J. 109, 1670–1677. https://doi.org/10.2134/AGRONJ2016.08.0483

Djodjic, F., Börling, K., Bergström, L., 2004. Phosphorus Leaching in Relation to Soil Type and Soil Phosphorus Content. J. Environ. Qual. 33, 678–684. https://doi.org/10.2134/jeq2004.6780

Dukes, M.D., Perry, C., 2006. Uniformity testing of variable-rate center pivot irrigation control systems. Precis. Agric. 7, 205–218. https://doi.org/10.1007/s11119-006-9020-y

Duong, T.T., Do, D.M., Yasuhara, K., 2019. Assessing the Effects of Rainfall Intensity and Hydraulic Conductivity on Riverbank Stability. Water 11, 741. https://doi.org/10.3390/w11040741

Filho, J.F.D.C.L., Ortiz, B. V, Damianidis, D., Balkcom, K.S., Dougherty, M., Knappenberger, T., 2020. Irrigation Scheduling to Promote Corn Productivity in Central Alabama. J. Agric. Sci. 12. https://doi.org/10.5539/jas.v12n9p34

Fridgen, J.J., Kitchen, N.R., Sudduth, K.A., Drummond, S.T., Wiebold, W.J., Fraisse, C.W., 2004. Management Zone Analyst (MZA). Agron. J. 96, 100–108. https://doi.org/10.2134/AGRONJ2004.1000

Gallardo, A., Paramá, R., 2007. Spatial variability of soil elements in two plant communities of NW Spain. Geoderma 139, 199–208. https://doi.org/10.1016/j.geoderma.2007.01.022

Gao, X., Xiao, Y., Deng, L., Li, Q., Wang, C., Li, B., Deng, O., Zeng, M., 2019. Spatial variability of soil total nitrogen, phosphorus and potassium in Renshou County of Sichuan Basin, China. J. Integr. Agric. 18, 279–289. https://doi.org/10.1016/S2095-3119(18)62069-6

Geisseler, D., Lazicki, P., Horwath, W.R., 2017. Plant Tissue Sampling. Univ. California, Davis. Retrieved from https://apps1.cdfa.ca.gov/FertilizerResearch/docs/Plant_Tissue_Sampling.pdf

Hanrahan, B.R., King, K.W., Williams, M.R., Duncan, E.W., Pease, L.A., LaBarge, G.A., 2019. Nutrient balances influence hydrologic losses of nitrogen and phosphorus across agricultural fields in northwestern Ohio. Nutr. Cycl. Agroecosystems 113, 231–245. https://doi.org/10.1007/s10705-019-09981-4

Harmel, R.D., Smith, D.R., Haney, R.L., Dozier, M., 2009. Nitrogen and phosphorus runoff from cropland and pasture fields fertilized with poultry litter. J. Soil Water Conserv. 64, 400–412. https://doi.org/10.2489/jswc.64.6.400

Huat, B.B.K., Ali, F.H.J., Low, T.H., 2006. Water infiltration characteristics of unsaturated soil slope and its effect on suction and stability. Geotech. Geol. Eng. 24, 1293–1306. https://doi.org/10.1007/s10706-005-1881-8

Irmak, S., Burgert, M.J., Yang, H.S., Cassman, K.G., Walters, D.T., Rathje, W.R., Payero, J.O.,

Grassini, P., Kuzila, M.S., Brunkhorst, K.J., Eisenhauer, D.E., Kranz, W.L., VanDeWalle, B., Rees, J.M., Zoubek, G.L., Shapiro, C.A., Teichmeier, G.J., Rees, J.M., Shapiro, C.A., Teichmeier, G.J., 2012. Large-Scale On-Farm Implementation of Soil Moisture-Based Irrigation Management Strategies for Increasing Maize Water Productivity. Trans. ASABE 55, 881–894. https://doi.org/10.13031/2013.41521

Irmak, S., Odhiambo, L.O., Kranz, W.L., Eisenhauer, D.E., 2011. Irrigation Efficiency and Uniformity, and Crop Water Use Efficiency. Univ. Nebraska–Lincoln Ext.

Jiang, G., Grafton, M., Pearson, D., Bretherton, M., Holmes, A., 2021. Predicting spatiotemporal yield variability to aid arable precision agriculture in New Zealand: a case study of maize-grain crop production in the Waikato region. New Zealand Journal of Crop and Horticultural Science, 49, 41–62. https://doi.org/10.1080/01140671.2020.1865413

Jiang, P., Thelen, K.D., 2004. Effect of Soil and Topographic Properties on Crop Yield in a North-Central Corn–Soybean Cropping System. Agron. J. 96, 252–258. https://doi.org/10.2134/AGRONJ2004.0252

Jiménez, A.F., Ortiz, B. V., Bondesan, L., Morata, G., Damianidis, D., 2020. Evaluation of Two Recurrent Neural Network Methods for Prediction of Irrigation Rate and Timing. Trans. ASABE 63, 1327–1348. https://doi.org/10.13031/TRANS.13765

Jones, J.B., Case, V.W., 2018. Sampling, Handling, and Analyzing Plant Tissue Samples. Soil Test. Plant Anal. 389–427. https://doi.org/10.2136/SSSABOOKSER3.3ED.C15

King, K.W., Williams, M.R., Macrae, M.L., Fausey, N.R., Frankenberger, J., Smith, D.R., Kleinman, P.J.A., Brown, L.C., 2015. Phosphorus Transport in Agricultural Subsurface Drainage: A Review. J. Environ. Qual. 44, 467–485. https://doi.org/10.2134/jeq2014.04.0163

Kumar, H., Srivastava, P., Lamba, J., Ortiz, B. V., Way, T.R., Sangha, L., Takhellambam, B.S., Morata, G., 2021a. Phosphorus Variability in the Irrigated Cropland During a growing season. Am. Soc. Agric. Biol. Eng. Annu. Int. Meet. ASABE 2021 4, 1-. https://doi.org/10.13031/AIM.202100886

Kumar, H., Srivastava, P., Ortiz, B. V., Morata, G., Takhellambam, B.S., Lamba, J., Bondesan, L., 2021b. Field-Scale Spatial and Temporal Soil Water Variability in Irrigated Croplands. Trans. ASABE 64, 1277–1294. https://doi.org/10.13031/TRANS.14335

Kumar, H., Srivastava, P., Ortiz, B.V., Takhellambam, B.S., Morata, G., Bondesan, L. and Lamba, J., 2020. Spatiotemporal Soil Moisture Variability in Corn and Cotton Fields with Uniform Irrigation During the Growing Season. In: AGU Fall Meeting Abstracts (Vol. 2020, pp. H209-05).

Lee, D., 2019. A guide to corn production in Georgia. Coop. Ext. Crop Soil Sci. University of Georgia Extention.

Lena, B.P., Bondesan, L., Ortiz, B.V., Pinheiro, E.A.R., Morata, G.T., Kumar, H., 2021. Evaluation of different negligible drainage flux for field capacity estimation and its

implication on irrigation depth for major soil types in Alabama, USA. Am. Soc. Agric. Biol. Eng. Annu. Int. Meet. ASABE 2021. https://doi.org/10.13031/AIM.202100415

Lena, B.P., Bondesan, L., Pinheiro, E.A.R., Ortiz, B. V., Morata, G.T., Kumar, H., 2022. Determination of irrigation scheduling thresholds based on HYDRUS-1D simulations of field capacity for multilayered agronomic soils in Alabama, USA. Agric. Water Manag. 259, 107234. https://doi.org/10.1016/J.AGWAT.2021.107234

Maestrini, B., Basso, B., 2018. Drivers of within-field spatial and temporal variability of crop yield across the US Midwest. Sci. Reports 2018 81 8, 1–9. https://doi.org/10.1038/s41598-018-32779-3

Malhotra, H., Vandana, Sharma, S., Pandey, R., 2018. Phosphorus Nutrition: Plant Growth in Response to Deficiency and Excess. Plant Nutr. Abiotic Stress Toler. 171–190. https://doi.org/10.1007/978-981-10-9044-8_7

Mallarino, A.P., Wittry, D.J., 2004. Efficacy of Grid and Zone Soil Sampling Approaches for Site-Specific Assessment of Phosphorus, Potassium, pH, and Organic Matter. Precis. Agric. 2004 52 5, 131–144. https://doi.org/10.1023/B:PRAG.0000022358.24102.1b

Mathew, M.M., Majule, A.E., Marchant, R., Sinclair, F., 2016. Variability of Soil Micronutrients Concentration along the Slopes of Mount Kilimanjaro, Tanzania. Appl. Environ. Soil Sci. 2016, 1–7. https://doi.org/10.1155/2016/9814316

McEntee, P.J., Bennett, S.J., Belford, R.K., 2019. Mapping the spatial and temporal stability of production in mixed farming systems: an index that integrates crop and pasture productivity to assist in the management of variability. Precis. Agric. 2019 211 21, 77–106. https://doi.org/10.1007/S11119-019-09658-6

Morales, L.A., Vidal Vázquez, E., Paz-Ferreiro, J., 2014. Spatial distribution and temporal variability of ammonium-nitrogen, phosphorus, and potassium in a rice field in Corrientes, Argentina. Sci. World J. 2014. https://doi.org/10.1155/2014/135906

Ortiz, B. V., Bondesan, L., Morata, G., McClendon, P., Kumar, H., 2021. Maintaining Water Application Uniformity in Irrigation Systems - Alabama Cooperative Extension System. Alabama Coop. Ext. Syst. https://www.aces.edu/blog/topics/crop-production/maintaining-water-application-uniformity-in-irrigation-systems/ (accessed 7.16.21).

Pereira, N.C.M., Galindo, F.S., Gazola, R.P.D., Dupas, E., Rosa, P.A.L., Mortinho, E.S., Filho, M.C.M.T., 2020. Corn Yield and Phosphorus Use Efficiency Response to Phosphorus Rates Associated With Plant Growth Promoting Bacteria. Front. Environ. Sci. 8, 40. https://doi.org/10.3389/FENVS.2020.00040

Peters, A., Iden, S.C., Durner, W., 2015. Revisiting the simplified evaporation method: Identification of hydraulic functions considering vapor, film and corner flow. J. Hydrol. 527, 531–542. https://doi.org/10.1016/J.JHYDROL.2015.05.020

Plach, J., Pluer, W., Macrae, M., Kompanizare, M., McKague, K., Carlow, R., Brunke, R., 2019.

Agricultural Edge-of-Field Phosphorus Losses in Ontario, Canada: Importance of the Nongrowing Season in Cold Regions. J. Environ. Qual. 48, 813–821. https://doi.org/10.2134/jeq2018.11.0418

Plach, J.M., Macrae, M.L., Ali, G.A., Brunke, R.R., English, M.C., Ferguson, G., Lam, W.V., Lozier, T.M., McKague, K., O'Halloran, I.P., Opolko, G., Van Esbroeck, C.J., 2018. Supply and Transport Limitations on Phosphorus Losses from Agricultural Fields in the Lower Great Lakes Region, Canada. J. Environ. Qual. 47, 96–105. https://doi.org/10.2134/jeq2017.06.0234

Plant, R.E., 2018. Spatial Data Analysis in Ecology and Agriculture Using R. Spat. Data Anal. Ecol. Agric. Using R. https://doi.org/10.1201/9781351189910

Qi, S., Vanapalli, S.K., 2015. Hydro-mechanical coupling effect on surficial layer stability of unsaturated expansive soil slopes. Comput. Geotech. 70, 68–82. https://doi.org/10.1016/j.compgeo.2015.07.006

Qin, C.Z., Zhu, A.X., Pei, T., Li, B.L., Scholten, T., Behrens, T., Zhou, C.H., 2011. An approach to computing topographic wetness index based on maximum downslope gradient. Precis. Agric. 12, 32–43. https://doi.org/10.1007/s11119-009-9152-y

Razaq, M., Zhang, P., Shen, H.L., Salahuddin, 2017. Influence of nitrogen and phosphorous on the growth and root morphology of Acer mono. PLoS One 12, e0171321. https://doi.org/10.1371/JOURNAL.PONE.0171321

Reid, K., Schneider, K., Joosse, P., 2019. Addressing Imbalances in Phosphorus Accumulation in Canadian Agricultural Soils. J. Environ. Qual. 48, 1156–1166. https://doi.org/10.2134/jeq2019.05.0205

Ridolfi, E., Kumar, H., Bárdossy, A., 2020. A methodology to estimate flow duration curves at partially ungauged basins. Hydrol. Earth Syst. Sci. 24, 2043–2060. https://doi.org/https://doi.org/10.5194/hess-24-2043-2020

Sangha, L., Lamba, J., Kumar, H., Srivastava, P., Dougherty, M., Prasad, R., 2020. An innovative approach to rainwater harvesting for irrigation based on El Niño Southern Oscillation forecasts. J. Soil Water Conserv. jswc.2020.00085. https://doi.org/10.2489/JSWC.2020.00085

SARE., 2007. Managing Cover Crops Profitably, 3rd Edition. Sustainable Agriculture Research and Education. https://www.sare.org/resources/managing-cover-crops-profitably-3rd-edition/ (accessed 4.8.22).

Schröder, J.J., Scholefield, D., Cabral, F., Hofman, G., 2004. The effects of nutrient losses from agriculture on ground and surface water quality: The position of science in developing indicators for regulation. Environ. Sci. Policy 7, 15–23. https://doi.org/10.1016/j.envsci.2003.10.006

Schroeder, P.D., Radcliffe, D.E., Cabrera, M.L., 2004. Rainfall Timing and Poultry Litter

Application Rate Effects on Phosphorus Loss in Surface Runoff. J. Environ. Qual. 33, 2201–2209. https://doi.org/10.2134/jeq2004.2201

Serrano, J.M., Peça, J.O., Marques da Silva, J.R., Shahidian, S., 2011. Spatial and temporal stability of soil phosphate concentration and pasture dry matter yield. Precis. Agric. 12, 214–232. https://doi.org/10.1007/s11119-010-9170-9

Sharpley, A.N., 1997. Rainfall Frequency and Nitrogen and Phosphorus Runoff from Soil Amended with Poultry Litter. J. Environ. Qual. 26, 1127–1132. https://doi.org/10.2134/jeq1997.00472425002600040026x

Shaw, A.N., Cleveland, C.C., 2020. The effects of temperature on soil phosphorus availability and phosphatase enzyme activities: a cross-ecosystem study from the tropics to the Arctic. Biogeochemistry 151, 113–125. https://doi.org/10.1007/S10533-020-00710-6

Slaets, J.I.F., Boeddinghaus, R.S., Piepho, H.P., 2021. Linear mixed models and geostatistics for designed experiments in soil science: Two entirely different methods or two sides of the same coin? Eur. J. Soil Sci. 72, 47–68. https://doi.org/10.1111/EJSS.12976

Smith, D.R., Owens, P.R., Leytem, A.B., Warnemuende, E.A., 2007. Nutrient losses from manure and fertilizer applications as impacted by time to first runoff event. Environ. Pollut. 147, 131–137. https://doi.org/10.1016/j.envpol.2006.08.021

Su, B., Zhao, G., Dong, C., 2018. Spatiotemporal variability of soil nutrients and the responses of growth during growth stages of winter wheat in northern China. PLoS One 13, e0203509. https://doi.org/10.1371/journal.pone.0203509

Tewolde, H., Buehring, N., Way, T.R., Feng, G., He, Z., Sistani, K.R., Jenkins, J.N., 2021. Yield and nutrient removal of cotton–corn–soybean rotation systems fertilized with poultry litter. Agron. J. https://doi.org/10.1002/AGJ2.20857

Tewolde, H., Sistani, K.R., Feng, G., Menkir, A., 2019. Does fertilizing corn with poultry litter enrich the grain with mineral nutrients? Agron. J. 111, 2472–2484. https://doi.org/10.2134/agronj2019.02.0094

Umali, B.P., Oliver, D.P., Forrester, S., Chittleborough, D.J., Hutson, J.L., Kookana, R.S., Ostendorf, B., 2012. The effect of terrain and management on the spatial variability of soil properties in an apple orchard. Catena 93, 38–48. https://doi.org/10.1016/j.catena.2012.01.010

USDA-NASS, 2019. 2017 Census of Agriculture. Washington. United States Department of Agriculture National Agriculture Statistics Service.

Williams, M.R., King, K.W., Duncan, E.W., Pease, L.A., Penn, C.J., 2018. Fertilizer placement and tillage effects on phosphorus concentration in leachate from fine-textured soils. Soil Tillage Res. 178, 130–138. https://doi.org/10.1016/j.still.2017.12.010

Wright, A.L., Wang, Y., Reddy, K.R., 2008. Loss-on-Ignition Method to Assess Soil Organic

Carbon in Calcareous Everglades Wetlands. Commun. Soil Sci. Plant Anal. 39, 3074–3083. https://doi.org/10.1080/00103620802432931

Yost, J.L., Huang, J., Hartemink, A.E., 2019. Spatial-temporal analysis of soil water storage and deep drainage under irrigated potatoes in the Central Sands of Wisconsin, USA. Agric. Water Manag. 217, 226–235. https://doi.org/10.1016/j.agwat.2019.02.045

Takhellambam, B.S., Srivastava, P., Lamba, J., McGehee, R.P., and Kumar, H., 2021. Potential changes in rainfall erosivity under climate change in southeastern United States. In: AGU Fall Meeting 2021.

Takhellambam, B.S., Srivastava, P., Lamba, J., Mcgehee, R.P., Kumar, H., Tian, D., 2022. Temporal disaggregation of hourly precipitation under changing climate over the Southeast United States. Sci. Data 2022 91 9, 1–14. https://doi.org/10.1038/s41597-022-01304-7

Chapter 4

Scheduling Site-Specific Irrigation Using One-Layer Zone-Specific Soil Hydraulic Properties and Inverse Modeling

4.1 Abstract

The adoption of irrigation practices has been increasing around the globe to meet irrigation water demands. Site-specific soil hydraulic properties (SHPs) are critical for determining irrigation thresholds and adopting the best irrigation practices. In this study, we optimized two single-layer SHPs for two management zones (namely, zone 1 and zone 2) delineated in a crop field using topographic attributes, soil texture, and historical crop yield to demonstrate the need for zone-specific SHPs. The HYDRUS-1D model was coupled with the shuffled complex evolution (SCE-UA) algorithm to optimize single-layer zone-specific SHPs using multilayered observed soil matric potential or soil water pressure head (h) measured using soil moisture sensors in both zones. Statistical indices for goodness of fit showed that single layer SHPs simulate the multilayered h during the growing season well. The irrigation thresholds and amounts determined using optimized SHPs were used to trigger irrigations in the two zones. Different irrigation scenarios using the top (15 cm), center (30 cm), and bottom (60 cm) soil depths as observation nodes were developed using the zone-specific optimized SHPs in the HYDRUS-1D model to meet irrigation water demand and reduce water stress during the growing season. A reference HYDRUS-1D model with actual water input (precipitation + irrigation) and No Irrigation (NI) model with no irrigation input were developed and compared for different irrigation scenarios. The ratio of actual root water uptake (ARWU) and potential root water uptake (PRWU) were calculated to compare improvements in satisfying daily water demand and to reduce the water stress under different irrigation scenarios. At 35% soil water depletion (SWD), the optimized irrigation threshold was at

an h value of 76 kPa, and the corresponding irrigation amount was 2.18 cm in the zone 1. However, in zone 2, the optimized irrigation threshold was at an h value of 59 kPa and the corresponding irrigation amount was 1.48 cm. Out of the total irrigation water triggered during the growing seasons, greater than 61% and 75% in zone 1 was triggered in July 2018 and in May-June 2019, respectively. However, greater than 73% in July 2018 and greater than 72% in May-June 2019 were triggered in zone 2. Based on the simulations of various irrigation scenarios in HYDRUS-1D, we found that installing sensors at 15 cm or 30 cm can help meet the daily crop water demand in a timely manner since sensors at these depths indicate the changes in h of irrigation thresholds much faster than sensors at 60 cm depth and 60 cm depth did not trigger irrigation in many irrigation scenarios. This study discusses the importance of critical water demands due to distribution of precipitation over the growing season and the need for site-specific irrigation management within the field. This study helps us to understand the importance of zone-specific SHPs for optimizing soil water dynamics to avoid discrepancies among laboratory determined SHPs and predicting the soil water movement in the field, and so determining the irrigation thresholds and amounts.

4.2 Introduction

Population growth and climate change are expected to increase freshwater demands (FAO, 2016). Also, more than 40% of the earth's population is already experiencing water scarcity problems (Kummu et al., 2016). Approximately 70% of available freshwater withdrawal is for meeting irrigation needs in agricultural production to meet the food demands. Thus, any improvements in current irrigation practices can help conserve limited water resources and promote sustainable agriculture (Himanshu et al., 2021; FAO, 2016). The future forecast of precipitation data showed the 14% increment in the annual average of precipitation by 2059, which would alter the time,

erosivity characteristics, and distribution of the precipitation events (Takhellambam et al., 2021, 2022). Depending on climate conditions, irrigation water demands vary greatly from arid to humid climate regions (O'Shaughnessy et al., 2018; Rolle et al., 2021). In humid climate regions, irrigation is needed due to non-uniform rainfall distribution (Sangha et al., 2020), distribution of precipitation over the growing season (Filho et al., 2020), and soil moisture variation within a crop field during a growing season (Kumar et al., 2020, 2021b). Within-field soil moisture variation can be due to the variability in soil properties, vegetation, and topographic gradients (Fontanet et al., 2020; Kumar et al., 2021b), which affect the irrigation rate, time, and depth during the crop growing period. Since uniform irrigation does not account for within-field variability in soil moisture and applies fixed irrigation amounts over the field, it can result in over- and under-application of water in different parts of a field. Water is expensive and its supply is limited, so irrigation needs to be optimized for applying the right amount, at the right place, and at the right time. Because of this, although uniform irrigation is currently the most common practice (Kumar et al., 2021b), farmers are increasingly adopting modern irrigation practices (Lena et al., 2020), for example, variable rate irrigation (VRI) based on management zones within a crop field.

To adopt VRI as the best irrigation practice, different management zones can be delineated within a field based on variations in crop yield, soil type, and topography (Kumar et al., 2021a). This has the potential to conserve water by meeting zone-specific crop water demands (Lowrance et al., 2016; Liakos et al., 2017). A VRI technology can trigger irrigations at zone-specific irrigation thresholds depending on plant available water within specific zones. This helps to increase irrigation water use efficiency, reduce leaching and runoff, reduce crop water stress, maximize crop yield and profitability, and reduce pressure on freshwater resources (Evans and Sadler, 2008; Stone et al., 2019; Yost et al., 2019). Sui and Yan (2017) found increased yield using VRI

compared to uniform irrigation in a humid climate. However, precise irrigation to meet zone-specific crop water demand requires continuous monitoring of soil water dynamics within the zones (Reyes et al., 2019; Fontanet et al., 2020).

In the past ten years, the sensor-based irrigation method has received much attention since this approach provides real-time soil water status, as soil water content-θ or soil matric potential (soil water pressure head)-h, which can be used for uniform irrigation and VRI. Locations of soil moisture sensors are selected based on variabilities (soil, topography, yield, etc.) in the field. Detailed information about sensor placement can be found in Irmak et al. (2012). Monitoring soil water dynamics in real-time not only improves irrigation timing and depth (Irmak et al., 2010), it also permits adequate water distribution using the VRI technique (O'Shaughnessy et al., 2018; Sharma and Irmak, 2020). To reduce crop water stress and potential crop yield losses, predefined soil water depletion (SWD) methods have been used by irrigation experts to determine irrigation thresholds using h or θ (Gu et al., 2020), where irrigation threshold, depth, and time are determined by maximum allowable SWD in each management zone (Allen et al., 1998; Irmak, 2016; Sui and Yan, 2017).

In sensor-based irrigation, soil water dynamics in the soil profile can be explained using knowledge on the soil hydraulic properties (SHPs), i.e., the soil water retention curve (SWRC) and the hydraulic conductivity curve (HCC). Soil hydraulic properties are required to understand root water uptake (Šimůnek and Hopmans, 2009) and to determine irrigation thresholds (Wang et al., 2017; Gu et al., 2020). Using one SWRC and HCC throughout the field does not account for zone-specific soil water dynamics and zone-specific characteristics in a crop field. Unfortunately, determination of both SWRC and HCC and using them to determine irrigation thresholds are rarely applied in irrigation applications. Even when these relationships are applied for determining

irrigation thresholds, investigations that optimize zone-specific SHPs (SWRC and HCC) and quantify their effect on irrigation threshold determination have not been conducted (Lena et al., 2022). Previous studies, such as Leininger et al. (2019) recommended a soil matric potential (h) value of 50 kPa (1 kPa = 10.1972 cm) as an irrigation threshold for very fine sandy loam textured soil in Mississippi. Irmak et al. (2016) recommended a range from 20 kPa to 25 kPa for fine sandy textured soils and a range from 90 kPa to 110 kPa for silt loam and silty clay loam textured soils in Nebraska. However, these studies used SHPs based on either laboratory determinations (raw) using undisturbed soil cores (Lena et al., 2022) or estimated based on soil texture and pedotransfer functions using particle size fractions (Iqbal et al., 2020). These SHPs were not optimized for observed h or θ in actual field conditions to determine irrigation thresholds and such SHPs cannot explain soil water movement within the soil profiles. Also, these studies did not consider significance of HCC, which influences the dynamic behavior of soil water movement. Irrigation scheduling using non-optimized SHPs does not account for the discrepancies between field observations of h or θ; such discrepancies can also result in the determination of irrigation thresholds and depths (Evett et al., 2019).

This study investigated the difference between uniform irrigation and zone-specific irrigation that accounts for zone-specific SHPs (both SWRC and HCC) in a farmer's field. We hypothesized that zone-specific irrigation thresholds and amounts greatly vary with optimized SHPs in each zone. Since field measurements are onerous, time-consuming, and include uncertainty in the measurements, it makes sense to establish a modeling setup to optimize accurate SHPs for zone-specific characterization, for more accurate irrigation and agricultural water management. Thus, for this investigation, we selected two different management zones of a irrigated cornfield. For each management zone, we optimized the SHPs using inverse modeling in HYDRUS-1D, a model

to simulate soil water and solute dynamics in unsaturated soil media (PC-Progress, 2022), and measured h coupled with the Shuffled Complex Evolution (SCE-UA) algorithm. Based on the optimized model, we compared the currently applied irrigation schedule (uniform application) with many different scenarios to schedule irrigation.

4.3 Materials and Methods

4.3.1 Study Area Description

This research was carried out in a cornfield belonging to a farmer located in the Town Creek Watershed in the Tennessee Valley Region of North Alabama, USA. The study region is classified as subtropical humid (Cfa, Köppen climate classification) (Kottek et al., 2006) with average annual precipitation is about 140 cm. The growing season usually occurs from April to October (Kumar et al., 2021b) and distribution of total monthly precipitation over the 2018 and 2019 growing seasons is shown in fig. 4.1. The study was conducted in a 120 ha area of cornfield. The field was delineated in three management zones (zone 1, zone 2, and zone 3). We used zone 1 and zone 2 in this study due to contrasting properties in these zones using the management zone analyst (MZA, USDA-ARS, Columbia, MO, USA) software (Fridgen et al., 2004) based on terrain elevation data collected using a John Deere StarFire^{TM} 6000 real-time kinematic GPS receiver (Deere and Company, Moline, IL, USA), historical yield data collected using a yield monitor mounted on a harvester, and soil texture. A similar approach was adopted to delineate the management zones in cornfields of Central Alabama (Filho et al., 2020) and South Alabama (Jiménez et al., 2020). For soil texture, a disturbed soil sampling campaign was conducted from several locations for soil characterization in the study field at three depths 0-15, 15-30, and 30-60 cm using the hydrometer method (Bouyoucos, 1962) (table 4.1). Corn grain yield varied from 3139 kg ha^{-1} to 18829 kg ha^{-1} in the field. The slope data were generated using the collected terrain elevation data and the slope

values varied from 0 to 10%. A topographic wetness index (TWI) was also generated (Beven et al., 1979), and TWI varied from 5.11 to 18. Two contrasting zones, namely, zone 1 and zone 2, differing in slope, soil, TWI, and grain yield were selected for this study (table 4.1). The zone 1 had lower slope, greater TWI, and greater grain yield as compared to zone 2, which had greater slope, lower TWI, and lower grain yield within the field. Zone 3 had properties between zone 1 and zone 2, and, therefore, it was not used in the study. Since about 95% of corn roots are distributed within the 0-60 cm soil layer (Zhou and Zhao, 2019), an array of three Watermark soil moisture sensors (Irrometer Co., Riverside, CA, USA) at multiple locations were installed in each zone to monitor zone-specific h at 0-15cm, 15-30 cm, and 30-60 cm soil depths during the growing season. Watermark sensors are electrical resistance devices to monitor h in different soil types in crop fields. Sensors were installed on 01 May 2019 and removed on 11 August 2019. The corn was planted on 28 March 2019 and harvested on 30 August 2019. During the 2018 growing season, corn was planted on 10 April and harvested on 03 September. An automatic weather station (Vantage Pro2 Plus, Davis Instruments, Hayward, CA, USA) was installed near field to record meteorological parameters (Kumar et al., 2021b).

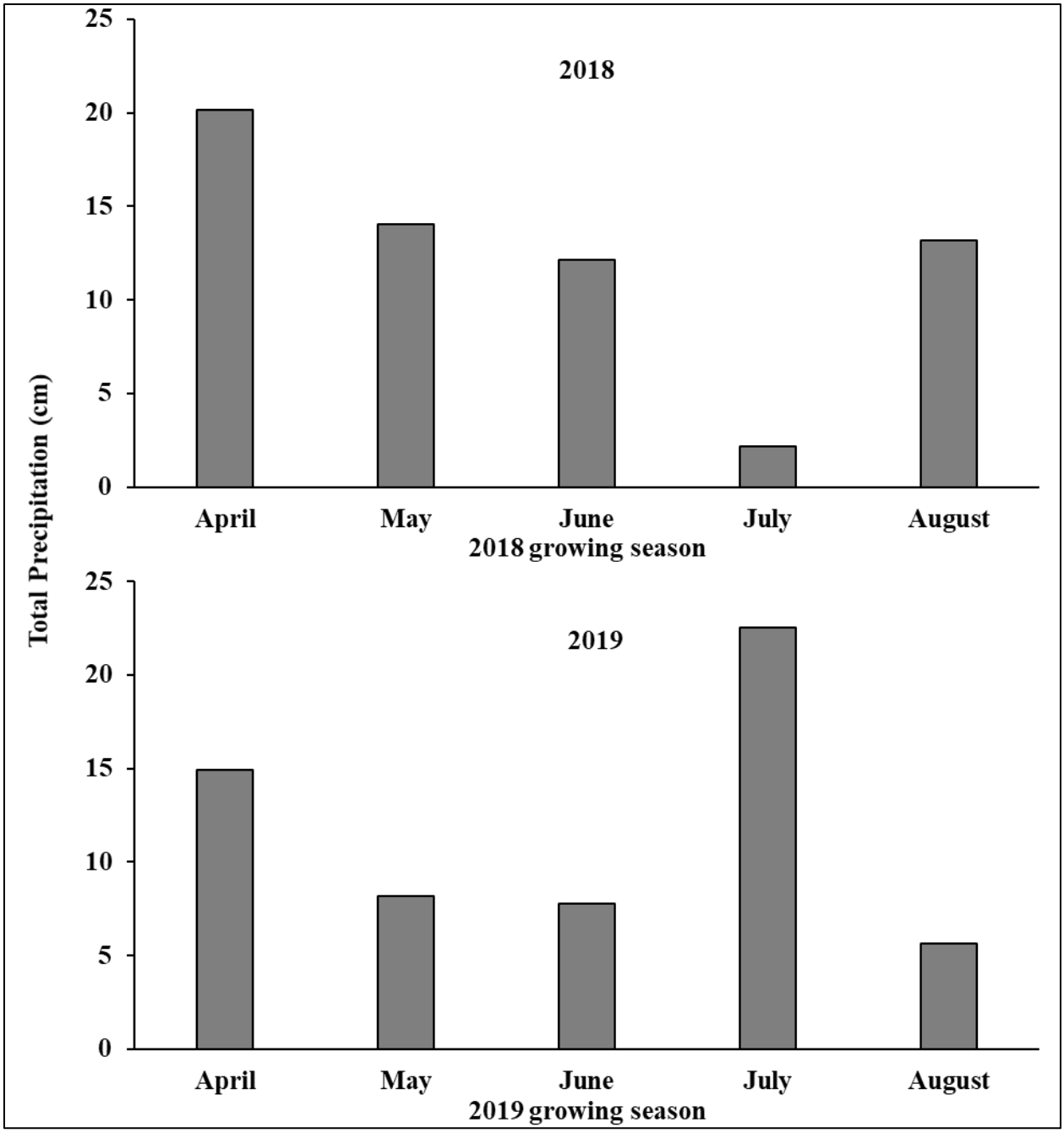

Figure 4.1 Distribution of precipitation over the growing seasons.

Table 4.1 Zone-specific soil properties in the crop field. (* indicate data retrieved from SSURGO 2022)

	Depth (cm)	Sand (%)	Silt (%)	Clay (%)	Texture	Soil Series*	Soil Family*
Zone 1	**0-15**	17.5	42.3	40.2	Silty clay	Abernathy-Emory	
	15-30	17.6	50.1	32.3	Silty clay loam		

	30-60	12.9	51.4	35.7	Silty clay loam		Fine-silty, siliceous, active, thermic Oxyaquic Hapludults
Zone 2	**0-15**	31.9	32.8	35.3	Clay loam	Decatur	Fine, kaolinitic, thermic Rhodic Paleudults
	15-30	30.1	29.6	40.3	Clay		
	30-60	29	24.4	46.8	Clay		

4.3.2 HYDRUS-1D numerical approximate model description

A numerically approximate one-dimensional model HYDRUS-1D was selected to simulate soil water dynamics in both zones during the growing season. HYDRUS-1D has been used as a reliable tool to model soil water dynamics of variably saturated soils in various field and laboratory conditions (Šimůnek et al., 2016; Mokari et al., 2019; Wyatt et al., 2021). The flow between soil surface and groundwater predominantly occurs in the vertical direction, and surface water ponding occurs as horizontal flow such as surface runoff or irrigation. Therefore, in this study, we used HYDRUS-1D instead of a 2D or 3D model (Li et al., 2014). HYDRUS-1D has been used extensively to simulate soil water dynamics and solute transport in different soil layers (González et al., 2015; Wang et al., 2016; Iqbal et al., 2020). HYDRUS-1D has been used in different scenarios such as rainfed agriculture (Iqbal et al., 2020), furrow irrigation (Tafteh and Sepaskhah, 2012), uniform irrigation (Fontanet et al., 2020), and root water uptake studies (Šimůnek and Hopmans, 2009; Zheng et al., 2017). HYDRUS-1D can optimize zone-specific SHPs and can simulate a well-defined K- θ- h relationship in field conditions during a growing season (Wang et al., 2021) to understand soil water dynamics for scheduling irrigation.

The model solves the governing Richard's equation (Šimůnek et al., 2016) by applying a finite element code. The one-dimensional equation for water flow in an unsaturated flow medium is described by equation (4.1)

$$\frac{\partial \theta}{\partial t} = \frac{\partial}{\partial z}\left[K\left(\frac{\partial h}{\partial z} + 1\right)\right] - S \tag{4.1}$$

where θ is soil water content [L^3L^{-3}]; h is soil water pressure head [L]; t is time [T]; z is the vertical spatial coordinate [L]; K is unsaturated hydraulic conductivity [LT^{-1}]; and S is sink term in the water flow equation accounting for water uptake by roots [$L^3L^{-3}T^{-1}$].

The zone-specific SHPs were modeled using van Genuchten (1980) to explain soil water retention and hydraulic conductivity functions.

$$\theta(h) = \begin{Bmatrix} \theta_r + \dfrac{\theta_s - \theta_r}{[1 + (\alpha|h|)^n]^m}; h < 0 \\ \theta_s; h \geq 0 \end{Bmatrix} \tag{4.2}$$

$$K(h) = \begin{Bmatrix} K_s S_e^l \left[1 - \left(1 - S_e^{\frac{1}{m}}\right)^m\right]^2; h < 0 \\ K_s;\ h \geq 0 \end{Bmatrix} \tag{4.3}$$

$$S_e = \frac{\theta - \theta_r}{\theta_s - \theta_r} \tag{4.4}$$

θ_r is residual soil water content [L^3L^{-3}]; θ_s is saturated soil water content [L^3L^{-3}]; α [L^{-1}], m [-], and n [-] are shape parameters, where $m = 1 - 1/n$; l [-] is shape parameter in hydraulic conductivity function; S_e is relative saturation or effective soil water content [-].

4.3.3 HYDRUS-1D Model Input Parameters

4.3.3.1 Determination of Zone-Specific SHPs

For each zone, undisturbed soil cores were collected using a sampler ring of stainless steel (5 cm in height and 8 cm in diameter). The sampler rings were carefully removed by digging out surrounding soils and stored in a container for transportation to develop the SHPs in the laboratory (raw SHPs). The sample cores were saturated in water for 24 hours before the soil water retention

measurements were made using the evaporation method with the HYPROP measurement system (Meter Group Inc., Pullman, WA, USA) (Peters and Durner, 2008; Peters et al., 2015). HYPROP measurements are limited by the cavitation point of the two tensiometers, and for this reason, water retention curves can be estimated from saturation until around pF 3. The pF is a logarithmic function of absolute h in cm. To determine the dry range of SWRCs, we used a dew-point hygrometer (WP4C PotentiaMeter, Meter Group, Pullman, WA, USA). A detailed procedure for developing SHPs is shown in Lena et al. (2021, 2022).

$$pF = log_{10}(|h|) \tag{4.5}$$

4.3.3.2 Dynamic Field Measurements

To input meteorological data, the surface water flux (precipitation and irrigation), minimum and maximum temperatures, relative humidity, solar radiation, and wind speed were collected from the installed weather station. Irrigation data for the 2018 and 2019 growing seasons were recorded in addition to precipitation for water input data in the model. The growth stages were recorded for corn to determine the associated crop coefficient during the growing season, for use in the model (Irmak, 2017). The plant heights and leaf area index (LAI) were also recorded in both zones during the field visits. The LAI was measured using an LAI-2200 Plant Canopy Analyzer (LI-COR Environmental, Lincoln, NE, USA) on the 57th, 72th, 92th and 128th day after planting during the growing season. The LAI was measured from four different locations within each zone with five replications for each location (Morata, 2020).

4.3.3.3 Initial and Boundary Conditions in the HYDRUS-1D model

The initial conditions were defined in terms of h in the model. Since this study is a field study, and the surface layer was subjected to the atmosphere, we defined the upper boundary condition (BC)

as atmospheric BC with surface runoff in the HYDRUS-1D model. The lower BC was set to free drainage boundary at 100 cm soil depth, indicating no interaction with the groundwater. A spatial discretization of 0.5 cm, leading to 201 nodes across the entire soil profile, and no hysteresis in soil water retention was used. The observed nodes (top, center, and bottom) were defined at the same depths of 15 cm, 30 cm, and 60 cm, respectively, where Watermark sensors were installed in both zones.

4.3.3.4 Root Water Uptake

HYDRUS-1D simulates root water uptake (RWU) of a crop during the growing season. The RWU, i.e., the sink term, S, in Richard's equation, was computed using equation 4.6 given by Feddes et al. (1978).

$$S = \alpha(h)\beta(z)T_p \tag{4.6}$$

where $\alpha(h)$ [-] is a dimensionless response function of h ($0 < \alpha(h) < 1$) which accounts for RWU stress; $\beta(z)$ is normalized water uptake distribution [L^{-1}]; T_p is a potential transpiration rate [LT^{-1}].

Water stress causes an RWU reduction, which is $\alpha(h)$, and can be explained as

$$\alpha(h) = \begin{cases} 0; & h > h_1 \text{ or } h < h_4 \\ \dfrac{h - h_1}{h_2 - h_1}; & h_1 > h > h_2 \\ 1; & h_2 \leq h \leq h_3 \\ \dfrac{h - h_4}{h_3 - h_4}; & h_3 > h > h_4 \end{cases} \tag{4.7}$$

where h_1 is called the anaerobiosis point, i.e., water uptake is considered to be zero close to the saturation ($h > h_1$); h_4 is pressure head at the wilting point and water uptake is also considered to be zero when $h < h_4$. Maximum RWU happens between h_2 and h_3, and it decreases or increases

linearly between the pressure heads h_3 and h_4 or h_1 and h_2, respectively (fig. 4.2). Since 95% of the corn roots are found within the 0-60 cm soil profile (Zhou and Zhao, 2019), and for this reason, we assumed linear root distribution function to a depth of 60 cm. The crop parameters of corn in Wesseling (1991) were selected for the root water uptake of corn in both zones.

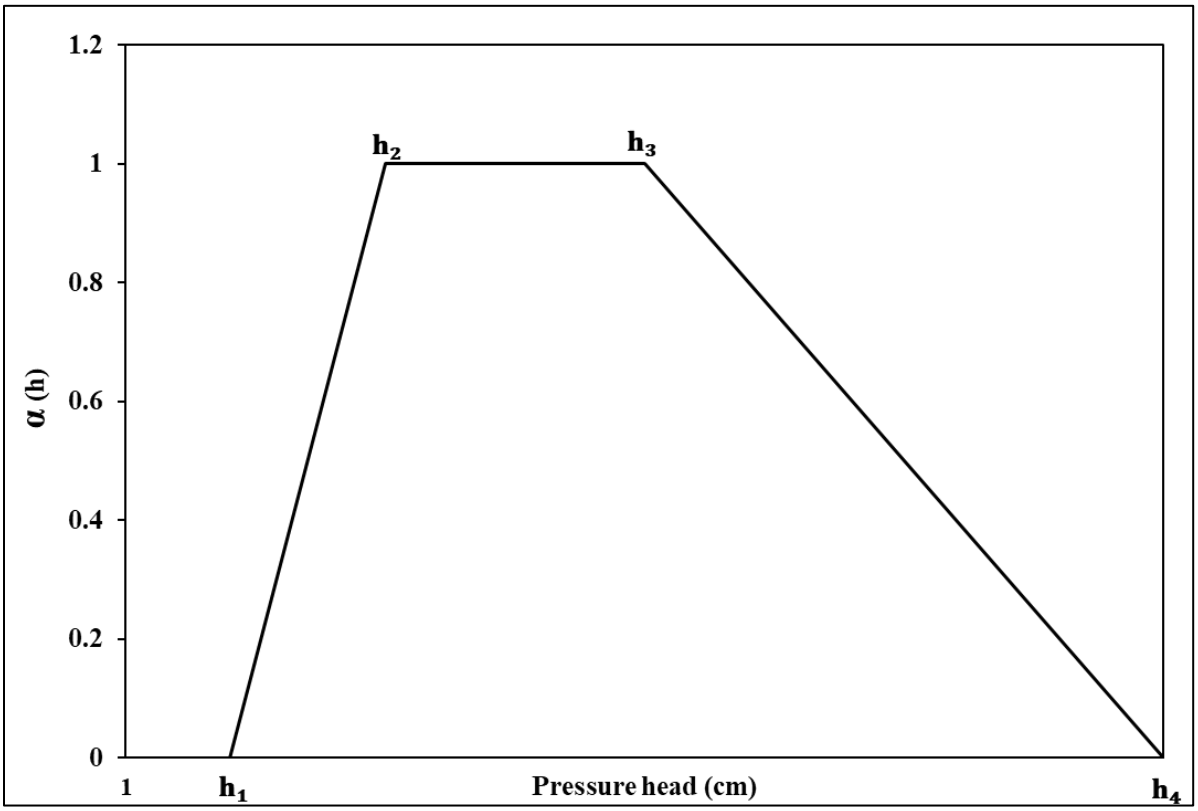

Figure 4.2 Schematic diagram of root water uptake stress response function.

4.3.4 Inverse Modeling to Optimize Zone-Specific SHPs-HYDRUS-1D as Reference Model

We used inverse modeling to optimize a single layer (0-100 cm) effective SHPs using h measured at three depths (0-15 cm, 15-30 cm, and 30-60 cm) in both zones. Due to fairly uniform soil layers and textural homogeneity within the soil depths in each zone, we used single-layer SHPs. We converted h into pF to perform inverse modeling in HYDRUS-1D. The HYDRUS-1D model was coupled with the SCE-UA developed by Duan et al. (1994) to perform optimization of SHPs

(Diamantopoulos et al., 2012; Qu et al., 2014). An objective function (Obj) was defined for minimization in the SCE-UA algorithm.

$$Obj = \sum_{j=1}^{nn} \left[pF_j - \widehat{pF_j}(x) \right]^2 \tag{4.8}$$

where $pF_j = \left[pF_{15cm,}\, pF_{30cm,}\, pF_{60cm} \right]$ is a vector of daily observations of h as pF values; $\widehat{pF_j} = \left[\widehat{pF}_{15cm,}\, \widehat{pF}_{30cm,}\, \widehat{pF}_{60cm} \right]$ a vector that contains daily HYDRUS-1D predictions of h as pF values; $x = (\theta_r, \theta_s, \alpha, n, K_s, l)$ is a vector of soil hydraulic parameters used in the van Genuchten model, K_s is saturated hydraulic conductivity, j is the number of each observation point, and nn is the total number of measurements at each soil depth. The model was set up from 05 April 2018 to 30 August 2019 when the corn was harvested. From 05 April 2018 until 30 April 2019, the model was trained to set initial conditions to run the simulations for the optimization of SHPs.

4.3.5 Goodness of Fit

Different indices of goodness of fit have been calculated: Root mean square error ($RMSE$), index of agreement (IA), and relative root mean square error ($RRMSE$) were used in this study.

$$RMSE = \sqrt{\frac{1}{nn} \sum_{j=1}^{nn} \left(\widehat{pF_j} - pF_j \right)^2} \tag{4.9}$$

$$IA = 1 - \frac{\sum_{j=1}^{nn} (\widehat{pF_j} - pF_j)^2}{\sum_{j=1}^{nn} (\left| \widehat{pF_j} - pF_{avg} \right| + \left| pF_j - pF_{avg} \right|)^2} \tag{4.10}$$

$$RRMSE = \frac{\sqrt{\frac{1}{nn} \sum_{j=1}^{nn} \left(\widehat{pF_j} - pF_j \right)^2}}{\sum_{j}^{nn} \left(pF_j \right)} \tag{4.11}$$

where nn is the total number of observations; $\widehat{pF_j}$ and pF_j are simulated and observed h as pF value, respectively, and pF_{avg} is average pF values. The lower the $RMSE$ value the better is the

model performance in predicting the data in terms of its absolute error. The IA value ranges from 0 to 1, and close to 1 indicates a better performance of the model. The $RRMSE$ indicates the performance of the model is excellent when $RRMSE < 0.1$, good if $0.1 \leq RRMSE \leq 0.2$, fair if $0.2 < RRMSE \leq 0.3$, and poor if $RRMSE > 0.3$ (Wang et al., 2018).

4.3.6 Irrigation Thresholds and Scheduling

We adopted a 35% SWD which is often recommended for most agronomic crops, especially corn (Girona et al., 2002; Irmak et al., 2016; Liang et al., 2016) to compute irrigation thresholds (Allen et al., 1998; Leininger et al., 2019). The thresholds at 35% SWD can be determined using the following equations.

$$|h|_{SWD} = \frac{\left\{\left[\frac{\theta_s - \theta_r}{\theta_{SWD} - \theta_r}\right]^{1/m} - 1\right\}^{1/n}}{\alpha} \tag{4.12}$$

$$\theta_{SWD} = \theta_{FC} - [SDW(\theta_{FC} - \theta_{PWP})] \tag{4.13}$$

$$I_{SWD} = \sum(\theta_{FC} - \theta_{SWD})Z \tag{4.14}$$

where $|h|_{SWD}$ is irrigation threshold value as h at 35% SWD [L]; θ_{SWD} is soil water content at 35% SWD [L^3L^{-3}]; θ_{FC} is soil water content at field capacity [L^3L^{-3}]; θ_{PWP} is soil water content at permanent wilting point [L^3L^{-3}]; I_{SWD} irrigation amount or depth [L]; Z is thickness of soil layer. Field capacity at an h value of 33 kPa and permanent wilting point at 1500 kPa were used to determine irrigation thresholds and schedule irrigation in this study.

The irrigation amounts were removed before running the simulations for irrigation scenarios in both zones. The precipitation was the only water input variable that was kept in the model. We defined these models as No Irrigation models (NI). The trigger irrigation module within the HYDRUS-1D model was selected to schedule the irrigations using the determined irrigation

thresholds and amounts at 35% SWD with zone-specific SHPs. The irrigation scheduling was performed using the observation nodes at 15 cm (node 1), 30 cm (node 2), and 60 cm (node 3), as the hypothetical depth of an installed sensor. At each observation node, multiple irrigation scenarios were created in each zone as summarized in table 2. We triggered the irrigations on the same day without delay (0Lag), after one day (1Lag), after two days (2Lag), after three days (3Lag), after four days (4Lag), and after five days (5Lag) when irrigation threshold reached (table 4.2). The idea of different irrigation scheduling was to bring the models of irrigation scenarios to the reference model status and reduce water stress or meet potential water requirements (Ramos et al., 2009).

Table 4.2 Descriptions of HYDRUS-1D models created for irrigation scheduling in both zones

Depth	Irrigation trigger description	Notations for Irrigation Scheduling Models
15 cm	0Lag	Top Node 0Lag
	1Lag	Top Node 1Lag
	2Lag	Top Node 2Lag
	3Lag	Top Node 3Lag
	4Lag	Top Node 4Lag
	5Lag	Top Node 5Lag
30 cm	0Lag	Center Node 0Lag
	1Lag	Center Node 1Lag
	2Lag	Center Node 2Lag
	3Lag	Center Node 3Lag
	4Lag	Center Node 4Lag
	5Lag	Center Node 5Lag
60 cm	0Lag	Bottom Node 0Lag
	1Lag	Bottom Node 1Lag
	2Lag	Bottom Node 2Lag
	3Lag	Bottom Node 3Lag
	4Lag	Bottom Node 4Lag
	5Lag	Bottom Node 5Lag

0Lag: Same day of threshold reached; 1Lag: After 1 day of threshold reached; 2Lag: After 2 days of threshold reached; 3Lag: After 3 days of threshold reached; 4Lag: After 4 days of threshold reached; 5Lag: After 5 days of threshold reached.

4.3.7 Actual Root Water Uptake and Irrigation Water for Various Irrigation Scenarios

We examined main components of soil water including potential root water uptake (PRWU), actual root water uptake (ARWU), and irrigation applied by different scenarios (Zheng et al., 2017; Zhou and Zhao, 2019). The HYDRUS-1D model tries to meet every day potential root water uptake (PRWU), and if the water is not available, a stress function reduces it to ARWU. The ratios of ARWU and PRWU for various scenarios were calculated to estimate the water stress in both zones. A value of close to one shows no water stress in the crop, and a value close to zero indicates severe water stress in the crop (Ramos et al., 2009) and inefficient irrigation. Increasing ARWU helps increase crop yield while ad decrease in ARWU results in yield reduction (Ramos et al., 2011).

4.4 Results and Discussion

4.4.1 Inverse HYDRUS-1D Model Performance for Optimizing SHPs

A single porosity model characterized the SHPs to satisfy the relation for both zones using HYPROP-FIT software (Mualem, 1976; van Genuchten, 1980). The raw SHPs in zone 1 and zone 2 obtained from HYPROP-FIT software are shown in fig. 4.3. These raw SHPs were used as input parameters in the inverse HYDRUS-1D model to start the simulations for optimizing SHPs. The raw SHPs showed the spatial variability between zone 1 and zone 2 (fig. 4.3). Both zones had distinct patterns of SHPs, which means invariable SHPs cannot be assumed throughout the field for irrigation management. It was inferred from the raw SHPs that considering uniform SHPs within the field can be a flawed irrigation strategy due to zone-specific variability. Using uniform SHPs will trigger irrigation at one threshold and one rate in the entire field. It was inferred from these raw SHPs that we need to consider spatial variability between the zones for better irrigation management and we need to adopt zone-specific SHPs. Although raw SHPs showed the

importance of zone-specific SHPs between the zones, the raw SHPs were not able to simulate field observations of soil matric potentials (h) measured during the growing season. This reason signified the need for optimizing zone-specific SHPs to simulate the soil water dynamics in each zone using field observations.

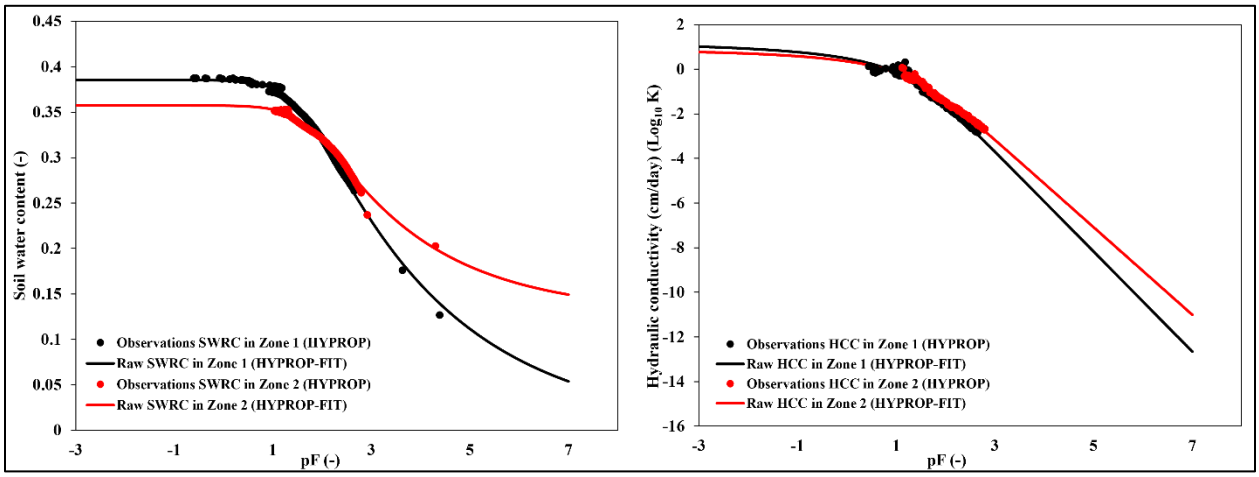

Figure 4.3 Raw soil hydraulic properties; Soil water retention curves (left), showing relation between volumetric soil water content and pF, and hydraulic conductivity curve (right). The observations (dots) were obtained from the HYPROP measurement system and fitted with HYPROP-FIT software.

Inverse solution using measured h indicated the importance and need for optimizing the zone-specific SHPs (fig. 4.4) in precision agriculture, for zone-specific irrigation improvements across the field to conserve agricultural water, and for the adoption of VRI technology. The optimized SHPs obtained using inverse HYDRUS-1D modeling were different from raw SHPs obtained from HYPROP-FIT software in the lab. Using the inverse solution in each zone, we found more effective zone-specific SHPs, which simulated soil water dynamics with good agreement in both zones (table 4.3). The simulated pF values fitted well with measured pF values for all the soil depths using optimized SHPs in both zones using optimized SHPs, as shown in fig. 4.5 and 4.6.

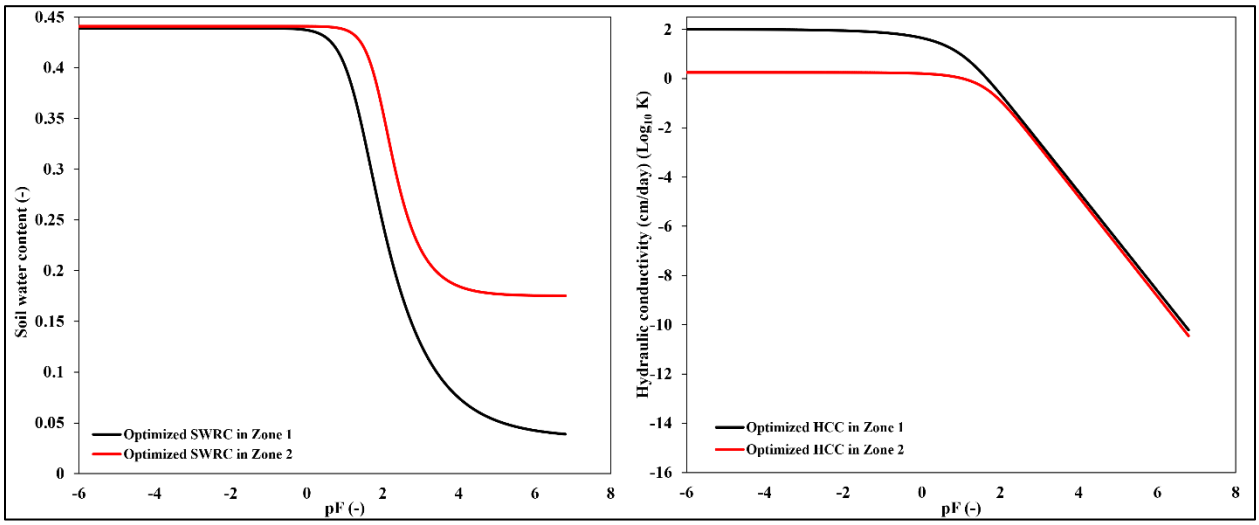

Figure 4.4 Zone-specific optimized SHPs; soil water retention curve(left), showing relation between volumetric soil water content and pF, and hydraulic conductivity curve (right) obtained from inverse modeling.

The HYDRUS-1D model described relatively well the observed data in all three soil layers in both zones using a single layer zone-specific optimized SHPs. The variability in soil water dynamics were due to the attributes considered in delineating management zones, for example, topographic attributes and soil texture. At the beginning of simulations, the gap between measured and simulated data was be due to the stabilization issues associated with the Watermark sensors, and it can take two to three weeks to stabilize the sensors in the crop fields (Irmak et al., 2016).

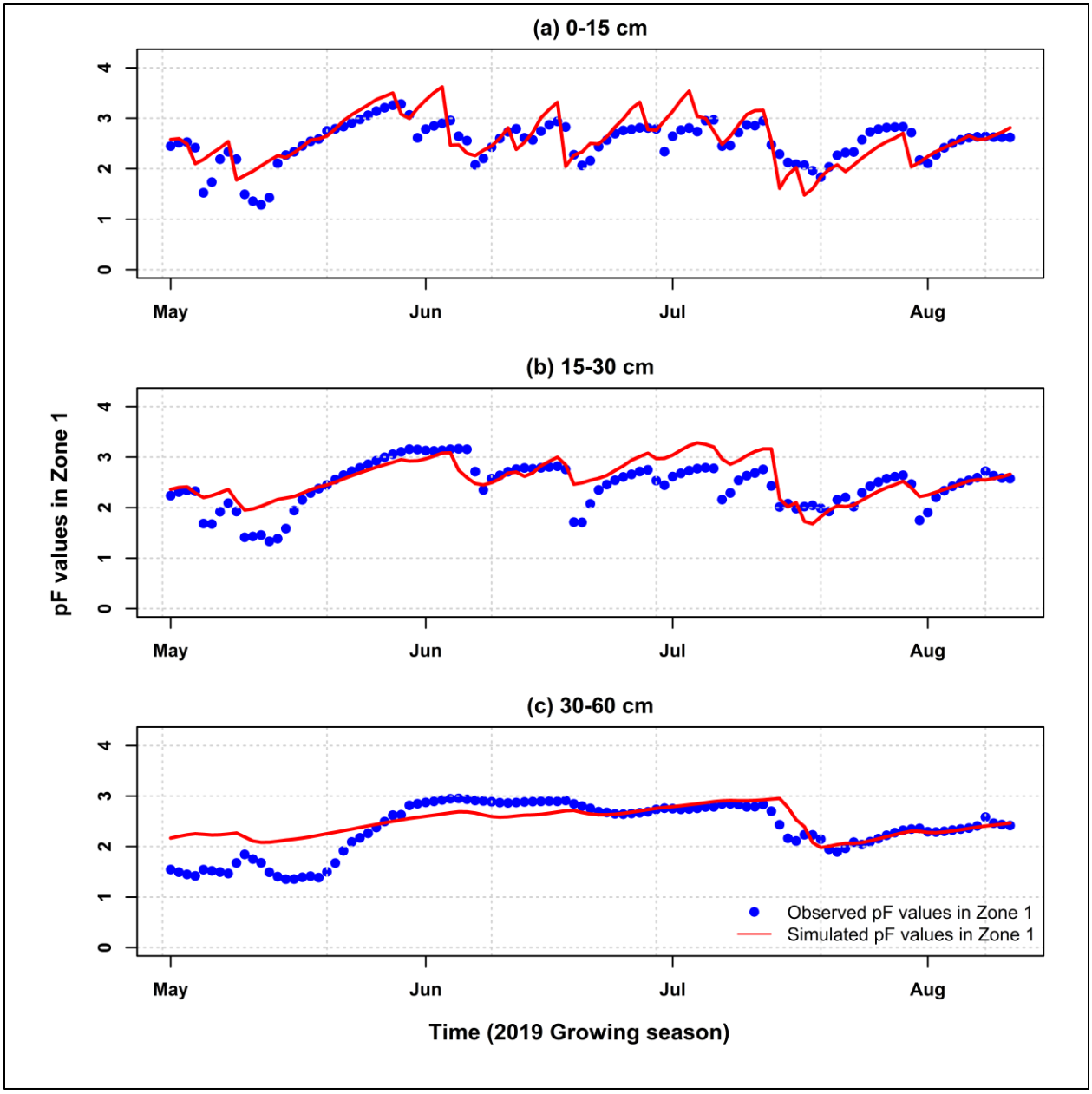

Figure 4.5 Observed and simulated pF values in zone 1 at (a) 0-15 cm, (b) 15-30 cm, and (c) 30-60 cm soil depths during the 2019 growing season.

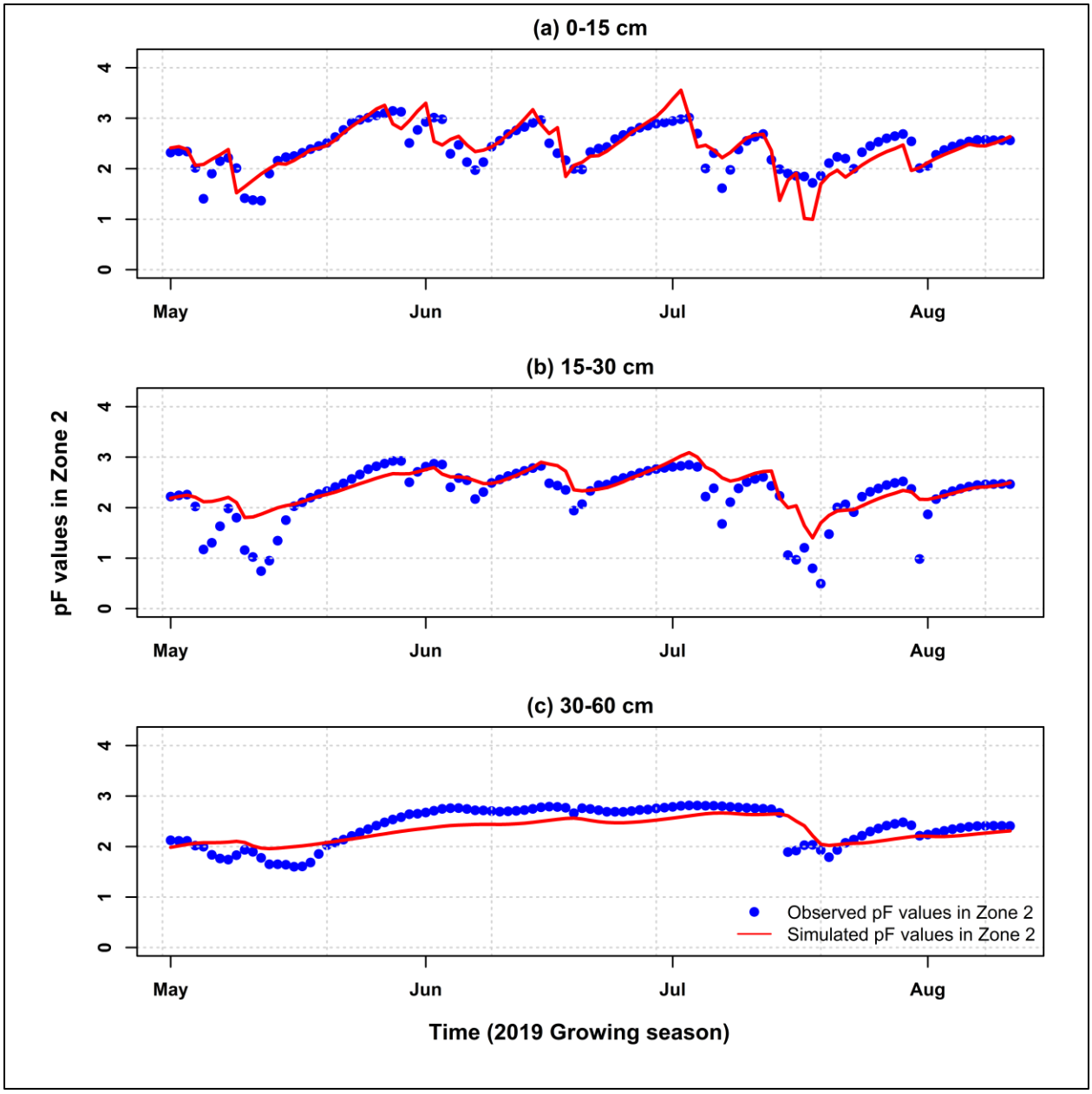

Figure 4.6 Observed and simulated pF values in zone 2 at (a) 0-15 cm, (b) 15-30 cm, and (c) 30-60 cm soil depths during the 2019 growing season.

Table 4.3 Statistical indices showing performance of inverse HYDRUS-1D model to simulate pF at each soil depth in both zones

Zones	Statistical indices	0-15 cm			15-30 cm			30-60 cm		
		RMSE (-)	IA (-)	RRMSE (-)	RMSE (-)	IA (-)	RRMSE (-)	RMSE (-)	IA (-)	RRMSE (-)
Zone 1	Mean	0.36	0.82	0.001	0.29	0.84	0.001	0.38	0.78	0.001
	Min.	0.33	0.78	0.001	0.22	0.83	0.001	0.35	0.78	0.001
	Max.	0.38	0.85	0.002	0.33	0.86	0.001	0.41	0.79	0.002

	Mean	0.33	0.83	0.001	0.38	0.79	0.002	0.40	0.71	0.001
Zone 2	Min.	0.27	0.75	0.001	0.35	0.76	0.001	0.24	0.62	0
	Max.	0.41	0.89	0.002	0.4	0.81	0.002	0.55	0.84	0.002

According to model testing at multiple locations in zone 1, among all soil depths in zone 1, the model performed best at a 15-30 cm soil depth with the best agreement and minimum error between observed and simulated data, followed by 0-15 cm and 30-60 cm (table 4.3). However, in zone 2, the observed and simulated data had the best agreement at 0-15 cm (table 4.3) with the lowest error among all soil depths. In comparison between the two zones, zone 1 performed better than zone 2 since the statistical indices were better in zone 1. The variation in the model performances in both zones was due to differences in the SHPs (fig. 4.4), differences in the topographic attributes (low slope and high TWI in zone 1 and high slope and low TWI in zone 2), and differences in root water uptake (fig. 4.7), which affected the soil water dynamics in both zones (fig. 4.6). It can also be noticed from the recorded plant height and LAI values, which were greater in zone 1 and lower in zone 2.

Please note that the one-layer optimized HYDRUS-1D model is a simplified version using single layer SHPs of the complex system, which can be used to simulate soil water dynamics at all three layers (fig. 4.5 and 4.6). However, comparing previous studies for HYDRUS-1D model performance using multilayer SHPs, Li et al. (2014) conducted a study in an irrigated rice field in China and the minimum average $RMSE$ achieved was 2.61 cm using the individual retention curves obtained from the RETC retention curves computer program for each layer from 0 to 100 cm at 20 cm increment depth. The RETC is a computer program that determines the soil hydraulic properties in the soil profile using parametric models such as van Genuchten and Brooks-Corey models (van Genuchten et al., 1991). Wyatt et al. (2017) reported an $RMSE$ ranged from 2.95 to 3.53 in terms of pF higher in deep soil layer in a study to estimate groundwater recharge at four

different sites in Oklahoma using the HYDRUS-1D model. However, these studies did not take all parameters of SWRC and HCC into account to find optimized SHPs. Some underpredictions and over-predictions of simulated data compared to observed data during the simulation period can be associated with soil water retention behavior of a fine-textured soil (Iqbal et al., 2020), hysteresis effect (Zhou and Zhao, 2019), and measurement errors associated with the sensors (Li et al., 2014; Mokari et al., 2019). Mokari et al. (2019) reported an IA that varied from 0.44 to 0.73. Discrepancies between observed and simulated data in the zones due to lateral leakage and macro-pores have also been reported in previous studies (Akay et al., 2008; Wang et al., 2011; Zhang et al., 2018). Based on the statistics to evaluate the goodness of fit, the model performance was evaluated as excellent to optimize zone-specific SHPs since our results were quite consistent and better than previous studies (Li et al., 2014; Mokari et al., 2019; Wyatt et al., 2017) using a single layer SHPs. Therefore, a single-layer with optimized SHPs can be utilized to predict h in deep soil layers more accurately with complete set of parameters.

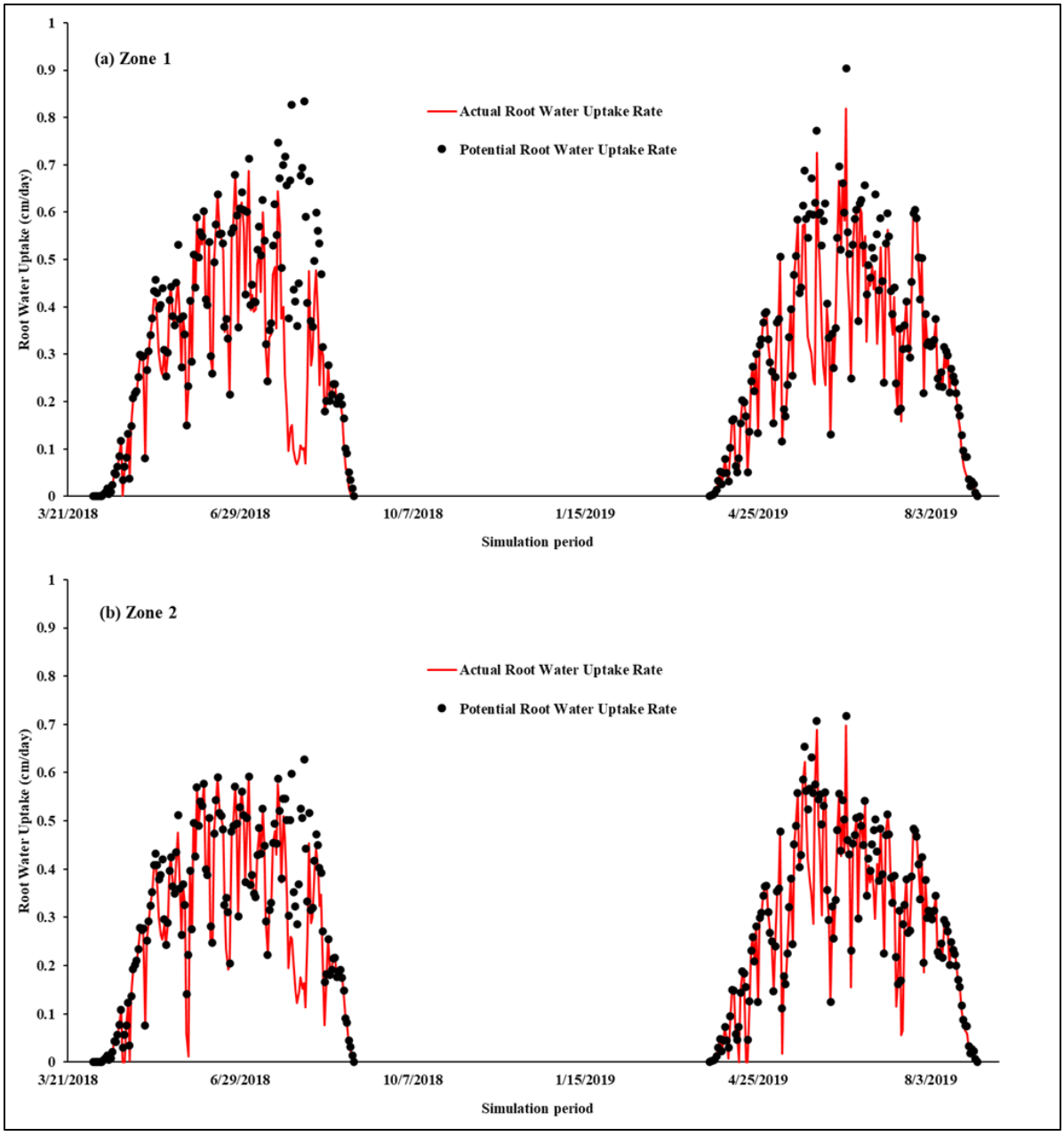

Figure 4.7 Root Water Uptake in (a) zone 1 and (b) zone 2 during 2018 and 2019 growing seasons

Fig. 4.7 shows the actual and potential RWU in both zones simulated using the optimized HYDRUS-1D model during the growing seasons of corn. During the seed germination stage, RWU was almost zero and increased with growing stages. The different patterns of RWU can be noticed in the 2018 and 2019 growing seasons in both zones. The actual RWU gradually increased and

reached a maximum of 0.69 cm day^{-1} in zone 1 and 0.59 cm day^{-1} in zone 2 around the 86^{th} day after planting in 2018, and 0.82 cm day^{-1} in zone 1 and 0.70 cm day^{-1} in zone 2 around the 80^{th} day after planting in the 2019 growing season. The RWU results are consistent with previous studies (Zhou and Zhao, 2019; Iqbal et al., 2020). The maximum RWU increased in both zones from the 2018 to 2019 growing seasons. The zone 1 had silty clay loam texture in the soil profile; however, zone 2 had clay texture. The clay texture has maximum water holding capacity and minimum water releasing property. Silt type soils have slightly less water holding capacity than clay, but have a greater water releasing property than clay soils. Also, plant available water (field capacity – permanent wilting point) in the soil profile of zone 1 was 1.6 times that of zone 2. Therefore, the ARWU was greater in zone 1 than zone 2 in both seasons. This variation of RWU in both zones and the differences in zone-specific SHPs had the impact on plant characteristics. For example, the maximum measured LAI was 4.13 cm2 cm^{-2} and 3.34 cm2 cm^{-2} in zone 1 and zone 2, respectively on the 92^{nd} day after planting during the 2019 growing season. On the same day of LAI measurements, the plant height was 225 cm and 195 cm in zone 1 and zone 2, respectively. These field measurements for plant characteristics explain the zone-specific differences in root water uptake, which is controlled by zone-specific SHPs. Similar observations have been found in previous studies (Wang et al., 2016; Aggarwal et al., 2017).

4.4.2 Determination of Irrigation Thresholds and Amounts

The accurate determination of an irrigation threshold and amount is critical for triggering zone-specific irrigation in crop fields. Table 4.4 summarized the irrigation thresholds and amounts determined using zone-specific optimized SHPs. It can be seen from table 4.4 that irrigation thresholds in both zones were different, which explicitly indicated the need to manage irrigation based on specific zones during the growing seasons. The irrigation thresholds were optimized to a

soil matric potential value of 76 kPa from a raw value of 102 kPa in zone 1 and 59 kPa from 69 kPa in zone 2. The corresponding irrigation amounts were optimized to 2.18 cm in zone 1 and 1.48 cm in zone 2. Optimizing zone-specific SHPs optimized the thresholds to trigger irrigation and reduced the irrigation amount to 2.18 cm in zone 1 and 1.48 cm in zone 2 (table 4.4). Among a very few studies that report irrigation thresholds, Irmak et al. (2016) suggested a range of irrigation thresholds from 90 kPa to 110 kPa for silt loam to silty clay loam soils in Nebraska. However, the range was not estimated using optimized SHPs in field conditions, and therefore, did not hold site-specific physical and hydraulic characteristics. Generally, farmers apply irrigation uniformly based on the feel of the soil or looking at the crop during the growing season (Kumar et al., 2021b). Delineating the irrigation management zones and adopting zone-specific irrigation strategies can help avoid water stress and water excess in the crop field. Irrigation threshold determined using raw SHPs can mislead the time and depth to trigger the irrigation since it did not simulate soil water dynamics within the zones. Optimizing the irrigation thresholds to trigger irrigation can help consider effective irrigation rate, time, and depth during the growing season. Based on our finding, we can reduce applied amounts as compared to raw SHPs obtained in the lab. This methodology can help in determining correct irrigation thresholds and amounts, which can be useful in site-specific management of irrigation water during the growing seasons, and which can help to avoid water stress and water excess in crop fields.

Table 4.4 Irrigation thresholds (soil matric potential values) and amounts using zone-specific optimized and raw SHPs at 35% SWD.

	Irrigation threshold		**Irrigation amount**	
	Optimized	**Raw**	**Optimized**	**Raw**
Zone 1	76 kPa	102 kPa	2.18 cm	2.6 cm
Zone 2	59 kPa	69 kPa	1.48 cm	1.9 cm

4.4.3 Irrigation Scheduling and Actual Root Water Uptake with Different irrigation Scenarios

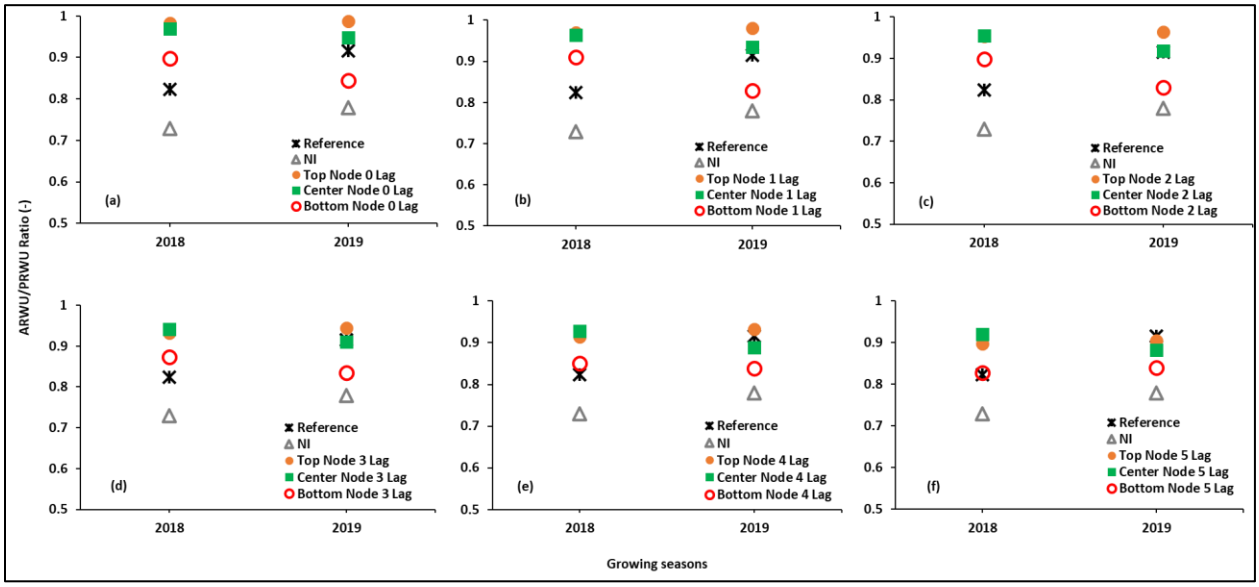

Figure 4.8 Actual to potential root water uptake ratios in zone 1 for (a) 0Lag, (b) 1Lag, (c) 2Lag, (d) 3Lag, (e) 4Lag, and (f) 5Lag irrigation scenarios during 2018 and 2019 growing seasons. Reference scenario is the inverse model and NI is the model without irrigation data.

The zone-specific determined thresholds and amounts using optimized SHPs were adopted in the HYDRUS-1D model to develop scenarios of irrigation scheduling. Among all different irrigation scenarios, scenarios with 0Lag, 1Lag, 2Lag, 3Lag, 4Lag, and 5Lag using the top node (15 cm) and center node (30 cm) in zone 1 reduced the crop water stress conditions and achieved an ARWU/PRWU ratio greater than or equivalent to the reference model (fig. 4.8) for both the 2018 and 2019 growing seasons. The actual irrigations applied in the field were 6.6 cm in 2018 and 8.76 cm in 2019, which were input in the reference model. The reference model had the ARWU/PRWU ratios of 0.8 in 2018 and 0.9 in 2019 in zone 1(fig. 4.8). Among all the scenarios, the maximum irrigation amount applied was 21.8 cm in 2018 and 19.62 in 2019 with 0Lag and 1Lag using the top node, and achieved an ARWU/PRWU ratio greater than 0.97 in both seasons. However, the minimum irrigation applied was 10.9 cm in 2018 with 5Lag and 6.54 cm in 2019 with 0Lag, 1Lag,

2Lag, and 3Lag using the bottom node (fig. 4.9). A minimum ARWU/PRWU ratio of 0.83 was achieved in both seasons. The distribution of precipitation over the growing seasons is the most critical component to decide the irrigation (Filho et al., 2020). Based on total precipitation distribution over the growing seasons, the maximum precipitation occurred in the beginning and near the end of the growing seasons (fig. 4.1). Therefore, looking at the actual irrigation data applied in the field, 71% of actual irrigations were triggered during July 2018 and 100% in May-June 2019. The reference model had the ARWU/PRWU ratios of 0.7 in July 2018 and 0.8 in May-June 2019. Out of total irrigations applied by the top and center nodes, more than 61% was triggered in July 2018 and more than 75% was triggered in May-June 2019. If no irrigation was applied during these periods, the crop was water-stressed with an AWRU/PRWU ratio of 0.44 in July 2018 and 0.68 in May-June 2019 due to lack of precipitation in this period (fig. 4.1). As an ideal case to adopt an irrigation scenario, the top and center nodes with 5Lag improved the RWU in plants and performed better than the reference model in 2018 and equivalent to reference model in 2019 in zone 1. The impact of lack of precipitation over the growing seasons and the need for irrigation can be understood with an example of the top node with 5Lag. The top node with 5Lag scenario applied 15.26 cm and 13.08 cm as total irrigation in 2018 and 2019 growing seasons, respectively (fig. 4.9), which was 8.6 cm and 4.26 cm of excess irrigation in 2018 and 2019, respectively. Applying this excess irrigation water increased the RWU and improved the ARWU/PRWU ratio. Of 15.26 cm and 13.08 cm of irrigation water amounts, 8.72 cm was applied in July 2018 and in May-June 2019. It was found that excess irrigation (8.6 cm in 2018 and 4.26 cm in 2019) contributed to the period of less precipitation in both growing seasons. Applying this excess irrigation water improved the ARWU/PRWU ratio in the water-stress months (July 2018 and May-June 2019) and entire growing season (fug. 4.8). The top and center nodes in zone 1 can

perform well to monitor h and to trigger irrigation with any lag scenario using HYDRUS-1D. Irrigation scenarios using the bottom node, which was at the 60 cm at the bottom of root zone in zone 1, increased the ARWU and improved the ARWU/PRWU ratio (fig. 4.8) for all irrigation scenarios compared to the reference model in 2018. However, the bottom node achieved a minimum ARWU/PRWU ratio of 0.83 in 2019 (fig. 4.8). The bottom node triggered minimum irrigation in both growing seasons (fig. 4.9) since soil matric potential did not reach irrigation thresholds frequently. Using the bottom node to trigger irrigation, greater than 60% of the irrigation amount was applied in July, and more than 67% was applied May-June of 2019

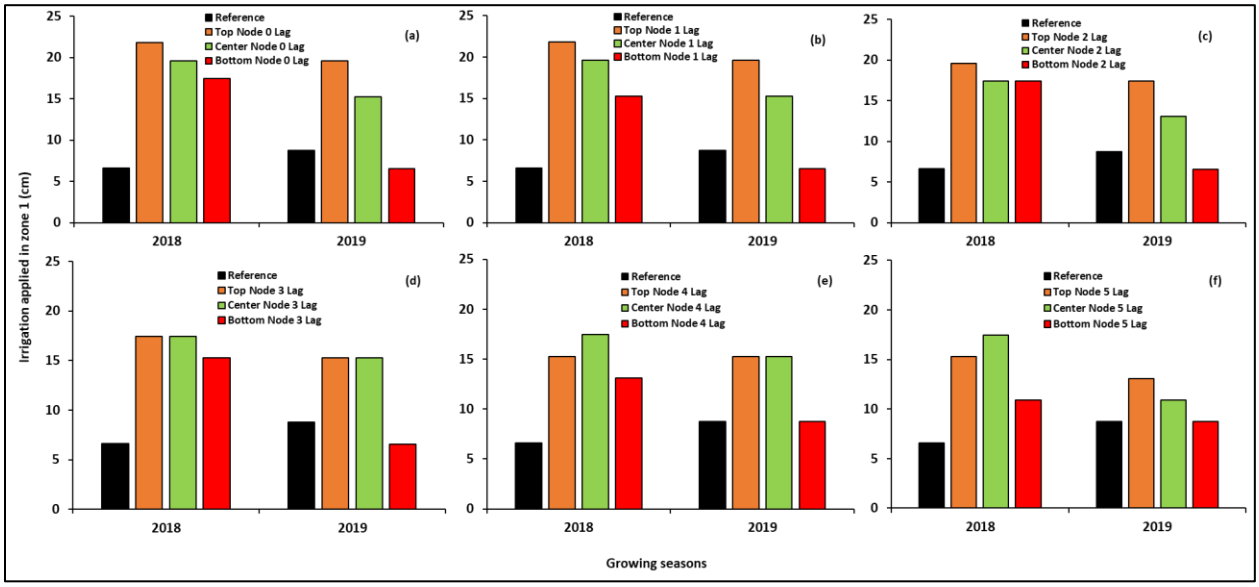

Figure 4.9 Total amount of irrigation applied in zone 1 for (a) 0Lag, (b) 1Lag, (c) 2Lag, (d) 3Lag, (e) 4Lag, and (f) 5Lag irrigation scenarios during 2018 and 2019 growing seasons.

In all the irrigation scenarios using top, center, and bottom nodes, RWU was mostly affected in the middle of the growing seasons, where minimum precipitation occurred. This middle period of the growing seasons was critical for the plants, which need maximum water uptake for plant growth and better yield production (Filho et al., 2020). A similar effect of precipitation distribution and the need for irrigation were found by Filho et al. (2020) in Alabama and Irmak et al. (2012) in

Nebraska. Also, the excess irrigation occurred during the water-stress period of the growing season (July 2018 and May-June 2019), which increased the ARWU and consequently AWRU/PRWU ratios. Although farmers trigger irrigation based on the feel of the soil and looking at the crop, they end up with over-irrigation in some areas and under-irrigation in others. It will be wise to adopt an irrigation strategy and install the sensors at 15 cm or 30 cm in zone 1 since these depths showed an increased ARWU/PRWU ratio relative to the reference scenario.

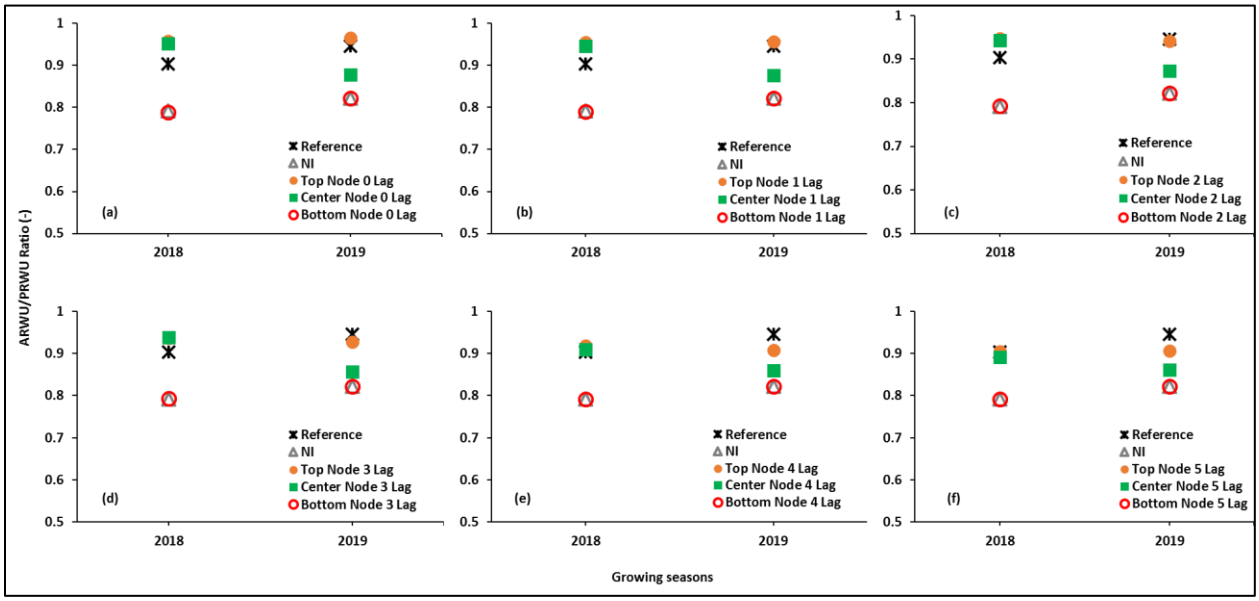

Figure 4.10 Actual to potential root water uptake ratios in zone 2 for (a) 0Lag, (b) 1Lag, (c) 2Lag, (d) 3Lag, (e) 4Lag, and (f) 5Lag irrigation models during 2018 and 2019 growing seasons.

In zone 2, the top node in 2018 and 2019 (except 4Lag and 5Lag in 2019) and center node in 2018 increased the ARWU, reduced the crop water stress, and produced a greater ARWU/PRWU ratio (fig. 4.10) as compared to the reference model for all irrigation scenarios in zone 2. The center node in zone 2 increased ARWU and achieved an ARWU/PRWU ratio greater than or equivalent to the reference model (fig. 4.10) for all scenarios of 2018, but not in 2019. These models showed improved RWU and reduced the water stress conditions in plants in 2018 the growing season. The minimum value of the ARWU/PRWU ratio using the center node to trigger irrigation was 0.86 in

2019 for 3Lag, 4Lag, and 5Lag scenarios. However, the bottom node did not trigger the irrigation during the 2019 growing season and triggered less irrigation than the reference scenario in 2018 except 0Lag and 1Lag irrigation scenarios (fig. 4.11). The bottom node did not improve the RWU and produced the ARWU/PRWU ratio equivalent to the NI model in both growing seasons (fig. 4.10). This suggested that the bottom node cannot be used to monitor h and cannot be used to trigger the irrigation in zone 2.

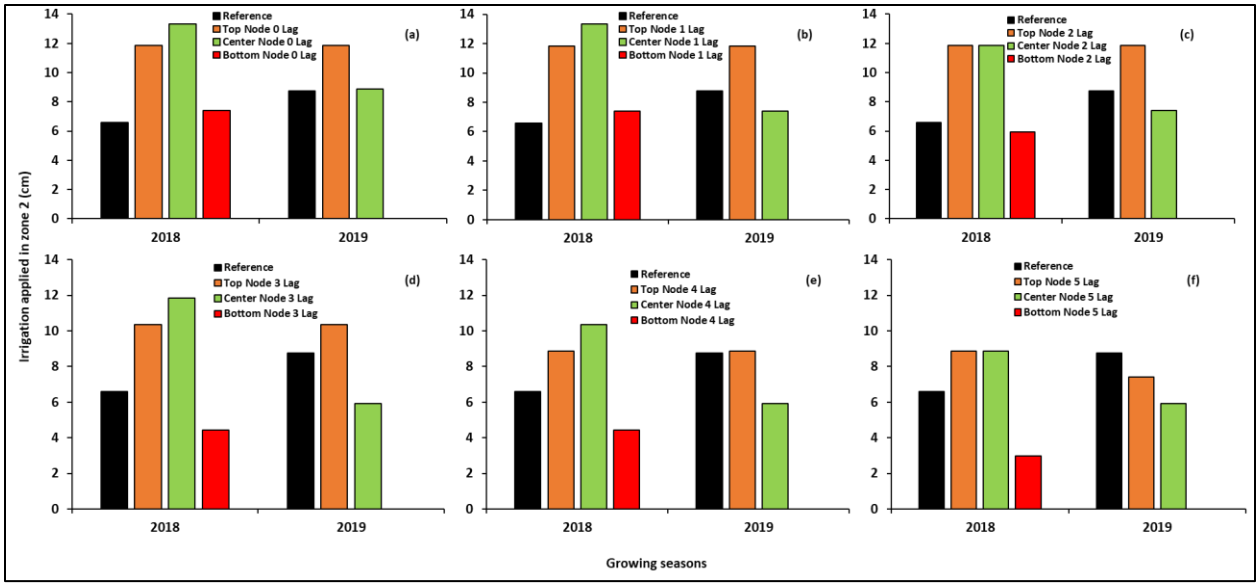

Figure 4.11 Total amount of irrigation applied in zone 2 for (a) 0Lag, (b) 1Lag, (c) 2Lag, (d) 3Lag, (e) 4Lag, and (f) 5Lag irrigation scenarios during 2018 and 2019 growing seasons.

As an ideal case to adopt an irrigation scenario in zone 2, the top node with 1Lag and 2Lag improved the RWU by plants in both seasons and performed better than the reference model. These models improved the ARWU/PRWU ratio to 0.96 in 2018 and 0.94 in 2019 (fig. 4.11) and reduced the water stress in the crop. The irrigation scenario using the top node with 3Lag had a better ARWU/PRWU ratio in 2018 and equivalent ratio in 2019 compared to the reference scenario. The maximum triggered irrigation was 13.32 cm with the center node (fig. 4.11) using the 0Lag and 1Lag scenario in 2018. However, the minimum irrigation was 0 cm using the bottom node (fig.

4.11). Similar to zone 1, most of the irrigations in zone 2 were triggered in July 2018 and May-June 2019 due to the lack of precipitation over the growing season (fig. 4.1). Irrigation scenarios using top and center nodes triggered greater than 73% of the total irrigation in July 2018 and greater than 72% May-June 2019. Without irrigation, NI scenarios had the ARWU/PRWU ratio of 0.58 and 0.76 in July 2018 and in May-June 2019, respectively, similar to the bottom node scenarios, which showed the crop water stress and lack of water in zone 2. For example, the top node with the 4Lag scenario applied 11.84 cm as the total irrigation in both growing seasons (fig. 4.11), which was 5.24 cm and 3.08 cm of excess irrigation in 2018 and 2019, respectively. Applying this excess irrigation water increased the RWU and improved the ARWU/PRWU ratio. Of 11.84 cm of irrigation water amount, 7.4 cm was applied in July 2018 and 8.88 cm in May-June 2019. It was found that excess irrigation (5.24 cm in 2018 and 3.08 cm in 2019) compensated for the period of less precipitation in both growing seasons. Irrigation scheduling using the top node performed better or equivalent to the reference model for various irrigation scenarios during the growing seasons in zone 2. Therefore, farmers can adopt an irrigation strategy in zone 2 by installing sensors at 15 cm soil depth to avoid water excess or severe crop water stress conditions during the growing season.

The model can achieve maximum RWU and reduce the crop water stress in both seasons. Also, assuming one irrigation threshold or using laboratory-drawn SHPs for the entire field can be a flawed irrigation management practice. Optimizing zone-specific SHPs can avoid discrepancies in field observation and result in better irrigation practices. Our results showed that each zone should be managed differently to improve water use and root water uptake. The results showed that optimizing irrigation thresholds can reduce the irrigation amount to be applied and simultaneously can increase the ARWU/PRWU ratio. However, if the calculated irrigation depth in any zones is

greater than the irrigation system capacity or the application rate exceeds the infiltration rate, the irrigation depth needs to be reduced while the frequency to irrigate should increase. Reduction in irrigation depth and increased frequency can simultaneously be achieved by adopting a lower threshold of SWD. Reducing the irrigation depth will provide more freedom to the plant for water uptake and increase the ARWU/PRWU ratio during the growing season. The lack of irrigation and crop water stress causes yield loss at any stage of the crop during the growing season (Çakir, 2004; Song et al., 2019). Therefore, meeting water demands by plants using zone-specific irrigation practices within a field can reduce the crop water stress and improve the crop yield during the growing season. Increasing the actual to potential root water uptake ratio can result in increasing crop yield (Ramos et al., 2009, 2011).

4.5 Summary and Conclusions

Zone-specific SHPs were estimated for two delineated irrigation management zones in a crop field with fine-textured soils. It can be concluded that both the zones also had spatial variability in SHPs along with the differences in soil texture, topographic attributes, and corn grain yield. The optimized inverse HYDRUS-1D model showed the impact on the shape and parameters of SHPs in both zones. A single layer HYDRUS-1D model simulated multilayered h very well for each zone using optimized SHPs. Determination of irrigation thresholds was highly dependent on zone-specific characteristics of SHPs and important for site-specific management of irrigation water. Optimizing the SHPs for each zone allowed us to develop zone-specific irrigation thresholds and irrigation amounts to schedule irrigation during the growing season. The determined irrigation thresholds can be used for efficient VRI and other irrigation water management. Based on our simulations in this study using optimized models, the irrigation thresholds with soil matric potential values of around 80 kPa in zone 1 and 60 kPa in zone 2 can arrive at different times or at

the same time during the growing season. The results showed conservation of irrigation water to trigger using optimized SHPs compared to laboratory drawn SHPs in both zones. Due to the lack of water available to the plants, especially in the middle of the growing season, the crop can suffer from severe crop water stress. Farmers can improve site-specific irrigation practices in both zones considering spatial variability in SHPs. Farmers can install the sensors at 15 cm or 30 cm depths in zone 1 and at 15 cm in zone 2 as optimal depths to monitor the soil matric potential, which can be used to trigger the irrigation using optimized SHPs. Improving the ARWU/PRWU by scheduling irrigation when needed can increase the crop yield by meeting the crop water demands on time. Uniform irrigation or assuming one threshold for irrigation and the use of raw SHPs within the zones would be less desirable irrigation strategies. Optimizing zone-specific SHPs showed that determining an accurate irrigation threshold in each zone can be an effective irrigation practice during the growing season. This study can best represent the site-specific irrigation scenarios. Therefore, additional research is needed to validate the suggested irrigation scenarios incorporating crop yield and implications of the irrigation management scenarios investigated in this study.

4.6 References

Aggarwal, P., Bhattacharyya, R., Mishra, A.K., Das, T.K., Šimůnek, J., Pramanik, P., Sudhishri, S., Vashisth, A., Krishnan, P., Chakraborty, D., Kamble, K.H., 2017. Modelling soil water balance and root water uptake in cotton grown under different soil conservation practices in the Indo-Gangetic Plain. Agric. Ecosyst. Environ. 240, 287–299. https://doi.org/10.1016/j.agee.2017.02.028

Akay, O., Fox, G.A., Šimůnek, J., 2008. Numerical Simulation of Flow Dynamics during Macropore–Subsurface Drain Interactions Using HYDRUS. Vadose Zo. J. 7, 909–918. https://doi.org/10.2136/VZJ2007.0148

Allen, R. G., Pereira, L. S., Raes, D., and Smith, M., 1998. FAO Irrigation and Drainage Paper. Irrig. Drain. 300, 300.

Beven, K.J., Kirkby, M.J., 1979. A physically based, variable contributing area model of basin hydrology / Un modèle à base physique de zone d'appel variable de l'hydrologie du bassin

versant. Hydrol. Sci. Bull. 24, 43–69. https://doi.org/10.1080/02626667909491834

Bouyoucos, G.J., 1962. Hydrometer Method Improved for Making Particle Size Analyses of Soils1. Agron. J. 54, 464–465. https://doi.org/10.2134/agronj1962.00021962005400050028x

Çakir, R., 2004. Effect of water stress at different development stages on vegetative and reproductive growth of corn. F. Crop. Res. 89, 1–16. https://doi.org/10.1016/J.FCR.2004.01.005

Diamantopoulos, E., Iden, S.C., Durner, W., 2012. Inverse modeling of dynamic nonequilibrium in water flow with an effective approach. Water Resour. Res. 48. https://doi.org/10.1029/2011WR010717

Duan, Q., Sorooshian, S., Gupta, V.K., 1994. Optimal use of the SCE-UA global optimization method for calibrating watershed models. J. Hydrol. 158, 265–284. https://doi.org/10.1016/0022-1694(94)90057-4

Evans, R.G., Sadler, E.J., 2008. Methods and technologies to improve efficiency of water use. Water Resour. Res. 44. https://doi.org/10.1029/2007WR006200

Evett, S.R., Stone, K.C., Schwartz, R.C., O'Shaughnessy, S.A., Colaizzi, P.D., Anderson, S.K., Anderson, D.J., 2019. Resolving discrepancies between laboratory-determined field capacity values and field water content observations: implications for irrigation management. Irrig. Sci. 37, 751–759. https://doi.org/10.1007/S00271-019-00644-4/FIGURES/8

FAO, 2016. Food and Agriculture Organization of the United Nations. AQUASTAT web- site. http://www.fao.org/nr/water/aquastat/water_use/index.stm/ website (accessed on December 7, 2021).

Feddes, R.A., Kowalik, P.J., Zaradny, H., 1978. Simulation of Field Water Use and Crop Yield. CropYield. John Wiley, New York, NY.

Filho, J.F.L.C. Da, Ortiz, B. V, Damianidis, D., Balkcom, K.S., Dougherty, M., Knappenberger, T., Franco, J., Cunha, D., Filho, L., 2020. Irrigation Scheduling to Promote Corn Productivity in Central Alabama. J. Agric. Sci. 12. https://doi.org/10.5539/jas.v12n9p34

Fontanet, M., Scudiero, E., Skaggs, T.H., Fernàndez-Garcia, D., Ferrer, F., Rodrigo, G., Bellvert, J., 2020. Dynamic Management Zones for Irrigation Scheduling. Agric. Water Manag. 238, 106207. https://doi.org/10.1016/j.agwat.2020.106207

Fridgen, J.J., Kitchen, N.R., Sudduth, K.A., Drummond, S.T., Wiebold, W.J. and Fraisse, C.W., 2004. Management Zone Analyst (MZA): Software for Subfield Management Zone Delineation. Agron. J. 96, 100-108. https://doi.org/10.2134/AGRONJ2004.1000

Girona, J., Mata, M., Fereres, E., Goldhamer, D.A., Cohen, M., 2002. Evapotranspiration and soil water dynamics of peach trees under water deficits. Agric. Water Manag. 54, 107–122. https://doi.org/10.1016/S0378-3774(01)00149-4

González, M.G., Ramos, T.B., Carlesso, R., Paredes, P., Petry, M.T., Martins, J.D., Aires, N.P., Pereira, L.S., 2015. Modelling soil water dynamics of full and deficit drip irrigated maize cultivated under a rain shelter. Biosyst. Eng. 132, 1–18. https://doi.org/10.1016/j.biosystemseng.2015.02.001

Gu, Z., Qi, Z., Burghate, R., Yuan, S., Jiao, X., Xu, J., 2020. Irrigation Scheduling Approaches

and Applications: A Review. J. Irrig. Drain. Eng. 146, 04020007. https://doi.org/10.1061/(asce)ir.1943-4774.0001464

Himanshu, S.K., Fan, Y., Ale, S., Bordovsky, J., 2021. Simulated efficient growth-stage-based deficit irrigation strategies for maximizing cotton yield, crop water productivity and net returns. Agric. Water Manag. 250, 106840. https://doi.org/10.1016/j.agwat.2021.106840

Iqbal, M., Kamal, M.R., M., M.F., Che Man, H., Wayayok, A., 2020. HYDRUS-1D Simulation of Soil Water Dynamics for Sweet Corn under Tropical Rainfed Condition. Appl. Sci. 10, 1219. https://doi.org/10.3390/app10041219

Irmak, S., 2017. Evapotranspiration Basics and Estimating Actual Crop Evapotranspiration from Reference Evapotranspiration and Crop-Specific Coefficients. Nebraska Ext.

Irmak, S., Burgert, M.J., Yang, H.S., Cassman, K.G., Walters, D.T., Rathje, W.R., Payero, J.O., Grassini, P., Kuzila, M.S., Brunkhorst, K.J., Eisenhauer, D.E., Kranz, W.L., VanDeWalle, B., Rees, J.M., Zoubek, G.L., Shapiro, C.A., Teichmeier, G.J., Rees, J.M., Shapiro, C.A., Teichmeier, G.J., 2012. Large-Scale On-Farm Implementation of Soil Moisture-Based Irrigation Management Strategies for Increasing Maize Water Productivity. Trans. ASABE 55, 881–894. https://doi.org/10.13031/2013.41521

Irmak, S., Payero, J.O., Vandewalle, B., Rees, J., Zoubek, G., Martin, D.L., Kranz, W.L., Eisenhauer, D.E., Leininger, D., 2016. Principles and Operational Characteristics of Watermark Granular Matrix Sensor to Measure Soil Water Status and Its Practical Applications for Irrigation Management in Various Soil Textures. Nebraska Ext.

Irmak, S., Rees, J.M., Zoubek, G.L., DeWalle, B.S. van, Rathje, W.R., DeBuhr, R., Leininger, D., Siekman, D.D., Schneider, J.W., Christiansen, A.P., 2010. Nebraska Agricultural Water Management Demonstration Network (NAWMDN): Integrating Research and Extension/Outreach. Appl. Eng. Agric. 26, 599–613. https://doi.org/10.13031/2013.32066

Jiménez, A.F., Ortiz, B. V., Bondesan, L., Morata, G., Damianidis, D., 2020. Evaluation of Two Recurrent Neural Network Methods for Prediction of Irrigation Rate and Timing. Trans. ASABE 63, 1327–1348. https://doi.org/10.13031/TRANS.13765

Kottek, M., Jurger, G., Beck, C., Rudolf, B., Rubel, F., 2006. World Map of the Köppen- Geiger climate classification updated. Meteorologische Zeitschrift 15 (3), 259–263. https://doi.org/10.1127/0941-2948/2006/0130.

Kumar, H., Srivastava, P., Lamba, J., Ortiz, B. V., Way, T.R., Sangha, L., Takhellambam, B.S., Morata, G., 2021a. Phosphorus variability in the irrigated cropland during a growing season. Am. Soc. Agric. Biol. Eng. Annu. Int. Meet. ASABE 2021. https://doi.org/10.13031/AIM.202100886

Kumar, H., Srivastava, P., Ortiz, B. V., Morata, G., Takhellambam, B.S., Lamba, J., Bondesan, L., 2021b. Field-Scale Spatial and Temporal Soil Water Variability in Irrigated Croplands. Trans. ASABE 64, 1277–1294. https://doi.org/10.13031/TRANS.14335

Kumar, H., Srivastava, P., Ortiz, B.V., Takhellambam, B.S., Morata, G., Bondesan, L. and Lamba, J., 2020. Spatiotemporal Soil Moisture Variability in Corn and Cotton Fields with Uniform Irrigation During the Growing Season. In: AGU Fall Meeting Abstracts (Vol. 2020, pp. H209-05).

Kummu, M., Guillaume, J.H.A., De Moel, H., Eisner, S., Flörke, M., Porkka, M., Siebert, S., Veldkamp, T.I.E., Ward, P.J., 2016. The world's road to water scarcity: shortage and stress in the 20th century and pathways towards sustainability. Sci. Reports 2016 61 6, 1–16. https://doi.org/10.1038/srep38495

Leininger, S.D., Krutz, L.J., Sarver, J.M., Gore, J., Henn, A., Bryant, C.J., Atwill, R.L., Spencer, G.D., 2019. Establishing Irrigation Thresholds for Furrow-Irrigated Peanuts. Crop. Forage Turfgrass Manag. 5, 180059. https://doi.org/10.2134/cftm2018.08.0059

Lena, B.P., Bondesan, L., Ortiz, B.V., Pinheiro, E.A.R., Morata, G.T., Kumar, H., 2021. Evaluation of different negligible drainage flux for field capacity estimation and its implication on irrigation depth for major soil types in Alabama, USA. Am. Soc. Agric. Biol. Eng. Annu. Int. Meet. ASABE 2021. https://doi.org/10.13031/AIM.202100415

Lena, B.P., Bondesan, L., Pinheiro, E.A.R., Ortiz, B. V., Morata, G.T., Kumar, H., 2022. Determination of irrigation scheduling thresholds based on HYDRUS-1D simulations of field capacity for multilayered agronomic soils in Alabama, USA. Agric. Water Manag. 259, 107234. https://doi.org/10.1016/J.AGWAT.2021.107234

Lena, B.P., Ortiz, B. V., Jiménez-López, A.F., Sanz-Sáez, Á., O'Shaughnessy, S.A., Durstock, M.K., Pate, G., 2020. Evaluation of infrared canopy temperature data in relation to soil water-based irrigation scheduling in a humid subtropical climate. Trans. ASABE 65, 1217–1231. https://doi.org/10.13031/TRANS.13912

Li, Y., Šimůnek, J., Jing, L., Zhang, Z., Ni, L., 2014. Evaluation of water movement and water losses in a direct-seeded-rice field experiment using Hydrus-1D. Agric. Water Manag. 142, 38–46. https://doi.org/10.1016/j.agwat.2014.04.021

Liakos, V., Porter, W., Liang, X., Tucker, M.A., McLendon, A., Vellidis, G., 2017. Dynamic Variable Rate Irrigation – A Tool for Greatly Improving Water Use Efficiency. Adv. Anim. Biosci. 8, 557–563. https://doi.org/10.1017/S2040470017000711

Liang, X., Liakos, V., Wendroth, O., Vellidis, G., 2016. Scheduling irrigation using an approach based on the van Genuchten model. Agric. Water Manag. 176, 170–179. https://doi.org/10.1016/j.agwat.2016.05.030

Lowrance, C., Fountas, S., Liakos, V., Vellidis, G., 2016. EZZone-An Online Tool for Delineating Management Zones, In: Proc. of the 13th International Conference on Precision Agriculture (unpaginated, online). Monticello, IL: International Society of Precision Agriculture.

Mokari, E., Shukla, M.K., Šimůnek, J., Fernandez, J.L., 2019. Numerical Modeling of Nitrate in a Flood-Irrigated Pecan Orchard. Soil Sci. Soc. Am. J. 83, 555–564. https://doi.org/10.2136/sssaj2018.11.0442

Morata, G.T., 2020. Evaluation of Deficit Irrigation Strategies and Management Zones Delineation for Corn Production in Alabama. MS thesis. Auburn, AL: Auburn University, Department of Crop, Soil and Environmental Sciences.

Mualem, Y., 1976. A new model for predicting the hydraulic conductivity of unsaturated porous media. Water Resour. Res. 12, 513–522. https://doi.org/10.1029/WR012I003P00513

O'Shaughnessy, S.A., Andrade, M.A., Stone, K.C., Vories, E.D., Sui, R., Evett, S.R., 2018. Adapting a VRI Irrigation Scheduling System for Different Climates, In: Irrigation

Association Show and Education Conference Proceedings on Irrigation Association, Fairfax, VA.

Peters, A., Durner, W., 2008. Simplified evaporation method for determining soil hydraulic properties. J. Hydrol. 356, 147–162. https://doi.org/10.1016/J.JHYDROL.2008.04.016

Peters, A., Iden, S.C., Durner, W., 2015. Revisiting the simplified evaporation method: Identification of hydraulic functions considering vapor, film and corner flow. J. Hydrol. 527, 531–542. https://doi.org/10.1016/J.JHYDROL.2015.05.020

Qu, W., Bogena, H.R., Huisman, J.A., Martinez, G., Pachepsky, Y.A., Vereecken, H., 2014. Effects of Soil Hydraulic Properties on the Spatial Variability of Soil Water Content: Evidence from Sensor Network Data and Inverse Modeling. Vadose Zo. J. 13, vzj2014.07.0099. https://doi.org/10.2136/vzj2014.07.0099

Ramos, T.B., Gonçalves, M.C., Castanheira, N.L., Martins, J.C., Santos, F.L., Prazeres, A., Fernandes, M.L., 2009. Effect of sodium and nitrogen on yield function of irrigated maize in southern Portugal. Agric. Water Manag. 96, 585–594. https://doi.org/10.1016/j.agwat.2008.09.023

Ramos, T.B., Šimůnek, J., Gonçalves, M.C., Martins, J.C., Prazeres, A., Castanheira, N.L., Pereira, L.S., 2011. Field evaluation of a multicomponent solute transport model in soils irrigated with saline waters. J. Hydrol. 407, 129–144. https://doi.org/10.1016/j.jhydrol.2011.07.016

Reyes, J., Wendroth, O., Matocha, C., Zhu, J., 2019. Delineating Site-Specific Management Zones and Evaluating Soil Water Temporal Dynamics in a Farmer's Field in Kentucky. Vadose Zo. J. 18, 180143. https://doi.org/10.2136/vzj2018.07.0143

Rolle, M., Tamea, S., Claps, P., 2021. ERA5-based global assessment of irrigation requirement and validation. PLoS One 16. https://doi.org/10.1371/JOURNAL.PONE.0250979

Sangha, L., Lamba, J., Kumar, H., Srivastava, P., Dougherty, M., Prasad, R., 2020. An innovative approach to rainwater harvesting for irrigation based on El Niño Southern Oscillation forecasts. J. Soil Water Conserv. jswc.2020.00085. https://doi.org/10.2489/JSWC.2020.00085

Sharma, V., Irmak, S., 2020. Economic comparisons of variable rate irrigation and fertigation with fixed (uniform) rate irrigation and fertigation and pre-plant fertilizer management for maize in three soils. Agric. Water Manag. 240, 106307. https://doi.org/10.1016/J.AGWAT.2020.106307

Šimůnek, J., van Genuchten, M.T., Šejna, M., 2016. Recent Developments and Applications of the HYDRUS Computer Software Packages. Vadose Zo. J. 15, 1–25. https://doi.org/10.2136/VZJ2016.04.0033

Šimůnek, J., Hopmans, J.W., 2009. Modeling compensated root water and nutrient uptake. Ecol. Modell. 220, 505–521. https://doi.org/10.1016/J.ECOLMODEL.2008.11.004

Song, L., Jin, J., He, J., 2019. Effects of Severe Water Stress on Maize Growth Processes in the Field. Sustain. 2019, Vol. 11, Page 5086 11, 5086. https://doi.org/10.3390/SU11185086

Stone, K.C., Bauer, P.J., Sigua, G.C., 2019. Potential Water Conservation Using Site-Specific Variable Rate Irrigation. Appl. Eng. Agric. 35, 881–888. https://doi.org/10.13031/aea.13108

Sui, R., Yan, H., 2017. Field Study of Variable Rate Irrigation Management in Humid Climates. Irrig. Drain. 66, 327–339. https://doi.org/10.1002/IRD.2111

Tafteh, A., Sepaskhah, A.R., 2012. Application of HYDRUS-1D model for simulating water and nitrate leaching from continuous and alternate furrow irrigated rapeseed and maize fields. Agric. Water Manag. 113, 19–29. https://doi.org/10.1016/j.agwat.2012.06.011

van Genuchten, M.T., 1980. A Closed-form Equation for Predicting the Hydraulic Conductivity of Unsaturated Soils. Soil Sci. Soc. Am. J. 44, 892–898. https://doi.org/10.2136/sssaj1980.03615995004400050002x

van Genuchten, M.T., Leij, F.J. and Yates, S.R., 1991. The RETC code for quantifying the hydraulic functions of unsaturated soils. U.S. Department of Agriculture, Agricultural Research Service Riverside, California

Wang, J., Huang, G., Li, J., Zheng, J., Huang, Q., Liu, H., 2017. Effect of soil moisture-based furrow irrigation scheduling on melon (Cucumis melo L.) yield and quality in an arid region of Northwest China. Agric. Water Manag. 179, 167–176. https://doi.org/10.1016/J.AGWAT.2016.04.023

Wang, S.Q., Song, X.F., Wei, S.C., Shao, J.L., 2016. Application of HYDRUS-1D in understanding soil water movement at two typical sites in the North China Plain. J. Groundw. Sci. Eng. 4, 1–11.

Wang, X., Li, Y., Chau, H.W., Tang, D., Chen, J., Bayad, M., 2021. Reduced root water uptake of summer maize grown in water-repellent soils simulated by HYDRUS-1D. Soil Tillage Res. 209, 104925. https://doi.org/10.1016/j.still.2020.104925

Wang, X., Li, Y., Si, B., Ren, X., Chen, J., 2018. Simulation of Water Movement in Layered Water-Repellent Soils using HYDRUS-1D. Soil Sci. Soc. Am. J. 82, 1101–1112. https://doi.org/10.2136/sssaj2018.01.0056

Wang, Y., Zhang, B., Lin, L., Zepp, H., 2011. Agroforestry system reduces subsurface lateral flow and nitrate loss in Jiangxi Province, China. Agric. Ecosyst. Environ. 140, 441–453. https://doi.org/10.1016/J.AGEE.2011.01.007

Wesseling, J., 1991. Meerjarige simulatie van grondwaterstroming voor verschillende bodemprofielen, grondwatertrappen en gewassen met het model SWATRE. 0924- 3070. 3070. DLO-Staring Centrum

Wyatt, B.M., Ochsner, T.E., Fiebrich, C.A., Neel, C.R., Wallace, D.S., 2017. Useful Drainage Estimates Obtained from a Large-Scale Soil Moisture Monitoring Network by Applying the Unit-Gradient Assumption. Vadose Zo. J. 16, vzj2017.01.0016. https://doi.org/10.2136/vzj2017.01.0016

Wyatt, B.M., Ochsner, T.E., Zou, C.B., 2021. Estimating root zone soil moisture across diverse land cover types by integrating in-situ and remotely sensed data. Agric. For. Meteorol. 307, 108471. https://doi.org/10.1016/J.AGRFORMET.2021.108471

Yost, J.L., Huang, J., Hartemink, A.E., 2019. Spatial-temporal analysis of soil water storage and deep drainage under irrigated potatoes in the Central Sands of Wisconsin, USA. Agric. Water Manag. 217, 226–235. https://doi.org/10.1016/j.agwat.2019.02.045

Zhang, Y., Zhao, W., He, J., Fu, L., 2018. Soil Susceptibility to Macropore Flow Across a Desert-

Oasis Ecotone of the Hexi Corridor, Northwest China. Water Resour. Res. 54, 1281–1294. https://doi.org/10.1002/2017WR021462

Zheng, C., Lu, Y., Guo, X., Li, H., Sai, J., Liu, X., 2017. Application of HYDRUS-1D model for research on irrigation infiltration characteristics in arid oasis of northwest China. Environ. Earth Sci. https://doi.org/10.1007/s12665-017-7151-2

Zhou, H., Zhao, W. zhi, 2019. Modeling soil water balance and irrigation strategies in a flood-irrigated wheat-maize rotation system. A case in dry climate, China. Agric. Water Manag. 221, 286–302. https://doi.org/10.1016/j.agwat.2019.05.011

Takhellambam, B.S., Srivastava, P., Lamba, J., McGehee, R.P., and Kumar, H., 2021. Potential changes in rainfall erosivity under climate change in southeastern United States. In: AGU Fall Meeting 2021.

Takhellambam, B.S., Srivastava, P., Lamba, J., Mcgehee, R.P., Kumar, H., Tian, D., 2022. Temporal disaggregation of hourly precipitation under changing climate over the Southeast United States. Sci. Data 2022 91 9, 1–14. https://doi.org/10.1038/s41597-022-01304-7

Chapter 5

Optimizing Zone-Specific Field Capacity and Irrigation Thresholds Using A Numerical Modeling Approach

5.1 Abstract

Accurate determination of irrigation thresholds and depths is crucial for timely adoption of best irrigation practices in crop fields, which help to reduce crop water stress, avoid excess water, and meet crop water demands on time. The accuracy in determining irrigation thresholds and depths is highly dependent on the accurate determination of field capacity (FC). The determination of FC, irrigation thresholds, and irrigation depths is characterized by site-specific soil hydraulic properties (SHPs). This study, conducted in two zones (zone 1 and zone 2) delineated based on soil, topography, and historical crop yield, focused on determining zone-specific optimized FC using a negligible drainage-flux (q_{fc}) criterion, optimizing irrigation thresholds and comparing with observed values of FC and irrigation thresholds. The HYDRUS-1D model, which was used to optimize zone-specific SHPs using measured soil matric potential (h) in both zones, determined the FCs at 0.01 cm/day as q_{fc}. The optimized FCs were also compared with benchmark FC (h of 33 kPa). The results showed that the optimized FC at q_{fc} was an h of 39.1 kPa in zone 1, which was greater than the benchmark FC and observed FC (14.7 kPa), and 24.6 kPa in zone 2 which was lower than the benchmark FC observed FC (59.1 kPa). Our method of determining zone-specific FC assesses the soil water dynamics by optimizing SHPs with measurements recorded in each zone; however, it is not the case with observed and benchmark FC values. Therefore, using observed and benchmark FC values can result in inefficient irrigation strategies. At flux-based FC, the optimized irrigation threshold and amount in zone 1 were greater and smaller, respectively, than the observed values. In zone 2, the optimized irrigation threshold and amount were smaller

and greater, respectively, than the observed values. The relationship between accumulated crop evapotranspiration (ET_c) and required irrigation amount determined using optimized SHPs showed a strong correlation in both zones, compared to using observed SHPs. The proposed method of optimizing zone-specific FC and irrigation thresholds can help with adopting timely best irrigation management schemes (e.g., variable-rate irrigation) in respective zones. The findings can help improve irrigation water use efficiency and reduce crop water stress during the growing season.

5.2 Introduction

The first definition of field capacity (FC) was proposed by Veihmeyer and Hendrickson (1931) as "the amount of soil water in the profile when downward water movement has decreased materially due to gravitational forces". The FC idea depicts the earliest effort of consolidating empirical measurements into a physically-based hydrologic criterion. The common FC criterion remains obscure for the well-defined hydrologic state of soils regardless of its importance in defining initial conditions for agronomic and hydrologic applications and for determining effective soil water available to plants. Traditionally, a static soil water pressure head or soil matric potential (h) of 10 kPa for coarse-textured soil and 33 kPa for fine-textured has been used to represent the soil condition at FC (Rivers and Shipp, 1972). However, studies have indicated discrepancies and uncertainty associated with the static nature of FC, and these values change based on soil physical and hydraulic characteristics and soil profile depth considered, which suggests FC is dynamic (Assouline and Or; 2014; Lena et al., 2022; Nemes et al., 2011; Twarakavi et al., 2009). As the upper limit of soil water holding capacity changes dynamically, the soil water available will change accordingly, ultimately varying irrigation recommendations (Lena et al., 2022). Defining such limits are imperative to improving irrigation water-use efficiency and agricultural water management practices (de Jong van Lier, 2017; Irmak et al., 2016; Pinheiro et al., 2019; Lena et

al., 2022; Romano et al., 2011) since it allows definition of irrigation triggering and depth considering a maximum allowable soil water depletion (SWD). Therefore, an accurate assessment of h at FC that accounts for site-specific soil characteristics is the first step when the objective is to implement irrigation best management practices and mitigate the negative impact associated with over- or under-application of irrigation water.

Due to high uncertainty, onerous, and time-consuming measurements of FC in the field and laboratory, the idea of internal drainage flux has been a topic of interest (Lena et al., 2022; Meyer and Gee, 1999; Twarakavi et al., 2009). Computer codes have been used to determine FC when the drainage flux at the bottom of a pre-defined soil profile depth reaches a negligible value. Schroeder et al. (1994) used HELP software to estimate FC at negligible drainage flux (q_{fc}) ranging from 0.001 cm/day to 0.1 cm/day depending on the application. Hillel (1998) recommended a value of 0.05 cm/day as q_{fc} to estimate FC. Meyer and Gee (1999) found consistency with the original range from 0.001 cm/day to 0.1 cm/day to interpret FC. Twarakavi et al. (2009) tested three q_{fc} values (0.001, 0.01, and 0.1 cm/day) using HYDRUS-1D model, a model to simulate soil water and solute dynamics in unsaturated soil media (PC-Progress, 2022), to determine FC for a 1 cm depth homogeneous soil profile, from soil surface to 1 cm deep, and a value of 0.01 cm/day was recommended to represent FC across a range of USA soils. Although many studies have proposed the use of different q_{fc} values to represent FC, the impact of different q_{fc} values on irrigation calculations is hardly ever investigated. One of the few examples is the study conducted by Lena et al. (2022) in which q_{fc} values of 0.01 cm/day and 0.025 cm/day were found to best represent soil conditions at FC for fine-textured and coarse-textured soils, respectively, and these values were used for irrigation recommendations in Alabama. This study

showed the importance of site-specific evaluation of q_{fc} to reduce the uncertainties in FC determination and irrigation recommendations.

The use of q_{fc} to estimate FC has been well accepted by the scientific community; however, the accurate determination of FC highly depends on well-defined soil hydraulic properties (SHPs), i.e., soil water retention curve (SWRC) and hydraulic conductivity curve (HCC). Field or laboratory measurements of SHPs have been considered the standard methods since they provide site-specific information about soil physical characteristics, but these methods are time consuming, onerous, and include disparities in the measurements. Additionally, a recent study indicated discrepancies between field observations and FC determined in the laboratory-based SHPs (raw or observed), and these discrepancies also impacted the irrigation scheduling (Evett et al., 2019). An alternative is to use estimated SHPs based on soil texture or pedo-transfer functions (Schaap et al., 2001), with the drawback of not being as precise as measured SHPs. One way to overcome the limitations regarding measured and estimated SHPs is the optimization of SHPs with h or soil water content (θ) measured using soil moisture sensors in the field. Accurate determinations of SWRC and hydraulic conductivity (K) help in characterizing the soil water dynamics, which are important in irrigation scheduling. Therefore, optimizing the K-θ-h relationship is quite desirable in q_{fc}-based determination of FC and irrigation scheduling to reduce uncertainty. Studies on the impact of optimized SHPs on FC determination and irrigation recommendations in field conditions have never been conducted. The accurate SHPs enable researchers and farmers to increase water use efficiency, improve crop yield, and maintain water resources by determining improved irrigation management strategies (Jabro et el., 2022). We hypothesize that optimized SHPs that also take into consideration differences in site-specific properties in a crop field will not only improve the determination of FC but also the irrigation threshold values over the measured or

estimated SHPs during the growing season, which can help with irrigation scheduling decisions. Thus, for site-specific management, it is best to delineate a crop field in different management zones based on soil, topography, historical crop yield, etc., (Filho et al., 2021a) and determine zone-specific FC to avoid discrepancies which would occur if one static FC is used throughout the field for irrigation water management.

Real-time h or θ monitoring, using soil moisture sensors in the soil profile to schedule irrigation has been gaining attention during the last decade (Fontanet et al., 2020). Although this sensor-based irrigation can improve irrigation efficiency and reduce crop water stress (Irmak et al., 2010; Leininger et al., 2019), these improvements are only achieved if the K-θ-h relationship is accurately and precisely defined. Due to variability in soil hydraulic and physical characteristics, different irrigation thresholds have been adopted to trigger irrigation among the soil types. Leininger et al. (2019) recommended a h of 50 kPa for very-fine sandy loam textured soil, and Irmak et al. (2014) recommended values ranging from 20 kPa to 25 kPa for fine sandy soils and from 90 kPa to 110 kPa for silt loam and silty clay loam soils. However, a single irrigation threshold has been adopted for the entire field and they do not account for site-specific variability in h or θ due to soil, topography, and soil water dynamics monitored within the field, and such values were recommended considering non-optimized SHPs. The determination of FC using q_{fc} has shown promise in determining irrigation thresholds. However, investigations to quantify the impact of zone-specific optimized SHPs and FC at q_{fc} on determination of zone-specific irrigation thresholds considering discrepancies in soil water dynamics monitored in the field are hardly ever conducted. The questions have always been asked and issues have been raised for future research to use optimized parameters to determine FC and irrigation thresholds. Zone-specific differences in h or θ can be due to soil properties, topographic gradient, and vegetation (Kumar et al., 2021b).

Hence, improved and optimized zone-specific SHPs accounting for measured h or θ can help in determining upper and lower limits of water holding capacity, consequently improving the irrigation timing during the growing season.

The overarching goals of this study were to investigate (1) the impact of zone-specific optimized SHPs (both SWRC and HCC) on the determination of zone-specific FC considering a q_{fc} criterion using the HYDRUS-1D model (Šimůnek et al., 2016), and (2) the effect of such optimized SHPs on the zone-specific irrigation thresholds and irrigation amounts using the determined FCs based on q_{fc} for varying SWD. The study was conducted in uniformly irrigated management zones of a delineated crop field. We used optimized and observed (raw i.e., laboratory drawn) zone-specific SHPs in this investigation. We hypothesized that the optimized SHPs greatly affect the determination of FCs and irrigation thresholds in the respective zones as compared to observed SHPs. The optimized FC determined using the q_{fc} criterion was compared with traditionally adopted FC (soil moisture potential of 33 kPa) as a benchmark.

5.3 Materials and Methods

5.3.1 Study Area Description

The research was performed in a field (34°43′06.46″ N and 87°23′13.53″ W) located in the Town Creek Watershed of the Tennessee Valley Region of North Alabama, USA in the 2019 growing season, which usually occurs from April to October. The area is classified as subtropical humid (Cfa Köppen climate classification) (Kottek et al., 2006) and has an annual average rainfall of about 140 cm. The total area of the field was 180 ha, and 120 ha was covered by a remotely controlled 625 m long Reinke center pivot irrigation system (Reinke Manufacturing Co., Inc.,

Deshler, NE, USA) with a mid-elevation spray application (MESA) sprinklers fitted with pressure regulators.

The field was delineated in three irrigation management zones (MZ-zone 1, zone 2, and zone 3) (Fridgen et al., 2004) based on soil texture, topography (slope), and historical yield data (Kumar et al., 2021a; Morata, 2020). However, we used zone 1 and zone 2 in this study due to their contrasting properties. A similar approach has been adopted to delineate the management zones in cornfields of Central Alabama (Filho et al., 2020) and South Alabama (Jiménez et al., 2020). Disturbed soil samples at 0-15 cm, 15-30 cm, and 30-60 cm soil depths were collected from several locations within the field to analyze the soil particle size distribution (Bouyoucos, 1962). The terrain elevation data were collected using a John Deere StarFireTM 6000 real-time kinematic GPS receiver (Deere and Company, Moline, IL, USA) mounted to the farmer's grain harvester. The slope was generated using terrain elevation data, and it varied from 0% to 10%. The corn grain yield was monitored using a yield monitor mounted on the combine, and corn grain yield varied from 3139 kg/ha to 18829 kg/ha. We also generated a topographic wetness index (TWI) in the field to differentiate the MZ for this study (Beven et al., 1979), and TWI varied from 5.11 to 18. Therefore, two MZ (zone 1 and zone 2), which were different in soil, topographic gradients (TWI and slope), and grain yield were selected. Zone 1 had a lower slope, greater TWI, and greater grain yield as compared to zone 2, which had a greater slope, lower TWI, and lower crop yield. Zone 3 had properties between zone 1 and zone 2, therefore, it was not used in the study. Table 5.1 shows the average soil particle distribution of zone 1 and zone 2. Based on soil particle distribution analysis of zone 1 and zone 2, the soil profiles in each MZ were fairly uniform. Since about 95% of corn roots are distributed within the 0-60 cm soil layer (Zhou and Zhao, 2019), an array of three Watermark soil moisture sensors (Irrometer Co., Riverside, CA, USA) at multiple locations were

installed in both MZ at 0-15 cm, 15-30 cm, and 30-60 cm soil depths during the growing season to monitor zone-specific h in the soil profile. The similar array of sensors has been used in soil moisture studies by Kumar et al. (2020, 2021b). Sensors were installed on 01 May 2019 and removed on 11 August 2019. An automated weather station (Vantage Pro2 Plus, Davis Instruments, Hayward, CA, USA) was installed near the field to record meteorological parameters.

Table 5.1 Zone-specific soil properties in the crop field. (* indicate data retrieved from SSURGO 2022).

Zone	Depth (cm)	Sand (%)	Silt (%)	Clay (%)	Texture	Soil Series*	Soil Family*
Zone 1	0-15	17.5	42.3	40.2	Silty clay	Abernathy-Emory	Fine-silty, siliceous, active, thermic Oxyaquic Hapludults
	15-30	17.6	50.1	32.3	Silty clay loam		
	30-60	12.9	51.4	35.7	Silty clay loam		
Zone 2	0-15	31.9	32.8	35.3	Clay loam	Decatur	Fine, kaolinitic, thermic Rhodic Paleudults
	15-30	30.1	29.6	40.3	Clay		
	30-60	29	24.4	46.8	Clay		

5.3.2 Zone-Specific Soil Hydraulic Property Determination

Undisturbed soil cores were collected for SHPs in both zones using a stainless steel sampler ring of 5 cm in height and 8 cm in diameter. The sampler rings were carefully removed by digging out surrounding soils and the soil sample was stored in a container for transportation, to measure the SHPs (SWRC and HCC) in the laboratory (raw or observed SHP). The sample cores were saturated in water for 24 hours before starting the soil water retention measurements. The ring was inserted at the hydraulic property analyzer (HYPROP 2, Meter Group, Pullman, WA, USA) for the determination of the wet end of the SWRC using the evaporation method (Peters et al., 2015). The h-θ data and weight of soil samples were automatically recorded by HYPROP-VIEW software (version 4.2.2.0, Meter Group, Pullman, WA, USA) every 30 minutes. After h-θ data measurements, the soil samples were removed from the hydraulic property analyzer and placed into an oven at 105ºC to determine the dry weight. After the determination of the wet end of

SWRC, the soil was removed from the sampler ring and four replicates of small disturbed samples were taken for the measurement of the dry end of SWRC using a dew point hygrometer (WP4C PotentiaMeter, Meter Group, Pullman, WA, USA). The soil sample was placed in the chamber of dew point hygrometer to measure h for the dry end. The permanent wilting point (PWP) was measured at a soil matric potential of 1500 kPa in both zones. Soil samples were weighed immediately for wet weight and placed in the oven for dry weight. Detailed procedures for determining the wet and dry end of SWRC are shown in Lena et al. (2022). The h-θ pairs measured by the hydraulic property analyzer and dew point hygrometer were input into HYPROP-FIT software (version 4.2.2.0, Meter Group, Pullman, WA, USA) to generate the SWRC. A single porosity model (Mualem, 1976; van Genuchten, 1980) characterized the soil hydraulic properties to satisfy the relation in both MZs. The generated SHPs in the laboratory are referred to as raw or observed SHPs in the following sections.

5.3.3 Inverse Modeling for SHP Optimization and Sensitivity Analysis of HYDRUS-1D

The HYDRUS-1D is a numerically approximate model which has been widely used to simulate soil water dynamics in different soil types and field conditions. The model uses an axisymmetric finite element code to solve Richard's equation numerically (Šimůnek et al., 2016). A HYDRUS-1D model was set up and coupled with the Shuffled Complex Evolution algorithm (SCE-UA) (Diamantopoulos et al., 2012; Duan et al., 1994; Qu et al., 2014) to optimize the SHPs of zone 1 and zone 2. The measured h from the array of three Watermark sensors at 0-15 cm, 15-30 cm, and 30-60 cm soil depths were used to optimize the SHPs to simulate the soil water dynamics in each zone. Due to fairly uniform soil profiles and textural homogeneity within the soil depths of each zone, we used single-layer zone-specific observed SHPs in each zone and optimized with multi-depth measured h. The model was set up for a 100 cm soil profile to run the HYDRUS simulations

to consider dynamic soil water processes. An objective function (Obj) was defined for minimization in the SCE-UA algorithm. We converted h into pF to perform inverse modeling in the HYDRUS-1D model. The pF is a logarithmic function of absolute h in cm.

$$Obj = \sum_{j=1}^{nn} \left[pF_j - \widehat{pF_j}(x)\right]^2 \tag{5.1}$$

$$pF = log_{10}|h| \tag{5.2}$$

where $pF_j = \left[pF_{15cm,}\, pF_{30cm,}\, pF_{60cm}\right]$ is a vector of daily pF observations, $\widehat{pF_j} = \left[\widehat{pF}_{15cm,}\widehat{pF}_{30cm,}\, \widehat{pF}_{60cm}\right]$ is a vector containing daily HYDRUS-1D predictions of pF value, $x = (\theta_r, \theta_s, \alpha, n, K_s, l)$ is a vector of soil hydraulic parameters used in the van Genuchten Mualem model, j is the measurement time, and nn is the total number of measurements at each soil depth. To fully use the zone-specific SHPs, we consider all parameters of the van Genuchten Mualem model to optimize and simulate soil water dynamics accurately in both zones.

To set up an inverse HYDRUS-1D model for optimization, we selected time-variable boundary conditions to input meteorological data collected from the weather station. The initial conditions were defined in terms of h in the model. Since this study is a field study, and the surface layer was subjected to the atmosphere, we defined the upper boundary condition (BC) as atmospheric BC with surface runoff in the water movement for the HYDRUS-1D model. The lower BC was set to free drainage boundary at 100 cm soil depth, indicating no interaction with the groundwater. A spatial discretization of 0.5 cm, leading to 201 nodes across the entire soil profile and no hysteresis in soil water retention was used. The Feddes et. al (1978) model and the Wesseling (1991) parameters were selected for the root water uptake of corn in HYDRUS-1D in both zones.

The performance of the HYDRUS-1D model was checked using different statistical indices of goodness of fit: Root mean square error ($RMSE$), index of agreement (IA), and relative root mean square error ($RRMSE$) were used in this study.

$$RMSE = \sqrt{\frac{1}{nn}\sum_{j=1}^{nn}\left(\widehat{pF_j} - pF_j\right)^2} \tag{5.3}$$

$$IA = 1 - \frac{\sum_{j=1}^{nn}(\widehat{pF_j} - pF_j)^2}{\sum_{j=1}^{nn}(|\widehat{pF_j} - pF_{avg}| + |pF_j - pF_{avg}|)^2} \tag{5.4}$$

$$RRMSE = \frac{\sqrt{\frac{1}{nn}\sum_{j=1}^{nn}\left(\widehat{pF_j} - pF_j\right)^2}}{\sum_{j}^{nn}\left(pF_j\right)} \tag{5.5}$$

where nn is the total number of observations, $\widehat{pF_j}$ and pF_j are simulated and observed pF value, respectively, and pF_{avg} is the average observed pF value. The lower the $RMSE$ value, the better the performance of the model to predict the data in terms of its absolute error. The IA value ranges from 0 to 1, and a value close to 1 indicates a good performance of the model. The $RRMSE$ indicates the performance of the model is excellent when $RRMSE$ < 0.1, good if 0.1 ≤ $RRMSE$ ≤ 0.2, fair if 0.2 < $RRMSE$ ≤ 0.3, and poor if $RRMSE$ > 0.3 (Wang et al., 2018).

5.3.4 Estimation of FC using Negligible Drainage Flux

Once the SHPs (optimized and observed SHPs) were generated in both MZs, the determination of FC using the q_{fc} criterion was performed using HYDRUS-1D (Šimůnek et al., 2016). Since the soils in zone 1 and zone 2 presented fine textures, we adopted a q_{fc} value of 0.01 cm/day to represent the FC estimation for both zones, following the recommendation of Lena et al. (2022). For the model setup, an effective root depth (60 cm) was considered, the upper BC was fixed as

constant zero flux and the lower BC as free drainage. The initial condition was defined as soil matric potential of 0.98 kPa (10 cm of water). The zone-specific optimized and observed SHPs were used as inputs in the HYDRUS-1D model for water flow simulations for a 100 cm soil depth, from the soil surface to 100 cm below the soil surface. When the bottom of the soil profile reached the desired q_{fc} of 0.01 cm/day, the profile was assumed to be at the FC condition. The model setup was used to simulate the zone-specific q_{fc}-based FC using optimized and observed SHPs. The FC determined using optimized SHPs was named as optimized FC, and the FC using observed SHPs was named as observed FC. The optimized FC values using the q_{fc} criterion in both zones were compared with the observed FC values in zone 1 and zone 2. Additionally, the benchmarked FC value at the soil matric potential of 33 kPa for fine-textured soil was also compared with the q_{fc}-based FC values in both zones.

5.3.5 Determination of Irrigation Thresholds and Amounts

The SWD-based irrigation method is the most commonly adopted technique to determine irrigation thresholds or amounts to schedule irrigation which can reduce crop water stress and increase the crop yield (Kisekka et al., 2016). The irrigation thresholds and amounts can be determined using a predefined SWD in the following equations.

$$|h|_{SWD} = \frac{\left\{\left[\frac{\theta_s - \theta_r}{\theta_{SWD} - \theta_r}\right]^{1/m} - 1\right\}^{1/n}}{\alpha} \tag{5.6}$$

$$\theta_{SWD} = \theta_{FC} - [SDW(\theta_{FC} - \theta_{PWP})] \tag{5.7}$$

$$I_{SWD} = \sum(\theta_{FC} - \theta_{SWD})Z \tag{5.8}$$

where $|h|_{SWD}$ is irrigation threshold as soil matric potential (h) at predefined SWD [L]; θ_{SWD} is the soil water content at predefined SWD [L^3L^{-3}]; θ_{FC} is the soil water content at FC [L^3L^{-3}]; θ_{PWP} is the soil water content at PWP [L^3L^{-3}]; I_{SWD} is the irrigation amount or depth [L]; Z is the thickness of the soil layer [L]. The soil water content at FC using the q_{fc} criterion for each SHP and the soil water content at PWP (soil matric potential of 1500 kPa) in each MZ were used to determine the upper and lower limits of water holding capacity to derive irrigation thresholds and depths. The upper limit was set as 0% SWD (at FC), while the lower limit was set as 100% (at PWP).

5.3.6 Evaluation of Negligible Drainage Flux Criteria on Zone-Specific Irrigation Recommendations for Optimized and Observed SHPs

To evaluate the impact of a q_{fc} of 0.01 cm/day using zone-specific optimized and observed SHPs on irrigation recommendations, we implemented an analysis using observed h data in zone 1 and zone 2. We used three depths of installed sensors where the soil matric potential measurements were recorded during the growing season. For this analysis, the periods with no rainfall events were selected to calculate the required irrigation water as the amount of water required to replenish h measured with soil moisture sensors back to h_{FC} (soil matric potential at FC). The required irrigation water was calculated based on h_{FC} and θ_{FC} determined using a q_{fc} of 0.01 cm/day. We also calculated accumulated crop evapotranspiration ET_c for the same periods of irrigation water amounts. The daily ET_c values were calculated as (Allen et al., 1998):

$$ET_c = K_c * ET_0 \tag{5.9}$$

where K_c is crop coefficient and ET_0 is reference evapotranspiration. The daily K_c for corn was calculated using the growth stages recorded during the growing season (Irmak, 2017). The daily

grass based ET_0 values (Allen et al., 1998) were obtained from the installed weather station. The accumulated ET_c values were calculated as the sum of daily ET_c values for the selected interval between irrigation or rainfall events. For comparison, a regression model was fitted between required irrigation amounts based on 0.01 cm/day as q_{fc} and accumulated ET_c for the selected intervals in both zones using optimized and observed SHPs.

5.4 Results and Discussion

5.4.1 Goodness of fit analysis of inverse HYDRUS-1D modeling

Studies have shown that HYDRUS-1D is a reliable tool to describe the soil water dynamics in various types of variably saturated soils in different crops such as corn, wheat, and rice (Iqbal et al., 2020; Zhou and Zhao, 2019). A single porosity model characterized the SHPs to satisfy the relation for both zones using HYPROP-FIT software (Mualem, 1976; van Genuchten, 1980). The raw SHPs in zone 1 and zone 2 obtained from HYPROP-FIT software are shown in fig. 5.1a and 5.1b. These raw SHPs were used as input parameters in the inverse HYDRUS-1D model to start the simulations for optimizing SHPs. The raw SHPs showed the spatial variability between zone 1 and zone 2 (fig. 5.1a and 5.1b). Both zones had distinct patterns of SHPs, which means invariable SHPs cannot be assumed throughout the field for irrigation management. It was inferred from the raw SHPs that considering uniform SHPs within the field can be a flawed irrigation strategy due to zone-specific variability. Using uniform SHPs will trigger irrigation at one FC, one threshold, and one rate in the entire field. It was inferred from the raw SHPs that we need to consider spatial variability between the zones for better irrigation management and adopt zone-specific SHPs. Although raw SHPs showed the importance of zone-specific SHPs between the zones, the raw SHPs were not able to simulate field observations of h measured during the growing season. This reason signified the need for optimizing zone-specific SHPs to simulate the soil water dynamics

and find effective FC and irrigation thresholds in each zone using field observations. Inverse solution using measured h indicated the importance and need for optimizing the zone-specific SHPs (fig. 5.1c and 5.1d) in precision agriculture, for zone-specific irrigation improvements to conserve agricultural water, and for the adoption of variable-rate technology. The optimized SHPs obtained using inverse HYDRUS-1D modeling were different from raw SHPs obtained from HYPROP-FIT software. Using the inverse solution in each zone, we found effective zone-specific SHPs, which simulated soil water dynamics with good agreement in both zones (table 5.2).

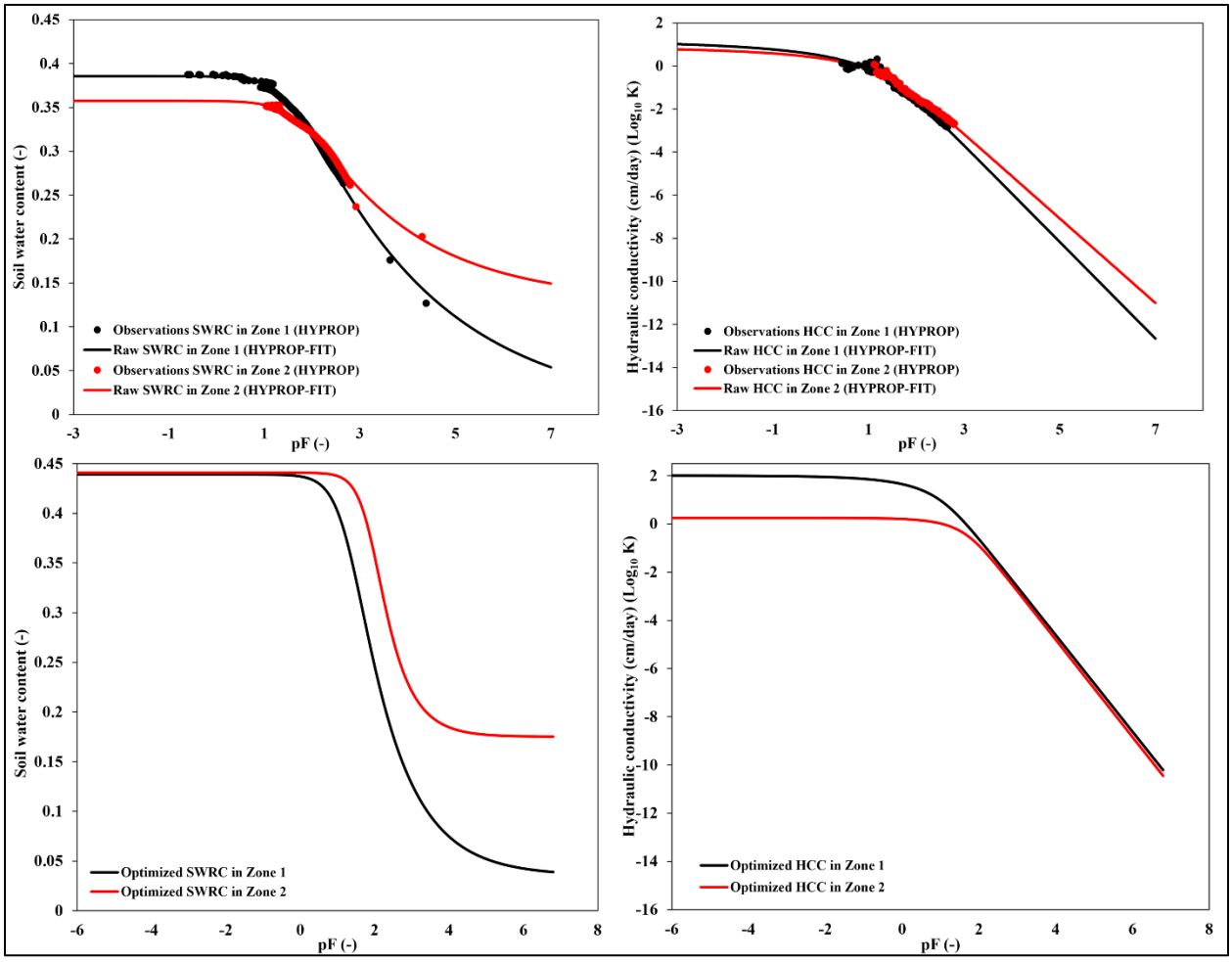

Figure 5.1 Soil hydraulic properties; (a) Laboratory drawn SWRC (we called them observed or raw) showing volumetric soil water content as function of pF and showing HYPROP measurements and fitted curves, (b) Laboratory drawn HCC showing observations and fitted

curves, (c) Optimized soil water retention curves showing volumetric soil water content as function of pF and, and (d) Optimized HCC in both zones. The observations (dots) shown in (a) and (b) were obtained from the HYPROP measurement system and fitted with HYPROP-FIT software.

Table 5.2 Goodness of fit statistics of inverse HYDRUS-1D model to simulate pF in both zones.

Zone	Performance statistics	0-15 cm			15-30 cm			30-60 cm		
		RMSE (-)	IA (-)	RRMSE (-)	RMSE (-)	IA (-)	RRMSE (-)	RMSE (-)	IA (-)	RRMSE (-)
Zone 1	Mean	0.36	0.82	0.001	0.29	0.84	0.001	0.38	0.78	0.001
	Min.	0.33	0.78	0.001	0.22	0.83	0.001	0.35	0.78	0.001
	Max.	0.38	0.85	0.002	0.33	0.86	0.001	0.41	0.79	0.002
Zone 2	Mean	0.33	0.83	0.001	0.38	0.79	0.002	0.40	0.71	0.001
	Min.	0.27	0.75	0.001	0.35	0.76	0.001	0.24	0.62	0
	Max.	0.41	0.89	0.002	0.4	0.81	0.002	0.55	0.84	0.002

The performance of the HYDRUS-1D model was tested at multiple locations in each zone. The results showed that the simulated pF fitted well with measured values of pF at all three soil depths in both zones (table 5.2). Among all soil depths in zone 1, the model performed best at a 15-30 cm soil depth with the best agreement and minimum error between observed and simulated data, followed by 0-15 cm and 30-60 cm (table 5.2). However, in zone 2, the observed and simulated data had the best agreement at 0-15 cm (table 5.2) with the lowest error among all soil depths. In comparison between the two zones, zone 1 performed better than zone 2 since the statistical indices were better in zone 1. Discrepancies between the observed and simulated data in the zones can be due to lateral leakage and macro-pores which have also been reported in previous studies (Akay et al., 2008; Wang et al., 2011; Zhang et al., 2018). Li et al. (2014) conducted a study in an irrigated rice field in China and the minimum average RMSE achieved was 2.61 cm using the individual retention curves obtained from the RETC retention curves computer program for each layer from 0 to 100 cm at 20 cm increment depth. The RETC is a computer program that determines the soil hydraulic properties in the soil profile using parametric models such as van Genuchten and Brooks-

Corey models (van Genuchten et al., 1991). Wyatt et al. (2017) reported that the RMSE ranged from 2.95 to 3.53 with a greater RMSE in deep soil layer in a study to estimate groundwater recharge at four different sites in Oklahoma using the HYDRUS-1D model. Mokari et al. (2019) reported an IA that varied from 0.44 to 0.73. Based on the statistical indices to evaluate the performance of the HYDRUS-1D model, the performance was evaluated as excellent to optimize zone-specific SHPs since our results were quite consistent and better than previous studies. However, the studies did not consider all parameters to optimize the SHPs. Based on the performance criterion, single-layer SHPs can predict h in deep soil layers more accurately. In zone 2, the observed and simulated data had the best agreement at 0-15 cm with the lowest error among all soil depths. In comparison between the two zones, zone 1 performed better than zone 2 since the statistical indices were better in zone 1. The variation in the model performances in both zones was due to differences in the SHPs and differences in the topographic attributes (low slope and high TWI in zone 1 and high slope and low TWI in zone 2), which affected the soil water dynamics in both zones. The plant heights and LAI values were greater in zone 1 than in zone 2. Importantly, the one-layer optimized HYDRUS-1D model is a simplified version using single layer SHPs of the complex system, which can be used to simulate soil water dynamics in all three layers.

5.4.2 Evaluation of FC Estimation Using Drainage Flux Criterion in HYDRUS-1D Model

The drainage flux criterion assumes the negligible flux density to simulate FC at the desired depth. The intrinsic property of FC is associated with dynamic natural processes within the soils. This idea of FC estimation using a q_{fc} considers most of the natural processes, such as water movement through soil profiles. Based on the recommendation in the previous studies conducted by Twarakavi et al. (2009) and Lena et al. (2022), we used 0.01 cm/day as q_{fc} in HYDRUS-1D to determine zone-specific FC using single-layer zone-specific optimized and observed SHPs in the

field conditions. We conducted simulations using the q_{fc} criterion in the HYDRUS-1D model at the bottom of considered effective root depth. The idea of determining zone-specific FC using zone-specific observed SHPs was to comprehend the differences in the optimized FC values and the importance of optimizing zone-specific SHPs. The determined FC values using different SHPs are tabulated in table 5.3. The optimized FC (soil matric potential of 39.1 kPa) was greater than the observed FC (soil matric potential of 14.7 kPa) in zone 1. However, in zone 2, the optimized FC (soil matric potential of 24.6 kPa) was lower than the observed FC (soil matric potential of 59.3 kPa). A similar trend of FC was also found by Lena et al. (2022) using multilayered observed SHPs for fine-textured soil types. However, Lena et al. (2022) did not optimize SHPs and FC values. The differences in zone-specific optimized FC values show the dynamic soil water movement processes that occur in the actual field conditions, which were captured by h measurements recorded during the growing season. The differences in zone-specific FC values considerably affect the irrigation water management to meet the water demands required for a crop in each zone. Additionally, the optimized FC values compared to benchmark FC (soil matric potential of 33 kPa) were different in both zones. The optimized FC was higher in zone 1 and was lower in zone 2 than the benchmark FC in respective zones, which shows that benchmark FC did not hold zone-specific characteristics for soil water dynamics during the growing season. The differences in zone-specific FC can generate differences in the irrigation thresholds, and ultimately the time to trigger irrigation during the growing season.

Table 5.3 Determined FC soil matric potential (kPa) values using 0.01 cm/day as negligible drainage flux for SHPs (optimized and observed) and benchmark FC.

Zone	Optimized FC (kPa)	Observed FC (kPa)	Benchmark FC (kPa)
Zone 1	39.1	14.7	33
Zone 2	24.6	59.1	33

Defining irrigation trigger and the amount is highly dependent on the upper limit of soil water holding capacity; therefore, different FC values will result in differences in irrigation recommendations. The observed differences of estimated FC using optimized and observed SHPs suggested that irrigation recommendation could be improved when zone-specific SHPs are optimized using the HYDRUS-1D, ultimately promoting irrigation best management practices. The optimized FC in zone 1 and zone 2 hold different values, which indicate the difference in the upper limits of soil available water. Assuming benchmark FC value as soil matric potential of 33 kPa throughout the field for irrigation scheduling cannot be accurate for efficient irrigation water management during the growing season. It can over-or under-estimate the zone-specific irrigation thresholds, which can result in over-or under-irrigation in the zones. Therefore, determining accurate zone-specific FC values can help precise and zone-specific irrigation scheduling with a better irrigation threshold in each zone.

5.4.3 Determination of Zone-Specific Irrigation Thresholds and Amounts Based on Drainage Flux FC Criterion

The initial phase in irrigation water management using an efficient sensor-based irrigation approach is the determination of soil matric potential at FC (h_{FC}). This information allows the assessment of irrigation trigger and amount considering an allowable SWD, which can facilitate decision-making by farmers and crop consultants (Lena et al., 2022). This can improve irrigation water-use efficiency, reduce crop water stress, and satisfy the crop water demands on time in each zone. Irrigation practices do not perform effectively if the root depth, soil water dynamics, and water depletion are not considered in the crop field. It can result in incorrect timing and inaccurate irrigation depth, which can be water stress or water excess conditions for the crops.

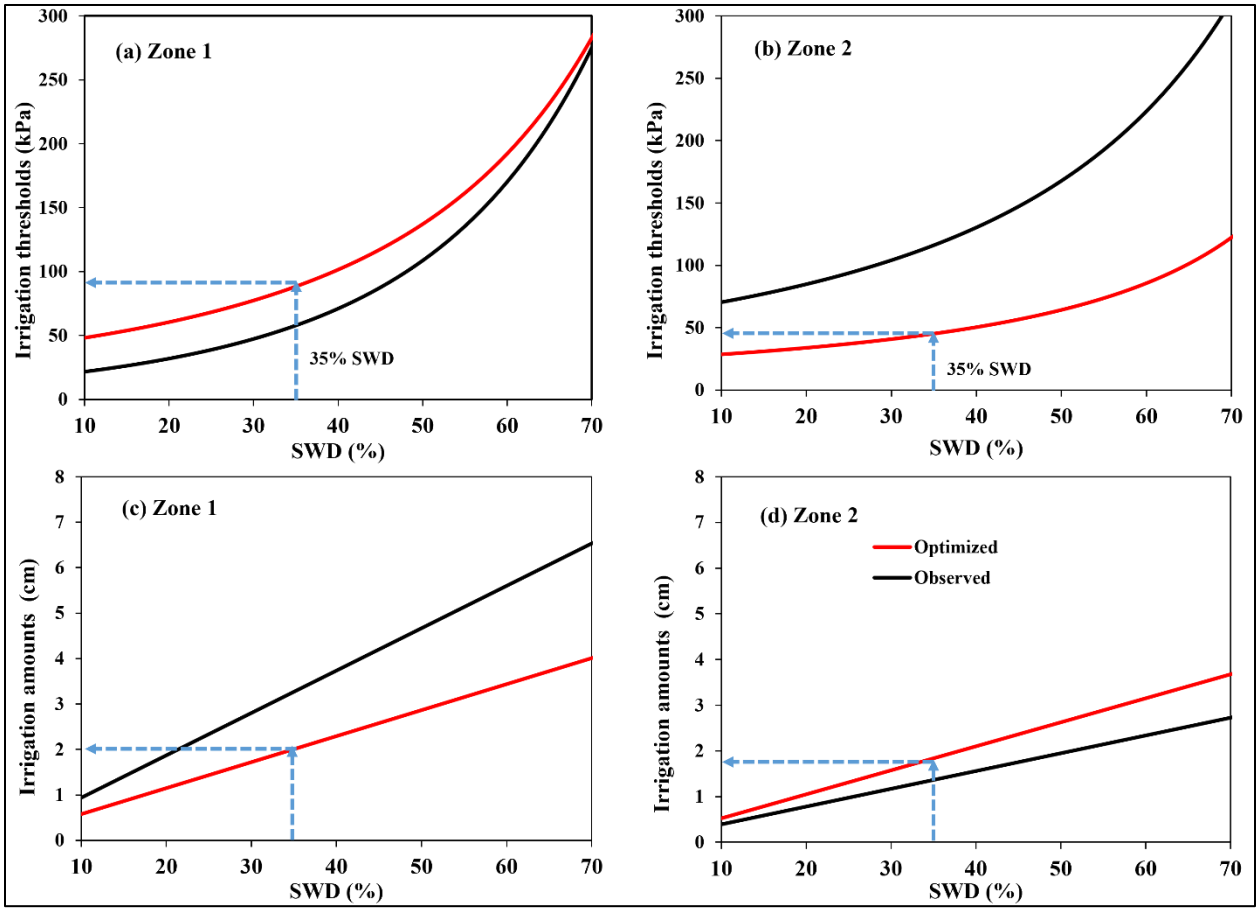

Figure 5.2 Determined irrigation thresholds (absolute values of soil matric potential) based on negligible drainage flux FC criterion in (a) zone 1 and (b) zone 2. Irrigation amounts in (c) zone 1 and (d) zone 2 with corresponding soil water depletion variation using optimized and observed SHPs. The blue dotted arrows show the values of irrigation thresholds corresponding to 35% soil water depletion.

The optimized irrigation thresholds and depths were determined with variation in SWD to trigger irrigation in both zones (fig. 5.2). In zone 1, we determined the optimized irrigation threshold was greater (fig. 5.2a) and optimized irrigation depth was lower (fig. 5.2c) than in other cases, which was due to differences in SHPs. The trend of the optimized and observed threshold curves indicate the two curves intersect at SWD values greater than 70% in zone 1 (fig. 5.2a), which illustrates the reduced differences due to higher depletion in the upper and lower limits with the shape of optimized and observed SHPs. In zone 2, the optimized irrigation thresholds were lower than the

observed thresholds (fig. 5.2b) and the optimized irrigation amounts were greater than the observed irrigation amounts (fig. 5.2d). Comparing optimized irrigation thresholds of both zones, the optimized irrigation thresholds were always greater than the observed irrigation thresholds in zone 1 and lower in zone 2. The optimized irrigation amounts were always lower than observed irrigation amounts in zone 1 and higher in zone 2. Differences in the pattern of irrigation threshold and amounts showed inaccuracy in irrigation scheduling using observed SHPs and FCs. Therefore, it is essential to optimize zone-specific SHPs and FC to adopt best irrigation practices in each zone.

Table 5.4 Irrigation threshold as absolute values of soil matric potential (kPa) and irrigation amounts (cm) at 35% SWD for negligible drainage flux-based FC and benchmark FC.

	Irrigation threshold (h_{35}) (kPa)				**Irrigation depths (cm)**			
	Zone 1		**Zone 2**		**Zone 1**		**Zone 2**	
	Flux	**Benchmark**	**Flux**	**Benchmark**	**Flux**	**Benchmark**	**Flux**	**Benchmark**
Optimized	88	76	45	59	2.00	2.18	1.84	1.50
Observed	58	102	116	70	3.27	2.59	1.36	1.90

For example, using a hypothetical 35% SWD as the irrigation trigger value, the optimized soil matric potential at 35% SWD (h_{35}) was 88 kPa with a corresponding irrigation amount of 2 cm for a 60 cm soil profile in zone 1. The optimized h_{35} in zone 2 was 45.32 kPa, and its corresponding irrigation amount was 1.84 cm (table 5.4). Differences in the optimized and observed irrigation thresholds at 35% SWD in both zones were due to discrepancies in soil hydraulic properties. These site-specific measurements were studied in the case of optimized computations but not in the observed computations.

From these findings, it was observed that accurate determination of irrigation threshold and irrigation amount is highly dependent on accurate and effective SHPs, which allowed zone-specific soil water dynamics and showed discrepancies in determination of FC values. The accurate threshold value will decide the moment to trigger irrigation and the corresponding irrigation

amount in each zone, which can be observed from sensor data installed in farmers' fields during the growing seasons. The decision of the right timing and amount of irrigation can result in efficient irrigation water management by maximizing crop yield, reducing crop water stress, and meeting crop water demands in the zones. As a result, irrigation scheduling using optimized parameters can be an efficient irrigation practice.

5.4.4 Determination of Irrigation Thresholds and Depths Based on Benchmark FC

As mentioned previously, a soil matric potential (h) value of 33 kPa was used to represent the benchmark FC value for the entire study site. We used the same SHPs to determine the irrigation thresholds and amounts in this scenario. Both zones had a similar pattern of irrigation thresholds and amounts variation with increasing SWD (fig. 5.3). The optimized irrigation thresholds (fig. 5.3a and 5.3b) and amounts (fig. 5.3c and 5.3d) were minimum considering benchmark FC in both zones. Assuming a static value of FC throughout the field can be flawed (Nemes et al., 2011) for irrigation recommendations as was seen in both zones. Although we had two different SHP curves, the zone-specific h-θ relation of FC controls the upper limits of SWRCs. We can conclude that assuming a single value of FC based on fine-textured soil might not be the best and most robust scheme to schedule irrigation.

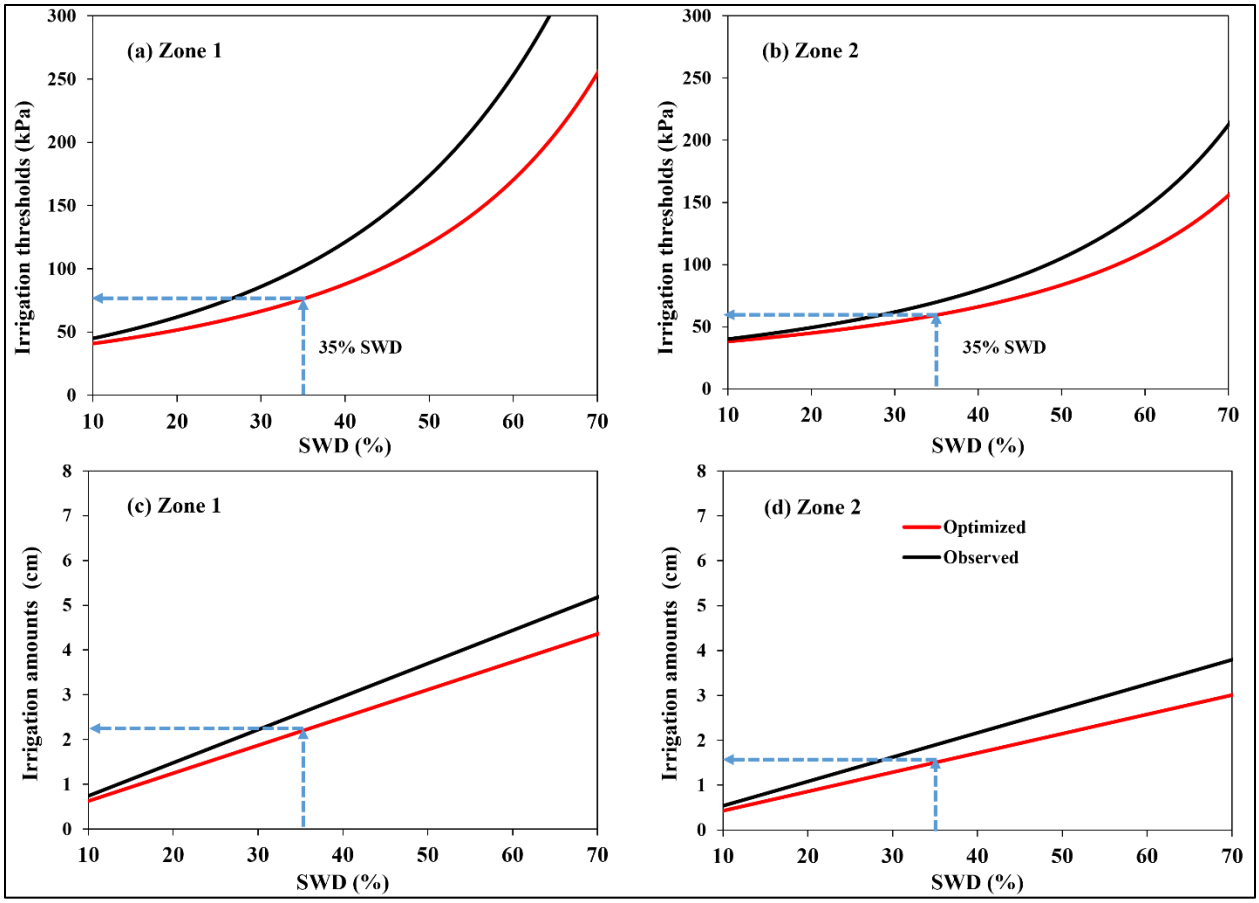

Figure 5.3 Determined irrigation thresholds (absolute values of soil matric potential) based on benchmark FC in (a) zone 1 and (b) zone 2. Irrigation amounts in (c) zone 1 and (d) zone 2 with corresponding soil water depletion variation using optimized and observed SHPs. The blue dotted arrows show the values of irrigation thresholds corresponding to 35% soil water depletion.

The optimized irrigation thresholds at flux-based FC (using optimized SHPs and optimized FC) were higher than optimized irrigation thresholds at benchmark FC (using optimized SHPs and benchmark FC) in zone 1. However, optimized irrigation thresholds at flux-based FC were lower than optimized irrigation thresholds at benchmark FC in zone 2 (fig. 5.4a). Observed irrigation thresholds at flux-based FC (using observed SHPs and observed FC) were lower and higher than observed irrigation thresholds at benchmark FC (using observed SHPs and benchmark FC) in zone 1 and zone 2, respectively (fig. 5.4b). Moreover, differences can be observed in irrigation thresholds of both zones for flux-based FC and benchmark FC.

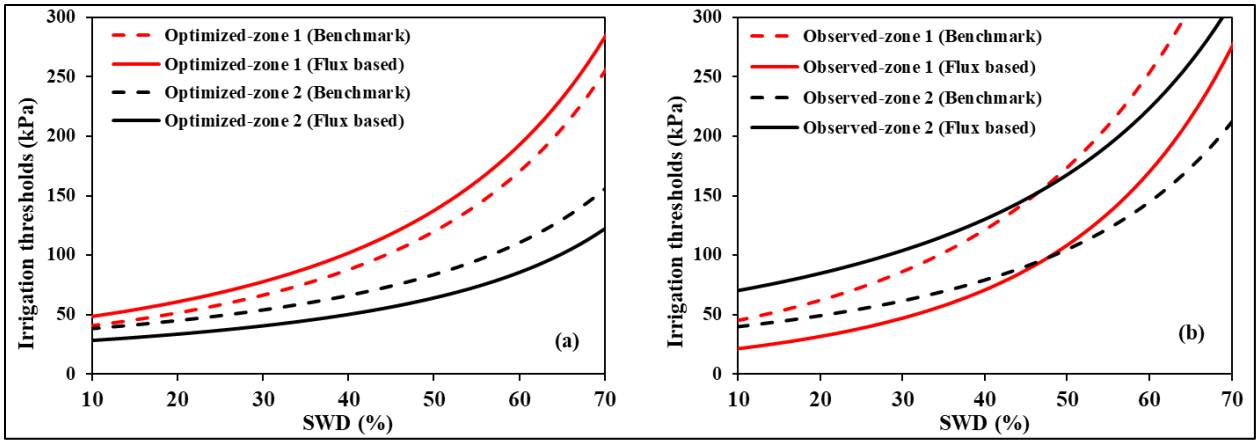

Figure 5.4 Comparison of irrigation thresholds (absolute values of soil matric potential) based on negligible drainage flux FC and benchmark FC in both zones using (a) Optimized (left) and (b) Observed SHPs (right) with corresponding soil water depletion variation.

We can understand the differences between zone-specific optimized and observed irrigation thresholds using flux-based FC with a hypothetical SWD of 35%. For example, the optimized h_{35}, i.e., irrigation threshold at 35% of SWD, using flux-based FC was 88.41 kPa in zone 1, which was greater than observed h_{35} (57.94 kPa) using flux-based FC, optimized h_{35} (76.27 kPa) using benchmark FC, and lower than observed h_{35} (101.94 kPa) using benchmark FC. In zone 2, optimized h_{35} was 45.32 kPa using flux-based FC, which was smaller than observed h_{35} (116 kPa) using flux-based FC, optimized h_{35} (59.51 kPa) using benchmark FC, and observed h_{35} (69.76 kPa) using benchmark FC as mentioned in table 5.4. The change in FC value resulted in different values of irrigation thresholds and amounts at a particular SWD. Different SHPs can lead to various FC and available water content in the soil. Therefore, a correct zone-specific FC value can help in efficient zone-specific irrigation water management within the crop field. It can be concluded that the determination of FC in field conditions and optimization of SHPs can be an essential and foremost step in adopting best irrigation practices.

The irrigation amount calculation can be done with growth stages and increasing root depths during the growing season. The soil depth element has been comprised in equation 5.8 of computations. Therefore, a decision can be made about the irrigation amount at a particular SWD with increasing root depths. This concept of optimizing zone-specific FC using optimized SHPs and irrigation thresholds within the zones can trigger irrigation with varying root depths, which ultimately can reduce water stress in crops in each zone of the field during the growing season. In the following section, we discuss if optimizing zone-specific FC using optimized SHPs can return an improved agreement for irrigation recommendations compared to observed FC and observed SHPs.

5.4.5 Assessment of Negligible Drainage Flux Criteria for Irrigation Recommendations Using Optimized and Observed SHPs

Based on FC recommendations using a negligible drainage flux of 0.01 cm/day for zone-specific irrigation management, we determined the irrigation recommendation for optimized and observed zone-specific SHPs in this study. The relationship between required irrigation and accumulated crop evapotranspiration (ET_c) was determined for zone-specific optimized and observed FC using zone-specific optimized and observed SHPs (fig. 5.5a for zone 1 and fig. 5.5b for zone 2). A linear model was fit to best represent the relationships for optimized and observed FC values in both zones. The discrepancies in irrigation amount reflect the effect of determined FC and adoption of optimized and observed SHPs in each zone. With smaller values of h_{FC} (absolute value), the irrigation amount required will be higher to replenish the soil water content back to FC from a given h since h_{FC} gets closer to zero. Also, the higher values of h_{FC} will require a smaller amount of irrigation water to replenish the soil water content back to FC from a given h since h_{FC} gets farther from zero. Based on the relationship between accumulated ET_c and required irrigation using

optimized and observed FC and SHPs, we found that optimized FC and optimized SHPs resulted in a stronger correlation than observed FC and observed SHPs in both zones (fig. 5.5a for zone 1 and fig. 5.5b for zone 2), which means that irrigation water is being used more efficiently. Although Lena et al. (2022) studied irrigation recommendations using FC based on 0.01 cm/day as q_{fc}, the authors did not optimize the zone-specific FC and SHPs, and information about the impact of optimizing zone-specific FC, which can help optimizing zone-specific irrigation recommendations, was still unknown.

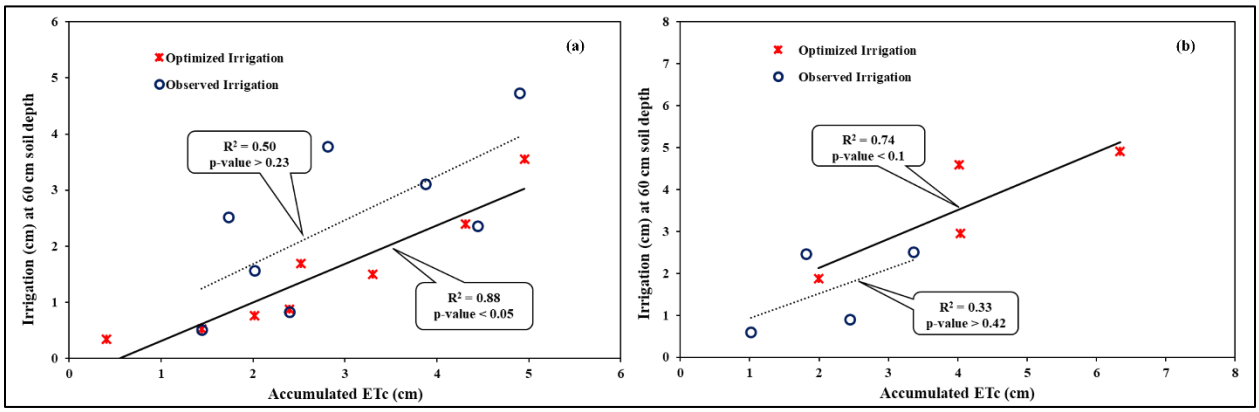

Figure 5.5 Relationship between the accumulated crop evapotranspiration (ET_c) and required irrigation in a soil profile of 60 cm depth using 0.01 cm/day as q_{fc} for field capacity simulations using zone-specific optimized and observed SHPs in (a) zone 1 and (b) zone 2. R^2 is the coefficient of determination for the fitted data.

The results found in this study suggest that evaluation of the impact of optimized and observed zone-specific FC on irrigation recommendations can improve the assessment of an accurate zone-specific FC. Based on the results obtained in this study, we recommend optimizing zone-specific FC values using an optimized HYDRUS-1D model for determining irrigation recommendations. The FC determination using soil cores in the lab, pedo-transfer function, or assuming benchmark may not be accurate and useful in irrigation management due to discrepancies between monitored h in the fields and assumed SHPs and FC. Such discrepancies between FC determined in the lab

and field soil water measurements have been discussed by Evett et al. (2019). We do not suggest obliterating the determination of FC using such SHP methods. The optimized threshold values for irrigation triggering showed the differences between the zones and resulted in promising results of zone-specific irrigation demands, which might result in the variable time of irrigation threshold arrival and frequency of irrigations in the zones.

5.5 Summary and Conclusions

In this study, zone-specific FC for optimized and observed SHPs based on a negligible drainage flux criterion was determined using the HYDRUS-1D numerical model in two managements zones delineated in a crop field. The FC estimated using q_{fc} were compared with benchmark FC value assumed as a soil matric potential (absolute value) of 33 kPa for fine-textured soils. The SHPs were optimized using observed soil matric potential measured at 0-15 cm, 15-30 cm, and 30-60 cm during the growing season in both zones. The optimized FC was greater in zone 1 compared to the observed and benchmark FC. However, in zone 2, optimized FC was lower than observed and benchmark FC. The zone-specific optimized FC values show that observed and benchmark FC values were underrepresented in zone 1 and overrepresented in zone 2. The observed and benchmark FC in both zones did not consider soil water dynamics for the discrepancies associated with FC and SHPs during field observations. Therefore, observed and benchmark FC may not be the best options in irrigation scheduling schemes without optimization. Also, assuming a single FC (benchmark) throughout the field may not be the best option for irrigation recommendations.

The determination of FC using zone-specific optimized and observed SHPs with a negligible drainage flux and benchmark methods showed differences in irrigation thresholds and amounts to trigger irrigation resulting from the differences in the K-h-θ relation of SHPs. The optimized flux-based irrigation threshold was greater than observed flux-based irrigation thresholds in zone 1 and

lower in zone 2 at any particular SWD value. Both the zones had different thresholds to trigger irrigation. Irrigation recommendations using zone-specific optimized FC and optimized SHPs showed a strong correlation between accumulated ET_c and required irrigation amount in both zones than observed FC and observed SHPs. Hence, we recommend that considering zone-specific optimized FC and optimized SHPs can be the best irrigation choice for irrigation water management. Therefore, adopting a variable rate irrigation scheme for efficient irrigation water management across the field can be a best irrigation practice. The irrigation thresholds and amounts using flux-based FC with optimized SHPs can reduce the water stress in the crops, increase irrigation water use efficiency, and conserve the water resources for irrigation.

5.6 References

Akay, O., Fox, G.A., Šimůnek, J., 2008. Numerical Simulation of Flow Dynamics during Macropore–Subsurface Drain Interactions Using HYDRUS. Vadose Zo. J. 7, 909–918. https://doi.org/10.2136/VZJ2007.0148

Allen, R.G., Pereira, L.S., Raes, D., Smith, M., 1998. Crop evapotranspiration-Guidelines for computing crop water requirements-FAO Irrigation and drainage paper 56. FAO, Rome, 300(9), p.D05109.

Assouline, S., Or, D., 2014. The concept of field capacity revisited: Defining intrinsic static and dynamic criteria for soil internal drainage dynamics. Water Resour. Res. 50, 4787–4802. https://doi.org/10.1002/2014WR015475

Beven, K.J. and Kirkby, M.J., 1979. A physically based, variable contributing area model of basin hydrology/Un modèle à base physique de zone d'appel variable de l'hydrologie du bassin versant. Hydrological sciences journal, 24(1), pp.43-69.

Bouyoucos, G.J., 1962. Hydrometer Method Improved for Making Particle Size Analyses of Soils. Agron. J. 54, 464–465. https://doi.org/10.2134/agronj1962.00021962005400050028x

Filho, J.F.D.C.L., Ortiz, B.V., Damianidis, D., Balkcom, K.S., Dougherty, M. and Knappenberger, T., 2020. Irrigation Scheduling to Promote Corn Productivity in Central Alabama. Journal of Agricultural Science, 12(9).

de Jong van Lier, Q., 2017. Field capacity, a valid upper limit of crop available water? Agric. Water Manag. 193, 214–220. https://doi.org/10.1016/J.AGWAT.2017.08.017

Diamantopoulos, E., Iden, S.C., Durner, W., 2012. Inverse modeling of dynamic nonequilibrium in water flow with an effective approach. Water Resour. Res. 48. https://doi.org/10.1029/2011WR010717

Duan, Q., Sorooshian, S., Gupta, V.K., 1994. Optimal use of the SCE-UA global optimization method for calibrating watershed models. J. Hydrol. 158, 265–284. https://doi.org/10.1016/0022-1694(94)90057-4

Evett, S.R., Stone, K.C., Schwartz, R.C., O'Shaughnessy, S.A., Colaizzi, P.D., Anderson, S.K., Anderson, D.J., 2019. Resolving discrepancies between laboratory-determined field capacity values and field water content observations: implications for irrigation management. Irrig. Sci. 37, 751–759. https://doi.org/10.1007/S00271-019-00644-4

Feddes, R.A., Kowalik, P.J., Zaradny, H., 1978. Simulation of Field Water Use and Crop Yield. Crop Yield. John Wiley, New York, NY.

Fridgen, J.J., Kitchen, N.R., Sudduth, K.A., Drummond, S.T., Wiebold, W.J. and Fraisse, C.W., SOFTWARE Management Zone Analyst (MZA): Software for Subfield Management Zone Delineation.

Fontanet, M., Scudiero, E., Skaggs, T.H., Fernàndez-Garcia, D., Ferrer, F., Rodrigo, G., Bellvert, J., 2020. Dynamic Management Zones for Irrigation Scheduling. Agric. Water Manag. 238, 106207. https://doi.org/10.1016/j.agwat.2020.106207

Hillel, D., 1998. Environmental Soil Physics: Fundamentals, Applications, and Environmental

Considerations. Environ. Soil Phys.

Iqbal, M., Kamal, M.R., M., M.F., Che Man, H., Wayayok, A., 2020. HYDRUS-1D Simulation of Soil Water Dynamics for Sweet Corn under Tropical Rainfed Condition. Appl. Sci. 10, 1219. https://doi.org/10.3390/app10041219

Irmak, S., 2017. Evapotranspiration Basics and Estimating Actual Crop Evapotranspiration from Reference Evapotranspiration and Crop-Specific Coefficients. Nebraska Ext.

Irmak, S., Djaman, K., Rudnick, D.R., 2016. Effect of full and limited irrigation amount and frequency on subsurface drip-irrigated maize evapotranspiration, yield, water use efficiency and yield response factors. Irrig. Sci. 34, 271–286. https://doi.org/10.1007/S00271-016-0502-z

Irmak, S., Rees, J.M., Zoubek, G.L., DeWalle, B.S. van, Rathje, W.R., DeBuhr, R., Leininger, D., Siekman, D.D., Schneider, J.W., Christiansen, A.P., 2010. Nebraska Agricultural Water Management Demonstration Network (NAWMDN): Integrating Research and Extension/Outreach. Appl. Eng. Agric. 26, 599–613. https://doi.org/10.13031/2013.32066

Jabro, J.D., Stevens, W.B., 2022. Soil-water characteristic curves and their estimated hydraulic parameters in no-tilled and conventionally tilled soils. Soil and Tillage Research, 219, p.105342.

Jiménez, A.F., Ortiz, B.V., Bondesan, L., Morata, G. and Damianidis, D., 2020. Evaluation of two recurrent neural network methods for prediction of irrigation rate and timing. Transactions of the ASABE, 63(5), pp.1327-1348.

Kargas, G., Londra, P.A., Sotirakoglou, K., 2021. Saturated Hydraulic Conductivity Measurements in a Loam Soil Covered by Native Vegetation: Spatial and Temporal Variability in the Upper Soil Layer. Geosci. 2021, Vol. 11, Page 105 11, 105. https://doi.org/10.3390/GEOSCIENCES11020105

Kisekka, I., Aguilar, J.P., Rogers, D.H., Holman, J., O'Brien, D.M. and Klocke, N., 2016. Assessing deficit irrigation strategies for corn using simulation. Transactions of the ASABE, 59(1), pp.303-317.

Kottek, M., Jurger, G., Beck, C., Rudolf, B., Rubel, F., 2006. World Map of the Köppen- Geiger climate classification updated. Meteorologische Zeitschrift 15 (3), 259–263. https://doi.org/10.1127/0941-2948/2006/0130.

Kumar, H., Srivastava, P., Lamba, J., Ortiz, B.V., Way, T.R., Sangha, L., Takhellambam, B.S. and Morata, G., 2021a. Phosphorus Variability in the Irrigated Cropland During a growing season. In 2021 ASABE Annual International Virtual Meeting (p. 1). American Society of Agricultural and Biological Engineers.

Kumar, H., Srivastava, P., Ortiz, B. V., Morata, G., Takhellambam, B.S., Lamba, J., Bondesan, L., 2021b. Field-Scale Spatial and Temporal Soil Water Variability in Irrigated Croplands. Trans. ASABE 64, 1277–1294. https://doi.org/10.13031/TRANS.14335

Kumar, H., Srivastava, P., Ortiz, B.V., Takhellambam, B.S., Morata, G., Bondesan, L. and Lamba, J., 2020. Spatiotemporal Soil Moisture Variability in Corn and Cotton Fields with Uniform Irrigation During the Growing Season. In: AGU Fall Meeting Abstracts (Vol. 2020, pp. H209-05).

Leininger, S.D., Krutz, L.J., Sarver, J.M., Gore, J., Henn, A., Bryant, C.J., Atwill, R.L., Spencer, G.D., 2019. Establishing Irrigation Thresholds for Furrow-Irrigated Peanuts. Crop. Forage Turfgrass Manag. 5, 180059. https://doi.org/10.2134/cftm2018.08.0059

Lena, B. P., Bondesan, L., Pinheiro, E.A.R., Ortiz, B., Morata, G., Kumar, H., 2022. Determination of irrigation scheduling thresholds based on HYDRUS-1D simulations of field capacity for multilayered agronomic soils in Alabama, USA. Agric. Water Manag. 259, 107234. https://doi.org/10.1016/J.AGWAT.2021.107234

Li, Y., Šimůnek, J., Jing, L., Zhang, Z., Ni, L., 2014. Evaluation of water movement and water losses in a direct-seeded-rice field experiment using Hydrus-1D. Agric. Water Manag. 142, 38–46. https://doi.org/10.1016/j.agwat.2014.04.021

Meyer, P.D., Gee, G.W., 1999. Flux-Based Estimation of Field Capacity. J. Geotech. Geoenvironmental Eng. 125, 595–599. https://doi.org/10.1061/(ASCE)1090-0241(1999)125:7(595)

Mokari, E., Shukla, M.K., Šimůnek, J. and Fernandez, J.L., 2019. Numerical Modeling of Nitrate in a Flood-Irrigated Pecan Orchard. Soil Science Society of America Journal, 83(3), pp.555-564.

Morata, G., 2020. Evaluation of Deficit Irrigation Strategies and Management Zones Delineation for Corn Production in Alabama. MS thesis. Auburn, AL: Auburn University, Department of Crop, Soil and Environmental Sciences.

Mualem, Y., 1976. A new model for predicting the hydraulic conductivity of unsaturated porous media. Water Resour. Res. 12, 513–522. https://doi.org/10.1029/WR012I003P00513

Nemes, A., Pachepsky, Y.A., Timlin, D.J., 2011. Toward Improving Global Estimates of Field Soil Water Capacity. Soil Sci. Soc. Am. J. 75, 807–812. https://doi.org/10.2136/SSSAJ2010.0251

Peters, A., Iden, S.C., Durner, W., 2015. Revisiting the simplified evaporation method: Identification of hydraulic functions considering vapor, film and corner flow. J. Hydrol. 527, 531–542. https://doi.org/10.1016/J.HYDROL.2015.05.020

Pinheiro, E.A.R., de Jong van Lier, Q., Inforsato, L., Šimůnek, J., 2019. Measuring full-range soil hydraulic properties for the prediction of crop water availability using gamma-ray attenuation and inverse modeling. Agric. Water Manag. 216, 294–305. https://doi.org/10.1016/J.AGWAT.2019.01.029

Qu, W., Bogena, H.R., Huisman, J.A., Martinez, G., Pachepsky, Y.A., Vereecken, H., 2014. Effects of Soil Hydraulic Properties on the Spatial Variability of Soil Water Content: Evidence from Sensor Network Data and Inverse Modeling. Vadose Zo. J. 13, vzj2014.07.0099. https://doi.org/10.2136/vzj2014.07.0099

Romano, N., Palladino, M., Chirico, G.B., 2011. Parameterization of a bucket model for soil-vegetation-atmosphere modeling under seasonal climatic regimes. Hydrol. Earth Syst. Sci. 15, 3877–3893. https://doi.org/10.5194/HESS-15-3877-2011

Schaap, M.G., Leij, F.J., van Genuchten, M.T., 2001. Rosetta: A computer program for estimating soil hydraulic parameters with hierarchical pedotransfer functions. J. Hydrol. 251, 163–176. https://doi.org/10.1016/S0022-1694(01)00466-8

Šimůnek, J., van Genuchten, M.T., Šejna, M., 2016. Recent Developments and Applications of the HYDRUS Computer Software Packages. Vadose Zo. J. 15, 1–25. https://doi.org/10.2136/VZJ2016.04.0033

Twarakavi, N.K.C., Sakai, M., Šimůnek, J., 2009. An objective analysis of the dynamic nature of field capacity. Water Resour. Res. 45. https://doi.org/10.1029/2009WR007944

van Genuchten, M.T., 1980. A Closed-form Equation for Predicting the Hydraulic Conductivity of Unsaturated Soils. Soil Sci. Soc. Am. J. 44, 892–898. https://doi.org/10.2136/SSSAJ1980.03615995004400050002X

van Genuchten, M.T., Leij, F.J. and Yates, S.R., 1991. The RETC code for quantifying the hydraulic functions of unsaturated soils. U.S. Department of Agriculture, Agricultural Research Service Riverside, California

Wang, X., Li, Y., Si, B., Ren, X., Chen, J., 2018. Simulation of Water Movement in Layered Water-Repellent Soils using HYDRUS-1D. Soil Sci. Soc. Am. J. 82, 1101–1112. https://doi.org/10.2136/sssaj2018.01.0056

Wang, Y., Zhang, B., Lin, L., Zepp, H., 2011. Agroforestry system reduces subsurface lateral flow and nitrate loss in Jiangxi Province, China. Agric. Ecosyst. Environ. 140, 441–453. https://doi.org/10.1016/J.AGEE.2011.01.007

Wesseling, J., 1991. Meerjarige simulatie van grondwaterstroming voor verschillende bodemprofielen, grondwatertrappen en gewassen met het model SWATRE. 0924- 3070. DLO-Staring Centrum.

Wyatt, B.M., Ochsner, T.E., Fiebrich, C.A., Neel, C.R., Wallace, D.S., 2017. Useful Drainage Estimates Obtained from a Large-Scale Soil Moisture Monitoring Network by Applying the Unit-Gradient Assumption. Vadose Zo. J. 16, vzj2017.01.0016. https://doi.org/10.2136/vzj2017.01.0016

Zhang, Y., Zhao, W., He, J., Fu, L., 2018. Soil Susceptibility to Macropore Flow Across a Desert-Oasis Ecotone of the Hexi Corridor, Northwest China. Water Resour. Res. 54, 1281–1294. https://doi.org/10.1002/2017WR021462

Zhang, Y., Zhao, W., Ochsner, T.E., Wyatt, B.M., Liu, H., Yang, Q., 2019. Estimating Deep Drainage Using Deep Soil Moisture Data under Young Irrigated Cropland in a Desert-Oasis Ecotone, Northwest China. Vadose Zo. J. 18, 1–10. https://doi.org/10.2136/vzj2018.10.0189

Zhou, H., Zhao, W. zhi, 2019. Modeling soil water balance and irrigation strategies in a flood-irrigated wheat-maize rotation system. A case in dry climate, China. Agric. Water Manag. 221, 286–302. https://doi.org/10.1016/j.agwat.2019.05.011

Chapter 6

Conclusions

6.1 General Conclusions

The increasing human population is increasing the demands for water and food all around the globe. The need to increase yield while reducing water and nutrient footprint have never been greater. Therefore, as irrigated agriculture intensifies to elevate food production, precision agriculture aims to reduce water and nutrient use through site-specific agricultural water and nutrient management. Excessive water withdrawal from the streams, lakes, and groundwater has started depleting the water resources. Also, climate change has changed the distribution of precipitation, especially over the growing season (Filho et al., 2020). The future forecast of precipitation data showed the 14% increment in the annual average of precipitation by 2059, which would alter the time, erosivity characteristics, and distribution of the precipitation events (Takhellambam et al., 2021, 2022). Irrigation is required to meet water demands due to lack of precipitation over the growing season or no precipitation during the periods of high water demand for crops. Meeting site-specific crop water demands on time by scheduling irrigation can increase crop yield. The need for site-specific crop water demands can be identified by monitoring soil moisture within the crop fields (Kumar et al., 2020, 2021b). Knowing the spatial and temporal variation in soil moisture can help in determining irrigation depths. Also, proper site-specific nutrient management can help reduce nutrient loss, increase nutrient uptake, and increase crop yield (Kumar et al., 2021a). Understanding site-specific spatial and temporal variability in soil moisture and nutrient can help understand the problems scientifically and improve the best management practices adopted by farmers. Evaluating the impact of uniform application of

irrigation and nutrient in the crop field can provide a glimpse into challenges that lie ahead for long-term sustainable agriculture management.

Understanding the spatial variability in soil water and nutrients indicated the adoption of variable-rate irrigation and nutrient management practices in the crop field. The field hydrology and topographic variability across the field influence the decisions for both agricultural water and nutrient management during the growing season. Evaluating the spatial and temporal variability in soil water in corn and cotton fields has shown that soil water is a key variable in determining irrigation. Soil water dynamics in different soil profiles can be used to optimize the irrigation amount, time, and rate (Dissertation Objective 1). The spatiotemporal variability in soil water in corn and cotton fields has an impact on the intermediate soil layer due to water input from the top and suction from the bottom soil layers. Determining a representative location to determine the average soil water can help to know the range of irrigation water demands within the field. Knowing the spatial and temporal variability in soil water and average soil water in the field helped identify the above-and-below soil water conditions compared to the average. A single soil moisture sensor location can be useful in scheduling uniform irrigation in a crop field during the growing season. To capture the maximum spatial and temporal variability in soil water, the number of sensors can be optimized for a maximum absolute error. Reducing the number of sensors installed can help farmers to reduce the cost, time, and labor. The meteorological factors had an impact on soil water variability due to canopy and root growth differences in corn and cotton crops. Among all field attributes, topography in the cornfield and soil properties in the cotton field were influential factors in soil water variability and determining the representative location. The management zones analysis incorporating nutrient variability can be helpful practice in precision

agricultural management. The distribution of sensors throughout the field can be categorized into different management zones based on the variability in soil water, nutrient, and soil characteristics.

Uniform application of nutrients (P and N) can lead to adequate nutrient concentrations in some areas and inadequate nutrients in others. Such site-specific spatial and temporal variability had an impact on plant growth and development in the study cornfield during the 2019 growing season (Dissertation Objective 2). The higher soil nutrient concentration area (HY zone) had better plant growth since the plants in the HY zone had higher nutrient uptake. However, the lower soil nutrient concentration area (LY zone) had reduced plant growth since the plants in the LY zone had reduced nutrient uptake due to a lack of availability of nutrients. The soil nutrient variability, nutrient variability in plants, and plant growth variability had a similar pattern, which affected the crop yield in the respective zones. The higher nutrient zone had higher crop yield and the lower nutrient zone had lower crop yield. The topographic wetness index (TWI), slope, and soil hydraulic properties were determined as responsible factors for within-field nutrient and crop yield variability across the crop field (Kumar et al., 2021a). These hydrological properties within a field caused the surface runoff loss of nutrients in the LY zone, which reduced the crop yield during the 2019 growing season. Incorporating spatial nutrient variability in management zone delineation can be an effective way to improve the adoption of precision agricultural management.

Assuming a single irrigation threshold to trigger irrigation can result in over-irrigation in some parts and under-irrigation in others. Delineating a field in different irrigation management zones and determining zone-specific irrigation thresholds can be a better irrigation strategy. The topographic attributes play an important role in the distribution of soil moisture sensors throughout the field. Uniform SHPs cannot be considered with contrasting topographically variable fields and cannot optimize the soil water dynamics. The selection of soil moisture sensors to optimize the

SHPs can be made using uniformity within the zones. Although irrigation threshold can be determined using laboratory-drawn SHPs, such SHPs do not consider discrepancies associated with field observations. Therefore, optimizing the SHPs resulted in accurate zone-specific irrigation thresholds. Optimizing zone-specific SHPs can avoid discrepancies in field observation and result in better irrigation practice. The results showed (Dissertation Objective 3) that each zone should be managed differently to improve water use and root water uptake. Knowing actual soil water dynamics in each zone, plants can increase root water uptake to meet potential root water demand. Based on our simulations in this study using optimized SHPs at 35% soil water depletion, the irrigation thresholds were at absolute soil matric potential value of 76 kPa in zone 1 and 59 kPa in zone 2, and corresponding irrigation application rates were reduced to 2.18 cm and 1.48 cm in zone 1 and zone 2, respectively. Farmers can delay irrigation by a few days depending upon the depth of irrigation in zone 1 and zone 2 to increase crop water demands.

Conventionally, an absolute soil matric potential value of 33 kPa is considered as benchmark field capacity in fine-textured soil without considering the particle size fractions, study region, and actual soil water dynamics. The zone-specific FC was determined using numerical modeling with HYDRUS-1D considering negligible flux criterion with optimized SHPs. The results from this study (Dissertation Objective 4) have shown that zone-specific optimized FC had a contrasting pattern compared to the benchmark and observed FC. The optimized FC values were found to be greater in zone 1 and lower in zone 2 compared to observed and benchmark FC. The observed and benchmark FC in both zones did not consider soil water dynamics for the discrepancies associated with FC and SHPs during field observations. Therefore, observed and benchmark FC may not be the best options in irrigation scheduling schemes without optimization. Irrigation recommendations using zone-specific optimized FC and optimized SHPs showed a strong

correlation between accumulated crop evapotranspiration and required irrigation amount in both zones, compared to observed FC and observed SHPs.

6.2 Future Work

Future research that can be performed using this study and its findings as a groundwork for further contributing to the science and improving the sustainability of agriculture and environment in the precision agriculture are listed below:

1. Assess and validate the optimized irrigation thresholds and field capacity scenarios to evaluate irrigation water use efficiency and crop yield.

2. Evaluate the two- and three-layer HYDRUS-1D models to see the impact of soil heterogeneity on soil water dynamics and root water uptake within the soil profiles.

3. Evaluate the dynamic irrigation thresholds and field capacity incorporating three-dimensional soil hydraulic properties.

4. Evaluate the HYDRUS-1D model for simulating soil nutrients in contrasting areas.

6.3 References

Filho, J.F.D.C.L., Ortiz, B.V., Damianidis, D., Balkcom, K.S., Dougherty, M. and Knappenberger, T., 2020. Irrigation Scheduling to Promote Corn Productivity in Central Alabama. Journal of Agricultural Science, 12(9).

Kumar, H., Srivastava, P., Ortiz, B.V., Takhellambam, B.S., Morata, G., Bondesan, L. and Lamba, J., 2020. Spatiotemporal Soil Moisture Variability in Corn and Cotton Fields with Uniform Irrigation During the Growing Season. In: AGU Fall Meeting Abstracts (Vol. 2020, pp. H209-05).

Kumar, H., Srivastava, P., Lamba, J., Ortiz, B. V., Way, T.R., Sangha, L., Takhellambam, B.S., Morata, G., 2021a. Phosphorus variability in the irrigated cropland during a growing season. Am. Soc. Agric. Biol. Eng. Annu. Int. Meet. ASABE 2021. https://doi.org/10.13031/AIM.202100886

Kumar, H., Srivastava, P., Ortiz, B. V., Morata, G., Takhellambam, B.S., Lamba, J., Bondesan, L.,

2021b. Field-Scale Spatial and Temporal Soil Water Variability in Irrigated Croplands. Trans. ASABE 64, 1277–1294. https://doi.org/10.13031/TRANS.14335

Takhellambam, B.S., Srivastava, P., Lamba, J., McGehee, R.P., and Kumar, H., 2021. Potential changes in rainfall erosivity under climate change in southeastern United States. In: AGU Fall Meeting 2021.

Takhellambam, B.S., Srivastava, P., Lamba, J., Mcgehee, R.P., Kumar, H., Tian, D., 2022. Temporal disaggregation of hourly precipitation under changing climate over the Southeast United States. Sci. Data 2022 91 9, 1–14. https://doi.org/10.1038/s41597-022-01304-7